

The Constrained Exceptional Supersymmetric Standard Model

P. Athron^a, S.F. King^b, D.J. Miller^c, S. Moretti^{b,d} and R. Nevzorov^{c1}

^a *Institut für Kern und Teilchenphysik, TU Dresden, Dresden, D-01062, Germany.*

^b *School of Physics and Astronomy, University of Southampton, Southampton, SO17 1BJ, U.K.*

^c *Department of Physics and Astronomy, University of Glasgow, Glasgow G12 8QQ, U.K.*

^d *Dipartimento di Fisica Teorica, Università degli Studi di Torino, Via Pietro Giuria 1, 10125 Torino, Italy*

Abstract

We propose and study a constrained version of the Exceptional Supersymmetric Standard Model (E₆SSM), which we call the cE₆SSM, based on a universal high energy scalar mass m_0 , trilinear scalar coupling A_0 and gaugino mass $M_{1/2}$. We derive the Renormalisation Group (RG) Equations for the cE₆SSM, including the extra $U(1)_N$ gauge factor and the low energy matter content involving three 27 representations of E_6 . We perform a numerical RG analysis for the cE₆SSM, imposing the usual low energy experimental constraints and successful Electro-Weak Symmetry Breaking (EWSB). Our analysis reveals that the sparticle spectrum of the cE₆SSM involves a light gluino, two light neutralinos and a light chargino. Furthermore, although the squarks, sleptons and Z' boson are typically heavy, the exotic quarks and squarks can also be relatively light. We finally specify a set of benchmark points which correspond to particle spectra, production modes and decay patterns peculiar to the cE₆SSM, altogether leading to spectacular new physics signals at the Large Hadron Collider (LHC).

¹On leave of absence from the Theory Department, ITEP, Moscow, Russia

1. Introduction

Supersymmetry (SUSY) provides an attractive framework that allows one to link gravity with the other fundamental forces of nature. Indeed, it is well known that local SUSY (Supergravity) leads to a partial unification of the Electro-Weak (EW), strong and gravitational interactions [1]. At some high energy scale local SUSY in Supergravity (SUGRA) models can be spontaneously broken in a hidden sector. Then the low-energy limit of such a theory is described by a global SUSY Lagrangian plus a set of soft SUSY-breaking terms [2] which do not induce quadratic divergences, thus preserving the Supersymmetric solution to the hierarchy problem [3] (for a recent review see [4]). A set of soft SUSY-breaking terms involves gaugino masses M_a , soft scalar masses m_i^2 , plus bilinear (B_i) and trilinear (A_i) scalar couplings [5]. If the SUSY-breaking scale is within a few TeV then the $SU(3)_C$, $SU(2)_W$ and $U(1)_Y$ gauge couplings converge to a common value near the scale $M_X \simeq 2 - 3 \cdot 10^{16}$ GeV [6], which allows one to embed SUSY extensions of the Standard Model (SM) into Grand Unified Theories (GUTs) [7]. The rational $U(1)_Y$ charges, which are postulated *ad hoc* in the SM, then appear in a natural way in the context of SUSY GUT models after the breakdown of the extended symmetry – such as $SU(5)$, $SO(10)$ or E_6 – at the scale M_X .

However, the incorporation of the simplest SUSY extension of the SM — the Minimal Supersymmetric Standard Model (MSSM) — into SUGRA or SUSY GUT models leads to the μ -problem [4]. The Superpotential of the MSSM contains one bilinear term $\mu \hat{H}_d \hat{H}_u$ that can be present before SUSY is broken. One would naturally expect the parameter μ to be either zero or of the order of the Planck scale. On the one hand, if $\mu \simeq M_{\text{Pl}}$ then the Higgs scalars acquire a huge positive contribution $\sim \mu^2$ to their squared masses and EW Symmetry Breaking (EWSB) does not occur. On the other hand, if $\mu = 0$ at some scale Q the mixing between Higgs doublets is not generated at any scale below Q due to non-renormalisation theorems [8] so that $\langle H_d \rangle = 0$ and down-type quarks and charged leptons remain massless. The correct pattern of EWSB requires μ to be of the order of the SUSY-breaking (or EW) scale.

An elegant solution to the μ -problem naturally arises in the framework of Superstring inspired E_6 models. Ten-dimensional heterotic Superstring theory based on $E_8 \times E'_8$ [9] can play a role in the ultraviolet completion of the non-renormalisable SUGRA models. In the strong coupling regime of an $E_8 \times E'_8$ heterotic string theory, which is described by eleven dimensional Supergravity (M-theory) [10], the string scale can be compatible with the unification scale M_X [11]. Compactification of the extra dimensions results in the breakdown of E_8 down to E_6 or one of its subgroups in the observable sector [12]. The remaining E'_8 couples to the usual matter representations of the E_6 group only by virtue

of gravitational interactions and comprises a hidden sector that gives rise to spontaneous breakdown of local SUSY. At low energies the hidden sector decouples from the observable one. The only signal it produces is a set of soft SUSY-breaking terms characterised by the gravitino mass ($m_{3/2}$) scale¹ which spoil the degeneracy between bosons and fermions within one Supermultiplet.

At the string scale, E_6 can be broken via the Hosotani mechanism [14]. The breakdown of the E_6 symmetry results in several models based on rank-5 or rank-6 gauge groups. Therefore Superstring inspired E_6 models may lead to low-energy gauge groups with one or two additional $U(1)'$ factors in comparison to the SM. In particular, E_6 can be broken directly to the rank-6 subgroup $SU(3)_C \times SU(2)_W \times U(1)_Y \times U(1)_\psi \times U(1)_\chi$. Two anomaly-free $U(1)_\psi$ and $U(1)_\chi$ symmetries of the rank-6 model are defined by [15]: $E_6 \rightarrow SO(10) \times U(1)_\psi$, $SO(10) \rightarrow SU(5) \times U(1)_\chi$. This rank-6 model can be reduced further to an effective rank-5 model with only one extra gauge symmetry $U(1)'$ which is a linear combination of $U(1)_\chi$ and $U(1)_\psi$:

$$U(1)' = U(1)_\chi \cos \theta + U(1)_\psi \sin \theta. \quad (1)$$

If $\theta \neq 0$ or π the extra $U(1)'$ gauge symmetry forbids an elementary μ term but allows an interaction of the extra SM singlet Superfield \hat{S} with the Higgs Supermultiplets \hat{H}_d and \hat{H}_u in the Superpotential: $\lambda \hat{S} \hat{H}_d \hat{H}_u$. After EWSB the scalar component of the SM singlet Superfield \hat{S} acquires a non-zero VEV breaking $U(1)'$ and an effective μ -term of the required size is automatically generated [16]. Thus in Superstring inspired E_6 models the μ -problem is solved in a similar way to the Next-to-Minimal Supersymmetric Standard Model (NMSSM) [17], but without the accompanying problems of singlet tadpoles or domain walls [18].

E_6 inspired SUSY models with an extra $U(1)'$ have been extensively studied [15], [19]. In general the models predict extra exotic matter beyond the MSSM and NMSSM. The large couplings of exotic quarks (D, \bar{D}) to the SM singlet S of the form $\kappa S(D\bar{D})$ may induce radiative breakdown of the extra $U(1)'$ symmetry [20], [21]–[24]. An important feature of E_6 inspired SUSY models is that the mass of the lightest Higgs particle can be substantially larger in these scenarios than in the MSSM and NMSSM [24]. Previously, the implications of E_6 inspired SUSY models with an additional $U(1)'$ gauge symmetry have been studied for EWSB [21]–[24], neutrino physics [25]–[26], leptogenesis [27]–[28], EW baryogenesis [29], muon anomalous magnetic moment [30], electric dipole moment of electron [31] and lepton flavour violating processes like $\mu \rightarrow e\gamma$ [32].

Recent publications have focused on a particular E_6 inspired SUSY model with an extra $U(1)_N$ gauge symmetry in which right handed neutrinos do not participate in the

¹In the most general case a complete set of expressions for the soft SUSY-breaking parameters can be found in [13].

gauge interactions. This corresponds to $\theta = \arctan \sqrt{15}$. Only in this Exceptional Supersymmetric Standard Model (E₆SSM) [33]–[34] right-handed neutrinos may be superheavy, shedding light on the origin of the mass hierarchy in the lepton sector and providing a mechanism for the generation of lepton and baryon asymmetry of the universe [27]–[28]. Supersymmetric models with an additional $U(1)_N$ gauge symmetry in which right-handed neutrinos have zero charge have been studied in [26] in the context of non-standard neutrino models with extra singlets, in [35] from the point of view of $Z - Z'$ mixing, in [23] and [35]–[36] where the neutralino sector was explored, in [23] where the RG flow of couplings was examined and in [22]–[24] where EWSB was studied.

In a recent letter [37] we presented predictions from a constrained version of the above E₆SSM, referred to as the cE₆SSM², in which the soft SUSY-breaking scalar masses, gaugino masses and the trilinear scalar couplings are each assumed to be universal at the scale M_X , i.e. $m_i^2(M_X) = m_0^2$, $M_i(M_X) = M_{1/2}$ and $A_i(M_X) = A_0$. We discussed scenarios of the cE₆SSM with the lowest values of m_0 and $M_{1/2}$ consistent with both EWSB and experimental constraints, leading to very light exotic quarks, inert Higgs/Higgsinos and Z' masses. As such these represented scenarios which could be discovered early at the LHC using “first data”. Since the emphasis was on early discovery we did not explore the cE₆SSM parameter space thoroughly and did not present a set of benchmarks which represent all the qualitatively different spectra of TeV scale cE₆SSM scenarios. For brevity we also omitted the renormalisation group equations (RGEs) used in our analysis and did not provide full details of our mass spectra calculations.

In this paper we provide a comprehensive study of the parameter space of the cE₆SSM and the TeV scale predictions of the model. We present two-loop RGEs for the gauge and Yukawa couplings together with two-loop RGEs for the gaugino masses and trilinear scalar couplings as well as one-loop RGEs for the soft scalar masses, in order to calculate the values of all masses and couplings at the EW scale for each set of fundamental parameters at the GUT scale M_X . Two-loop corrections to the β -functions are important for the analysis of the particle spectrum because in E_6 inspired SUSY models the β -function of the $SU(3)$ gauge coupling and the gluino mass vanish in the one-loop approximation. We perform a numerical RG analysis for the cE₆SSM, imposing the usual low energy experimental constraints and enforcing successful EWSB. Our analysis reveals that there is a substantial part of the cE₆SSM parameter space where the correct breakdown of the gauge symmetry can be achieved and all experimental constraints can be satisfied. We then perform a scan of the parameter space of the cE₆SSM and specify a set of benchmark points that highlight particular characteristics of the particle spectrum within the cE₆SSM parameter space. A general feature of the benchmark spectra is a light sector of SUSY

²See also Ref. [38] for a preliminary account.

particles consisting of a light gluino, two light neutralinos and a light chargino, resulting from the relative smallness of the low energy gaugino masses M_i due to the stronger gauge running. Although the squarks, sleptons and Z' boson are typically much heavier, the exotic quarks and squarks can be also relatively light leading to spectacular new physics signals at the LHC.

The paper is organised as follows. In the next section we introduce the E_6 SSM and define the cE_6 SSM. In section 3 we discuss the breakdown of gauge symmetry in the cE_6 SSM. In section 4 we provide analytical expressions for the mass matrices and masses of all new particles appearing in our model. In section 5 we study the RG flow of all masses and couplings and summarise the results of our studies of the particle spectrum. Section 6 is reserved for our conclusions and outlook. Appendix A contains explicit expressions for the one-loop corrections to the mass matrix of the CP-even Higgs bosons calculated in the leading approximation. In Appendix B we specify the complete system of RGEs that we use in our analysis.

2. From the E_6 SSM to the cE_6 SSM

The E_6 SSM is based on the $SU(3)_C \times SU(2)_W \times U(1)_Y \times U(1)_N$ gauge group which is a subgroup of E_6 . The extra $U(1)_N$ gauge symmetry is defined such that right-handed neutrinos carry zero charges. The E_6 SSM can originate from an E_6 GUT gauge group which is broken at the GUT scale M_X . In E_6 theories the anomalies are cancelled automatically; all models that are based on the E_6 subgroups and contain complete representations of E_6 should be anomaly-free. Consequently, in order to make a Supersymmetric model with an extra $U(1)_N$ anomaly-free, one is forced to augment the minimal particle spectrum by a number of exotics which, together with ordinary quarks and leptons, form complete fundamental 27 representations of E_6 . Thus the particle content of the E_6 SSM involves at least three fundamental representations of E_6 at low energies. These multiplets decompose under the $SU(5) \times U(1)_N$ subgroup of E_6 as follows:

$$27_i \rightarrow \left(10, \frac{1}{\sqrt{40}}\right)_i + \left(5^*, \frac{2}{\sqrt{40}}\right)_i + \left(5^*, -\frac{3}{\sqrt{40}}\right)_i \\ + \left(5, -\frac{2}{\sqrt{40}}\right)_i + \left(1, \frac{5}{\sqrt{40}}\right)_i + (1, 0)_i. \quad (2)$$

The first and second quantities in brackets are the $SU(5)$ representation and extra $U(1)_N$ charge respectively, while i is a family index that runs from 1 to 3. An ordinary SM family, which contains the doublets of left-handed quarks Q_i and leptons L_i , right-handed up- and down-quarks (u_i^c and d_i^c) as well as right-handed charged leptons, is assigned to

$\left(10, \frac{1}{\sqrt{40}}\right)_i + \left(5^*, \frac{2}{\sqrt{40}}\right)_i$. Right-handed neutrinos N_i^c should be associated with the last term in Eq. (2), $(1, 0)_i$. The next-to-last term, $\left(1, \frac{5}{\sqrt{40}}\right)_i$, represents SM-singlet fields S_i , which carry non-zero $U(1)_N$ charges and therefore survive down to the EW scale. The pair of $SU(2)_W$ -doublets $(H_i^d$ and $H_i^u)$ that are contained in $\left(5^*, -\frac{3}{\sqrt{40}}\right)_i$ and $\left(5, -\frac{2}{\sqrt{40}}\right)_i$ have the quantum numbers of Higgs doublets. They form either Higgs or Inert Higgs $SU(2)_W$ multiplets³. Other components of these $SU(5)$ multiplets form colour triplets of exotic quarks \overline{D}_i and D_i with electric charges $-1/3$ and $+1/3$, respectively.

In E_6 models the renormalisable part of the Superpotential arises from the $27 \times 27 \times 27$ decomposition of the E_6 fundamental representation. The most general renormalisable Superpotential that is allowed by the E_6 symmetry can be written in the following form:

$$W_{E_6} = W_0 + W_1 + W_2, \quad (3)$$

$$\begin{aligned}
 W_0 = & \lambda_{ijk} \hat{S}_i (\hat{H}_1^d \hat{H}_k^u) + \kappa_{ijk} \hat{S}_i (\hat{D}_j \hat{\overline{D}}_k) + h_{ijk}^N \hat{N}_i^c (\hat{H}_j^u \hat{L}_k) + h_{ijk}^U \hat{u}_i^c (\hat{H}_j^u \hat{Q}_k) \\
 & + h_{ijk}^D \hat{d}_i^c (\hat{H}_j^d \hat{Q}_k) + h_{ijk}^E \hat{e}_i^c (\hat{H}_j^d \hat{L}_k), \quad (4)
 \end{aligned}$$

$$W_1 = g_{ijk}^Q \hat{D}_i (\hat{Q}_j \hat{Q}_k) + g_{ijk}^a \hat{\overline{D}}_i \hat{d}_j^c \hat{u}_k^c, \quad (5)$$

$$W_2 = g_{ijk}^N \hat{N}_i^c \hat{D}_j \hat{d}_k^c + g_{ijk}^E \hat{e}_i^c \hat{D}_j \hat{u}_k^c + g_{ijk}^D (\hat{Q}_i \hat{L}_j) \hat{\overline{D}}_k. \quad (6)$$

From Eq. (3) one can see that the E_6 symmetry does not forbid lepton and baryon number violating operators that result in rapid proton decay. Moreover, exotic particles in E_6 inspired SUSY models give rise to new Yukawa interactions that in general induce unacceptably large non-diagonal flavour transitions. To suppress these effects, an approximate Z_2^H symmetry can be postulated. All Superfields except one pair of \hat{H}_i^d and \hat{H}_i^u (say $\hat{H}_d \equiv \hat{H}_3^d$ and $\hat{H}_u \equiv \hat{H}_3^u$) and one SM-type singlet field ($\hat{S} \equiv \hat{S}_3$) are odd under this symmetry. In this case, only one Higgs doublet H_d interacts with the down-type quarks and charged leptons and only one Higgs doublet H_u couples to up-type quarks, while the couplings of all other exotic particles to the ordinary quarks and leptons are forbidden. This eliminates any problems related to non-diagonal flavour transitions.

However, in the E_6 SSM the Z_2^H symmetry can only be approximate. Indeed, this symmetry forbids all terms in W_1 and W_2 . As a consequence the Lagrangian is invariant not only with respect to $U(1)_L$ and $U(1)_B$ but also $U(1)_D$ symmetry transformations,

$$D \rightarrow e^{i\alpha} D, \quad \overline{D} \rightarrow e^{-i\alpha} \overline{D}. \quad (7)$$

This $U(1)_D$ invariance forces the lightest exotic quark to be stable. Any heavy stable particle would have been copiously produced during the very early epochs of the Big

³We use the terminology ‘‘Inert Higgs’’ to denote Higgs-like doublets that do not develop VEVs.

Bang, and the strong or electromagnetically interacting fermions and bosons which survive annihilation would subsequently have been confined in heavy hadrons which would annihilate further. The remaining heavy hadrons originating from the Big Bang should be present in terrestrial matter. There are very strong upper limits on the abundances of nuclear isotopes which contain such stable relics in the mass range from 1 GeV to 10 TeV. Different experiments set limits on their relative concentrations from 10^{-15} to 10^{-30} per nucleon [39]. At the same time various theoretical estimates [40] show that if remnant particles would exist in nature today their concentration is expected to be at the level of 10^{-10} per nucleon. Thus E_6 inspired models with stable exotic quarks are ruled out.

Therefore this Z_2^H symmetry must be broken, but in such a way as to avoid rapid proton decay. There are two ways to overcome this problem: the Lagrangian must be invariant with respect to either a Z_2^L symmetry, under which all Superfields except lepton ones are even (Model I), or a Z_2^B discrete symmetry, which implies that exotic quark and lepton Superfields are odd whereas the others remain even (Model II). If the Lagrangian is invariant under the Z_2^B symmetry then all terms in W_1 are forbidden and the exotic quarks are leptoquarks, i.e. they carry baryon ($B_D = 1/3$ and $B_{\overline{D}} = -1/3$) and lepton ($L_D = 1$ and $L_{\overline{D}} = -1$) numbers simultaneously. If Z_2^L is imposed, then all terms in W_2 are forbidden and baryon number conservation requires exotic quarks to be diquarks, i.e. $B_D = -2/3$ and $B_{\overline{D}} = 2/3$. In summary, the two possible models are,

$$W_{E_6SSM I} = W_0 + W_1, \quad W_{E_6SSM II} = W_0 + W_2. \quad (8)$$

Since Z_2^H violating operators lead to non-diagonal flavour interactions, the corresponding Yukawa couplings are expected to be small, and must preserve either the Z_2^B or Z_2^L symmetry to ensure proton stability. In order to guarantee that the contribution of new particles and interactions to $K^0 - \overline{K}^0$ oscillations and to the muon decay $\mu \rightarrow e^- e^+ e^-$ are suppressed in accordance with experimental limits, it is necessary to assume that the Yukawa couplings of exotic particles to ordinary quarks and leptons are less than $10^{-3} - 10^{-4}$. In this case, they do not affect the RG flow of other masses and couplings and can safely be ignored in our analysis of the particle spectrum.

In addition to the complete 27_i multiplets the low energy matter content of the E_6 SSM is supplemented by an $SU(2)_W$ doublet \hat{H}' and anti-doublet $\overline{\hat{H}'}$ from the extra $27'$ and $\overline{27'}$, in order to preserve gauge coupling unification. These components of the E_6 fundamental representation originate from $\left(5^*, \frac{2}{\sqrt{40}}\right)$ of $27'$ and $\left(5, -\frac{2}{\sqrt{40}}\right)$ of $\overline{27'}$ by construction. The analysis performed in [41] shows that the unification of gauge couplings in the E_6 SSM can be achieved for any phenomenologically acceptable value of $\alpha_3(M_Z)$ consistent with the measured low energy central value, unlike in the MSSM which, ignoring the effects of high energy threshold corrections, requires significantly higher values of $\alpha_3(M_Z)$, well

above the experimentally measured central value. The splitting of $27'$ and $\overline{27}'$ multiplets can be naturally achieved, for example, in the framework of orbifold GUTs [42].

Hence the low energy matter content of the E_6 SSM may be summarised as:

$$3 \left[(\hat{Q}_i, \hat{u}_i^c, \hat{d}_i^c, \hat{L}_i, \hat{e}_i^c, \hat{N}_i^c) \right] + 3(\hat{S}_i) + 3(\hat{H}_i^u) + 3(\hat{H}_i^d) + 3(\hat{D}_i, \hat{\bar{D}}_i) + \hat{H}' + \hat{H}', \quad (9)$$

where the right-handed neutrinos \hat{N}_i^c are expected to gain masses at some intermediate scale, while the remaining matter survives down to the EW scale near which the gauge group $U(1)_N$ is broken. Thus, in addition to a Z' corresponding to the $U(1)_N$ symmetry, the E_6 SSM involves extra matter beyond the MSSM with the quantum numbers of three $5 + 5^*$ representations of $SU(5)$ plus three $SU(5)$ singlets with $U(1)_N$ charges. The presence of a Z' boson and exotic quarks predicted by the E_6 SSM provides spectacular new physics signals at the LHC which were discussed in [33]–[34], [43].

The Z_2^H symmetry reduces the structure of the Yukawa interactions in the Superpotential of the E_6 SSM to

$$\begin{aligned} W_{E_6SSM I, II} \longrightarrow & \lambda_i \hat{S}(\hat{H}_i^d \hat{H}_i^u) + \kappa_i \hat{S}(\hat{D}_i \hat{\bar{D}}_i) + f_{\alpha\beta} \hat{S}_\alpha(\hat{H}_d \hat{H}_\beta^u) + \tilde{f}_{\alpha\beta} \hat{S}_\alpha(\hat{H}_\beta^d \hat{H}_u) \\ & + \frac{1}{2} M_{ij} \hat{N}_i^c \hat{N}_j^c + \mu'(\hat{H}' \hat{\bar{H}}') + h_{4j}^E(\hat{H}_d \hat{H}') \hat{e}_j^c + h_{4j}^N(\hat{H}_u \hat{H}') \hat{N}_j^c \\ & + W_{MSSM}(\mu = 0), \end{aligned} \quad (10)$$

where $\alpha, \beta = 1, 2$ and $i, j = 1, 2, 3$. In Eq. (10) we choose the basis $H_\alpha^d, H_\alpha^u, D_i$ and \bar{D}_i so that the Yukawa couplings of the singlet field S have flavour diagonal structure. We define $\lambda \equiv \lambda_3$. The $SU(2)_W$ doublets \hat{H}_u and \hat{H}_d , that are even under the Z_2^H symmetry, play the role of Higgs fields generating the masses of quarks and leptons after EWSB. The singlet field S must also acquire a large VEV in order to induce sufficiently large masses for the exotic charged fermions and Z' boson and avoid conflict with direct particle searches at present and past accelerators. This requires the Yukawa couplings λ_i and κ_i to be reasonably large. If λ_i or κ_i are large at the GUT scale they affect the evolution of the soft scalar mass m_S^2 of the singlet field S rather strongly resulting in negative values of m_S^2 at low energies that triggers the breakdown of the $U(1)_N$ symmetry.

Since H_u, H_d and S generate masses of all quarks, leptons and exotic fermions, it is natural to assume that only these fields acquire non-zero VEVs. To guarantee this, a certain hierarchy between the Yukawa couplings is imposed, $\kappa_i \sim \lambda_3 \gtrsim \lambda_{1,2} \gg f_{\alpha\beta}, \tilde{f}_{\alpha\beta}, h_{4j}^E, h_{4j}^N$. Although $f_{\alpha\beta}$ and $\tilde{f}_{\alpha\beta}$ are expected to be considerably smaller than λ_i and κ_i , they cannot be negligibly small since the fermion components of the Superfields \hat{S}_1 and \hat{S}_2 would become extremely light. The induced masses of singlinos \tilde{S}_1 and \tilde{S}_2 should be as large as a few MeV, otherwise the extra states could contribute to the universe expansion rate prior to nucleosynthesis, thereby changing nuclear abundances.

The Superpotential of the E_6 SSM includes two types of bilinear terms. One of these, $\mu' \hat{H}' \hat{\overline{H}'}$, is solely responsible for the masses of the charged and neutral components of \hat{H}' and $\hat{\overline{H}'}$. The corresponding mass term is not suppressed by the E_6 symmetry and is not involved in the process of the EWSB, and therefore, the parameter μ' remains arbitrary. Nevertheless, if the mass parameter μ' is too large it can spoil gauge coupling unification. Recent analyses revealed that gauge coupling unification is consistent with $\mu' \lesssim 100$ TeV [41]. Within SUGRA models the appropriate term $\mu' \hat{H}' \hat{\overline{H}'}$ in the Superpotential (10) can be induced after the breakdown of local SUSY if the Kähler potential contains an extra term ($Z(H' \overline{H}') + h.c.$) [44]⁴.

Another bilinear term in the Superpotential, $\frac{1}{2} M_{ij} \hat{N}_i^c \hat{N}_j^c$, determines the spectrum of the right-handed neutrinos. These mass terms are forbidden by E_6 and can be generated only after its breakdown [45]. Suppose N_H^c and \overline{N}_H^c are components of some extra 27_H and $\overline{27}_H$ representations which develop VEVs along the D -flat direction $\langle N_H^c \rangle = \langle \overline{N}_H^c \rangle \simeq \Lambda$. Then the right-handed neutrino mass terms can be induced through the non-renormalisable interactions of 27_i and $\overline{27}_H$ of the form $\frac{\eta_{ij}}{M_{Pl}} (\overline{27}_H 27_i) (\overline{27}_H 27_j)$. As a result, right-handed neutrinos gain masses M_i of the order of the intermediate mass scale⁵, $\frac{\Lambda^2}{M_{Pl}} \ll M_X$. We assume that the masses of the right-handed neutrinos are much larger than the SUSY-breaking scale.

Since the right-handed neutrinos are heavy, the three known doublet neutrinos ν_e , ν_μ and ν_τ , acquire small Majorana masses via the see-saw mechanism. This allows for a comprehensive understanding of the mass hierarchy in the lepton sector and neutrino oscillation data. At the same time the heavy Majorana right-handed neutrinos may decay into final states with lepton number $L = \pm 1$, thereby creating a lepton asymmetry in the early universe [46]. The flavour dependent lepton CP-asymmetries were calculated within the E_6 SSM in [28]. Since the Yukawa couplings of exotic particles are not constrained by neutrino oscillation data, substantial values of the CP-asymmetries can be induced even for a relatively small mass of the lightest right-handed neutrino ($M_1 \sim 10^6$ GeV) so that successful thermal leptogenesis may be achieved without encountering a gravitino problem [47]. At low energies the generated lepton asymmetry is partially converted into a baryon asymmetry via sphaleron processes [48].

⁴This mechanism is the same one used in the MSSM to solve the μ -problem. But in E_6 inspired models the bilinear terms involving \hat{H}_d and \hat{H}_u are forbidden by the E_6 symmetry both in the Kähler potential and Superpotential. As a result the mechanism mentioned above cannot be applied for the generation of $\mu \hat{H}_d \hat{H}_u$ in the E_6 SSM Superpotential.

⁵A similar mechanism could be applied for the generation of the μ' term discussed earlier. However, it is rather difficult to use the same fields N_H^c and \overline{N}_H^c in both cases because the values of the corresponding mass parameters are too different. In order to obtain μ' in the TeV range one should assume the existence of an additional pair of $N_H^{c'}$ and $\overline{N}_H^{c'}$ which acquire VEVs of order 10^{11} GeV.

The hierarchical structure of the Yukawa interactions allows one to simplify the Superpotential substantially. Integrating out heavy Majorana right-handed neutrinos and keeping only Yukawa interactions whose couplings are allowed to be of order unity we find

$$\begin{aligned}
W_{E_6SSM} \simeq & \lambda \hat{S}(\hat{H}_d \hat{H}_u) + \lambda_\alpha \hat{S}(\hat{H}_\alpha^d \hat{H}_\alpha^u) + \kappa_i \hat{S}(\hat{D}_i \hat{\bar{D}}_i) \\
& + h_t(\hat{H}_u \hat{Q}) \hat{t}^c + h_b(\hat{H}_d \hat{Q}) \hat{b}^c + h_\tau(\hat{H}_d \hat{L}) \hat{\tau}^c + \mu'(\hat{H}' \hat{\bar{H}}'),
\end{aligned} \tag{11}$$

where the Superfields $\hat{L} = \hat{L}_3$, $\hat{Q} = \hat{Q}_3$, $\hat{t}^c = \hat{u}_3^c$, $\hat{b}^c = \hat{d}_3^c$ and $\tau^c = e_3^c$ belong to the third generation. In Eq. (11) we neglect the Yukawa couplings of the quarks and leptons of the first and second generation because they are small and therefore do not affect the RG flow of other masses and couplings. The large Yukawa couplings of the third generation (in particular, the top quark Yukawa coupling) play an important role. They facilitate the generation of the non-zero VEVs of H_u and H_d which break the $SU(2)_W$ symmetry [49]. The simplified Superpotential (11) that we use in our analysis of the cE₆SSM contains seven new couplings compared to the MSSM with $\mu = 0$: the parameter μ' and six new Yukawa couplings λ_i and κ_i .

The most general scalar potential of the E₆SSM that ensures soft SUSY-breaking can be presented as a sum

$$V = V_F + V_D + V_{soft}, \tag{12}$$

where V_F and V_D are the contributions of F and D terms respectively, while V_{soft} contains a set of soft SUSY-breaking couplings:

$$\begin{aligned}
V_{soft} = & m_{S_i}^2 |S_i|^2 + m_{H_i^u}^2 |H_i^u|^2 + m_{H_i^d}^2 |H_i^d|^2 + m_{D_i}^2 |D_i|^2 + m_{\bar{D}_i}^2 |\bar{D}_i|^2 + m_{Q_i}^2 |Q_i|^2 \\
& + m_{u_i^c}^2 |u_i^c|^2 + m_{d_i^c}^2 |d_i^c|^2 + m_{L_i}^2 |L_i|^2 + m_{e_i^c}^2 |e_i^c|^2 + m_{H'}^2 |H'|^2 + m_{\bar{H}'}^2 |\bar{H}'|^2 \\
& + \left[B' \mu' (H' \bar{H}') + h.c. \right] + \left[\lambda_i A_{\lambda_i} S(H_i^d H_i^u) + \kappa_i A_{\kappa_i} S(D_i \bar{D}_i) \right. \\
& \left. + h_t A_t (H_u Q) t^c + h_b A_b (H_d Q) b^c + h_\tau A_\tau (H_d L) \tau^c + h.c. \right].
\end{aligned} \tag{13}$$

The soft breakdown of SUSY gives rise to many new couplings. The six additional Yukawa couplings are accompanied by six extra trilinear scalar couplings, A_{λ_i} and A_{κ_i} (13). Soft SUSY-breaking also induces the bilinear scalar coupling B' that corresponds to the mass term $\mu' \hat{H}' \hat{\bar{H}}'$ in the Superpotential (11). In addition, the scalar potential of the E₆SSM includes 15 extra soft scalar masses: six masses of exotic squarks $m_{\bar{D}_i}$ and $m_{\bar{D}_i^-}$, four masses of Inert Higgs fields $m_{H_\alpha^d}$ and $m_{H_\alpha^u}$, two soft scalar masses of H' and \bar{H}' and three masses of SM singlet scalar fields $m_{S_i}^2$. Due to the extra Yukawa couplings, the parameter μ' and the new trilinear scalar and bilinear scalar couplings (that can be complex), even the simplified version of the Z_2^H -symmetric E₆SSM considered here involves 43 new

parameters in comparison to the MSSM with $\mu = 0$. Fourteen of them are phases, some of which (but not all) can be eliminated by an appropriate redefinition of the new fields. However, the number of fundamental parameters reduces drastically in the cE₆SSM, defined at the GUT scale M_X , where all gauge couplings coincide, i.e. $g_1(M_X) \simeq g_2(M_X) \simeq g_3(M_X) \simeq g'_1(M_X)$, while the off-diagonal gauge coupling $g_{11}(M_X)$ vanishes. Constrained SUSY models impose extra unification constraints on the soft SUSY-breaking parameters. In particular, all soft scalar masses are set to be equal to m_0^2 at the scale M_X . Gaugino masses $M_i(M_X)$ are equal to an overall gaugino mass $M_{1/2}$ at the GUT scale and all trilinear and bilinear scalar couplings coincide at this scale, i.e. $A_i(M_X) = A_0$ and $B_i(M_X) = B$. Thus the cE₆SSM is uniquely characterised by the set of Yukawa couplings $\lambda_i(M_X)$, $\kappa_i(M_X)$, $h_t(M_X)$, $h_b(M_X)$ and $h_\tau(M_X)$, the universal soft scalar mass m_0 , the universal gaugino mass $M_{1/2}$ and the universal trilinear scalar coupling A_0 . The phases of the dimensionless couplings in the Superpotential are selected by appropriate field redefinitions and are chosen so that all the dimensionless couplings are real. In order to guarantee correct EWSB, m_0^2 has to be positive. To simplify our analysis we also assume that A_0 is real and $M_{1/2}$ is positive — this then naturally leads to real VEVs of the Higgs fields.

The set of parameters mentioned above should be in principle supplemented by B' and μ' . However, since μ' is not constrained by EWSB and the term $\mu' \hat{H}' \hat{H}'$ in the Superpotential (11) is not suppressed by the E_6 symmetry, the parameter μ' can be as large as 10 TeV. Therefore we assume that the scalar and fermion components of the Superfields \hat{H}' and \hat{H}' are very heavy so that they decouple from the rest of the particle spectrum. As a consequence the parameters B' and μ' , that determine the masses of the survival components of $27'$ and $\overline{27'}$, are irrelevant for our analysis.

3. EWSB and Z – Z' mixing

As described in the previous section, the Higgs sector of the model involves two Higgs doublets H_u and H_d , as well as the SM-singlet field S . The corresponding Higgs effective potential is defined by the structure of the gauge interactions and by the Superpotential (11). It can be written as,

$$\begin{aligned}
V = & \lambda^2 |S|^2 (|H_d|^2 + |H_u|^2) + \lambda^2 |(H_d H_u)|^2 + \frac{g_2^2}{8} \left(H_d^\dagger \sigma_a H_d + H_u^\dagger \sigma_a H_u \right)^2 \\
& + \frac{g'^2}{8} (|H_d|^2 - |H_u|^2)^2 + \frac{g_1'^2}{2} \left(\tilde{Q}_1 |H_d|^2 + \tilde{Q}_2 |H_u|^2 + \tilde{Q}_S |S|^2 \right)^2 \\
& + m_S^2 |S|^2 + m_1^2 |H_d|^2 + m_2^2 |H_u|^2 + \left[\lambda A_\lambda S (H_u H_d) + h.c. \right] + \Delta V, \quad (14)
\end{aligned}$$

where $g' = \sqrt{3/5}g_1$ is the low energy (non-GUT normalised) gauge coupling and \tilde{Q}_1 , \tilde{Q}_2 and \tilde{Q}_S are the effective $U(1)_N$ charges of H_d , H_u and S defined below. The first two terms in Eq. (14) correspond to F-term contributions while the subsequent three represent D-term contributions associated with $SU(2)_W$, $U(1)_Y$ and $U(1)_N$ gauge interactions. At tree-level ($\Delta V = 0$) the soft SUSY-breaking parameters in the Higgs potential are the soft masses m_1^2 , m_2^2 , m_S^2 and the trilinear coupling A_λ . Since the only complex phase (of λA_λ) that appears in the tree-level scalar potential (14) can easily be absorbed by a suitable redefinition of the Higgs fields, CP-invariance is preserved in the Higgs sector at tree-level. In the limit where the gauge coupling of the extra $U(1)_N$, g'_1 , goes to zero the structure of the tree-level scalar potential (14) is exactly the same as in the NMSSM without the self-interaction of the singlet Superfield. The term in Eq. (14) proportional to $g'_1{}^2$ represent the D-term contribution due to the extra $U(1)_N$ interaction, which is not present in the MSSM or NMSSM. The value of g'_1 at the EW scale can be determined by assuming gauge coupling unification.

The last term in Eq. (14) ΔV represents the contribution of loop corrections to the Higgs effective potential. In general the inclusion of loop effects draws into the analysis many soft SUSY-breaking couplings which define masses of different Superparticles. Some of these parameters can be complex giving rise to CP-violation. Here we take into account only the dominant contribution to ΔV that comes from loop diagrams involving the top-quark and its Superpartners. In the leading one-loop approximation we find

$$\Delta V = \frac{3}{32\pi^2} \left[m_{\tilde{t}_1}^4 \left(\ln \frac{m_{\tilde{t}_1}^2}{Q^2} - \frac{3}{2} \right) + m_{\tilde{t}_2}^4 \left(\ln \frac{m_{\tilde{t}_2}^2}{Q^2} - \frac{3}{2} \right) - 2m_t^4 \left(\ln \frac{m_t^2}{Q^2} - \frac{3}{2} \right) \right] \quad (15)$$

where m_t , $m_{\tilde{t}_1}$, $m_{\tilde{t}_2}$ are the masses of the top quark and its Superpartners. The analytical expressions for $m_{\tilde{t}_1}$ and $m_{\tilde{t}_2}$ are specified in the next section.

At the physical minimum of the scalar potential (14) the Higgs fields develop VEVs

$$\langle H_d \rangle = \frac{1}{\sqrt{2}} \begin{pmatrix} v_1 \\ 0 \end{pmatrix}, \quad \langle H_u \rangle = \frac{1}{\sqrt{2}} \begin{pmatrix} 0 \\ v_2 \end{pmatrix}, \quad \langle S \rangle = \frac{s}{\sqrt{2}}. \quad (16)$$

The equations for the extrema of the Higgs boson potential are:

$$\begin{aligned} \frac{\partial V}{\partial s} &= m_S^2 s - \frac{\lambda A_\lambda}{\sqrt{2}} v_1 v_2 + \frac{\lambda^2}{2} (v_1^2 + v_2^2) s \\ &\quad + \frac{g_1'^2}{2} \left(\tilde{Q}_1 v_1^2 + \tilde{Q}_2 v_2^2 + \tilde{Q}_S s^2 \right) \tilde{Q}_S s + \frac{\partial \Delta V}{\partial s} = 0, \end{aligned} \quad (17)$$

$$\begin{aligned} \frac{\partial V}{\partial v_1} &= m_1^2 v_1 - \frac{\lambda A_\lambda}{\sqrt{2}} s v_2 + \frac{\lambda^2}{2} (v_2^2 + s^2) v_1 + \frac{\bar{g}^2}{8} (v_1^2 - v_2^2) v_1 \\ &\quad + \frac{g_1'^2}{2} \left(\tilde{Q}_1 v_1^2 + \tilde{Q}_2 v_2^2 + \tilde{Q}_S s^2 \right) \tilde{Q}_1 v_1 + \frac{\partial \Delta V}{\partial v_1} = 0, \end{aligned} \quad (18)$$

$$\begin{aligned} \frac{\partial V}{\partial v_2} &= m_2^2 v_2 - \frac{\lambda A_\lambda}{\sqrt{2}} s v_1 + \frac{\lambda^2}{2} (v_1^2 + s^2) v_2 + \frac{\bar{g}^2}{8} (v_2^2 - v_1^2) v_2 \\ &\quad + \frac{g_1'^2}{2} \left(\tilde{Q}_1 v_1^2 + \tilde{Q}_2 v_2^2 + \tilde{Q}_S s^2 \right) \tilde{Q}_2 v_2 + \frac{\partial \Delta V}{\partial v_2} = 0, \end{aligned} \quad (19)$$

where $\bar{g} = \sqrt{g_2^2 + g'^2}$. Instead of v_1 and v_2 , it is more convenient to use $\tan \beta = v_2/v_1$ and $v = \sqrt{v_1^2 + v_2^2} = 246$ GeV.

The VEVs of the Higgs fields (16) induce masses for the gauge bosons and lead to Z - Z' mixing. In this context, note that the $U(1)_Y$ and $U(1)_N$ mix at low energies even before EWSB. Gauge symmetries do not forbid a mixing term in the gauge kinetic part of the E_6 SSM Lagrangian,

$$\mathcal{L}_{mix}^{kin} = -\frac{\sin \chi}{2} F_{\mu\nu}^Y F_{\mu\nu}^N, \quad (20)$$

where $F_{\mu\nu}^Y$ and $F_{\mu\nu}^N$ are field strengths for the $U(1)_Y$ and $U(1)_N$ gauge interactions. Since $U(1)_Y$ and $U(1)_N$ arise from the breaking of the simple gauge group E_6 , the parameter $\sin \chi$ that parametrises the gauge kinetic term mixing is expected to be equal to zero at the GUT scale. Nevertheless a small value of $\sin \chi$ is generated at low energies due to loop effects. The mixing in the gauge kinetic part of the Lagrangian (20) can be easily eliminated by means of a non-unitary transformation of the two $U(1)$ gauge fields [21], [50]–[51]:

$$B_\mu^Y = B_{1\mu} - B_{2\mu} \tan \chi, \quad B_\mu^N = B_{2\mu} / \cos \chi, \quad (21)$$

where B_μ^Y and B_μ^N are the original $U(1)_Y$ and $U(1)_N$ gauge fields. In terms of the variables $B_{1\mu}$ and $B_{2\mu}$ the gauge kinetic part of the Lagrangian is now diagonal and the covariant derivative can be written in a compact form

$$D_\mu = \partial_\mu - iQ^T G B_\mu + \dots, \quad (22)$$

where $Q^T = (Q_i^Y, Q_i^N)$, $B_\mu^T = (B_{1\mu}, B_{2\mu})$, Q_i^Y and Q_i^N are the $U(1)_Y$ and $U(1)_N$ charges and G is a 2×2 matrix of gauge couplings

$$G = \begin{pmatrix} g_1 & g_{11} \\ 0 & g_1' \end{pmatrix}. \quad (23)$$

Now all physical phenomena related to the gauge kinetic term mixing can be described by using a new modified structure of the extra $U(1)_N$ interaction with matter fields which can be concealed in the effective $U(1)_N$ charges

$$\tilde{Q}_i \equiv Q_i^N + Q_i^Y \delta, \quad (24)$$

where $\delta = g_{11}/g'_1$ while the $U(1)_Y$ charges remain the same. As the gauge coupling constants are scale dependent, the effective $U(1)_N$ charges defined here as \tilde{Q}_i are scale dependent as well.

Initially the EWSB sector involves ten degrees of freedom. However, four of them are massless Goldstone modes which are eaten by the W^\pm , Z and Z' gauge bosons. The charged W^\pm bosons gain masses via the interaction with the neutral components of the Higgs doublets in the same way as in the MSSM so that $M_W = \frac{g_2}{2}v$. In contrast, the mechanism of neutral gauge boson mass generation differs significantly. Letting Z' be the gauge boson associated with $U(1)_N$, i.e.

$$Z'_\mu = B_{2\mu}, \quad Z_\mu = W_\mu^3 \cos \theta_W - B_{1\mu} \sin \theta_W, \quad (25)$$

the $Z - Z'$ mass squared matrix is given by,

$$M_{ZZ'}^2 = \begin{pmatrix} M_Z^2 & \Delta^2 \\ \Delta^2 & M_{Z'}^2 \end{pmatrix}, \quad (26)$$

where,

$$\begin{aligned} M_Z^2 &= \frac{\bar{g}^2}{4}v^2, & \Delta^2 &= \frac{\bar{g}g'_1}{2}v^2 \left(\tilde{Q}_1 \cos^2 \beta - \tilde{Q}_2 \sin^2 \beta \right), \\ M_{Z'}^2 &= g_1'^2 v^2 \left(\tilde{Q}_1^2 \cos^2 \beta + \tilde{Q}_2^2 \sin^2 \beta \right) + g_1'^2 \tilde{Q}_S^2 s^2. \end{aligned} \quad (27)$$

The eigenvalues of this matrix are,

$$M_{Z_1, Z_2}^2 = \frac{1}{2} \left[M_Z^2 + M_{Z'}^2 \mp \sqrt{(M_Z^2 - M_{Z'}^2)^2 + 4\Delta^4} \right], \quad (28)$$

corresponding to mass eigenstates Z_1 and Z_2 given by,

$$Z_1 = Z \cos \alpha_{ZZ'} + Z' \sin \alpha_{ZZ'}, \quad Z_2 = -Z \sin \alpha_{ZZ'} + Z' \cos \alpha_{ZZ'}, \quad (29)$$

where,

$$\alpha_{ZZ'} = \frac{1}{2} \arctan \left(\frac{2\Delta^2}{M_{Z'}^2 - M_Z^2} \right). \quad (30)$$

Phenomenological constraints typically require the mixing angle $\alpha_{ZZ'}$ to be less than $2 - 3 \times 10^{-3}$ [52] and the mass of the extra neutral gauge boson to be heavier than 860 GeV [53]. A suitable mass hierarchy and mixing between Z and Z' are maintained if the field S acquires a large VEV $s \gtrsim 1.5 - 2$ TeV. Then the mass of the lightest neutral gauge boson Z_1 is very close to M_Z whereas the mass of Z_2 is set by the VEV of the singlet field $M_{Z_2} \simeq M_{Z'} \approx g_1' \tilde{Q}_S s$.

4. Particle spectrum

4.1 The squarks and sleptons

In Supersymmetric theories, each quark and lepton state with a specific chirality has a scalar Superpartner. In principle, all scalars with the same electric charge, R-parity and colour quantum numbers can mix with one another. This means that the mass eigenstates of the squarks and sleptons should be obtained by diagonalising three 6×6 squared-mass matrices for up-type squarks $(\tilde{u}_L, \tilde{c}_L, \tilde{t}_L, \tilde{u}_R, \tilde{c}_R, \tilde{t}_R)$, down-type squarks $(\tilde{d}_L, \tilde{s}_L, \tilde{b}_L, \tilde{d}_R, \tilde{s}_R, \tilde{b}_R)$ and charged leptons $(\tilde{e}_L, \tilde{\mu}_L, \tilde{\tau}_L, \tilde{e}_R, \tilde{\mu}_R, \tilde{\tau}_R)$ and one 3×3 matrix for sneutrinos $(\tilde{\nu}_e, \tilde{\nu}_\mu, \tilde{\nu}_\tau)$. However, since the first and second family quarks and leptons have negligible Yukawa couplings the mixing angles of the corresponding squark and slepton states are very small so that their masses are set by the appropriate diagonal entries. Thus one finds,

$$m_{\tilde{d}_{Li}}^2 \simeq m_{Q_i}^2 + \left(-\frac{1}{2} + \frac{1}{3} \sin^2 \theta_W \right) M_Z^2 \cos 2\beta + \Delta_Q, \quad (31)$$

$$m_{\tilde{u}_{Li}}^2 \simeq m_{Q_i}^2 + \left(\frac{1}{2} - \frac{2}{3} \sin^2 \theta_W \right) M_Z^2 \cos 2\beta + \Delta_Q, \quad (32)$$

$$m_{\tilde{u}_{Ri}}^2 \simeq m_{u_i^c}^2 + \frac{2}{3} M_Z^2 \sin^2 \theta_W \cos 2\beta + \Delta_{u^c}, \quad (33)$$

$$m_{\tilde{d}_{Ri}}^2 \simeq m_{d_i^c}^2 - \frac{1}{3} M_Z^2 \sin^2 \theta_W \cos 2\beta + \Delta_{d^c}, \quad (34)$$

$$m_{\tilde{e}_{Li}}^2 \simeq m_{L_i}^2 + \left(-\frac{1}{2} + \sin^2 \theta_W \right) M_Z^2 \cos 2\beta + \Delta_L, \quad (35)$$

$$m_{\tilde{\nu}_i}^2 \simeq m_{L_i}^2 + \frac{1}{2} M_Z^2 \cos 2\beta + \Delta_L, \quad (36)$$

$$m_{\tilde{e}_{Ri}}^2 \simeq m_{e_i^c}^2 - M_Z^2 \sin^2 \theta_W \cos 2\beta + \Delta_{e^c}. \quad (37)$$

The first terms on the right-hand side of Eqs. (31)-(37) are soft scalar masses while all other terms come from the $SU(2)_W$, $U(1)_Y$ and $U(1)_N$ D-term quartic interactions in the scalar potential (12) when the Higgs fields get VEVs. In particular,

$$\Delta_\phi = \frac{g_1'^2}{2} \left(\tilde{Q}_1 v_1^2 + \tilde{Q}_2 v_2^2 + \tilde{Q}_S s^2 \right) \tilde{Q}_\phi, \quad (38)$$

are contributions of $U(1)_N$ D-term to the masses of squarks and sleptons. As in the MSSM the D-term contributions in the E_6 SSM induce ‘‘hyperfine’’ splitting for the masses of the left-handed squarks and sleptons, i.e.

$$m_{\tilde{u}_{Li}}^2 - m_{\tilde{d}_{Li}}^2 = m_{\tilde{\nu}_i}^2 - m_{\tilde{e}_{Li}}^2 = M_W^2 \cos 2\beta. \quad (39)$$

In general the terms in Eqs. (31)-(37) which are proportional to M_Z^2 or $g_1'^2 v^2$ are typically much smaller than the soft scalar masses squared and $g_1'^2 s^2$. As a consequence the D-term

contributions to the squark and slepton masses are governed by Δ_ϕ which in the leading approximation are given by

$$\Delta_Q \simeq \Delta_{u^c} \simeq \Delta_{e^c} \simeq \frac{1}{10} M_{Z'}^2, \quad \Delta_{d^c} \simeq \Delta_L \simeq \frac{1}{5} M_{Z'}^2. \quad (40)$$

We emphasise that the extra $U(1)_N$ D-term gives positive contributions to the masses of squarks and sleptons because the $U(1)_N$ charges of the SM-singlet Superfield S and the charges of quark and lepton Supermultiplets have the same sign.

Let us now consider the masses of squarks and sleptons of the third generation. In contrast with the first two families the top quark Yukawa coupling is always large at the EW scale resulting in substantial mixing between left-handed and right-handed top squarks. This mixing is induced when Higgs fields acquire non-zero VEVs. The corresponding mixing terms originate from the trilinear scalar interactions, which arise due to the soft breakdown of global SUSY (see Eq. (13)) and F-term contribution to the scalar potential (12). Diagonalising the 2×2 top squark mass matrix it is easy to see that

$$m_{\tilde{t}_1, \tilde{t}_2}^2 = \frac{1}{2} \left\{ m_{Q_3}^2 + m_{u_3^c}^2 + \frac{1}{2} M_Z^2 \cos 2\beta + \Delta_Q + \Delta_{u^c} + 2m_t^2 \mp \sqrt{\left[m_{Q_3}^2 - m_{u_3^c}^2 + \left[\frac{1}{2} - \frac{4}{3} \sin^2 \theta_W \right] M_Z^2 \cos 2\beta + \Delta_Q - \Delta_{u^c} \right]^2 + 4m_t^2 X_t^2} \right\}, \quad (41)$$

where $X_t = A_t - \frac{\lambda_s}{\sqrt{2} \tan \beta}$ is a stop mixing parameter. The large value of X_t induces a significant mixing in the stop sector which reduces the mass of the lightest top squark so that it may become one of the lightest eigenstates in the sparticle spectrum.

With increasing $\tan \beta$, the b -quark and τ -lepton Yukawa couplings grow. At large values of $\tan \beta \gg 10$ the couplings h_b and h_τ become comparable with the top quark Yukawa coupling at the EW scale. This leads to substantial mixing between left-handed and right-handed sbottoms as well as left-handed and right-handed staus. The eigenval-

ues of the corresponding 2×2 matrices are given by

$$m_{\tilde{b}_1, \tilde{b}_2}^2 = \frac{1}{2} \left\{ m_{Q_3}^2 + m_{d_3^c}^2 - \frac{1}{2} M_Z^2 \cos 2\beta + \Delta_Q + \Delta_{d^c} \right. \\ \left. \mp \sqrt{\left[m_{Q_3}^2 - m_{d_3^c}^2 + \left[-\frac{1}{2} + \frac{2}{3} \sin^2 \theta_W \right] M_Z^2 \cos 2\beta + \Delta_Q - \Delta_{d^c} \right]^2 + 4m_b^2 X_b^2} \right\}, \quad (42)$$

$$m_{\tilde{\tau}_1, \tilde{\tau}_2}^2 = \frac{1}{2} \left\{ m_{L_3}^2 + m_{e_3^c}^2 - \frac{1}{2} M_Z^2 \cos 2\beta + \Delta_L + \Delta_{e^c} \right. \\ \left. \mp \sqrt{\left[m_{L_3}^2 - m_{e_3^c}^2 + \left[-\frac{1}{2} + 2 \sin^2 \theta_W \right] M_Z^2 \cos 2\beta + \Delta_L - \Delta_{e^c} \right]^2 + 4m_\tau^2 X_\tau^2} \right\}, \quad (43)$$

where $X_b = A_b - \frac{\lambda_s}{\sqrt{2}} \tan \beta$ and $X_\tau = A_\tau - \frac{\lambda_s}{\sqrt{2}} \tan \beta$. From Eqs. (42)-(43) one can see that the magnitude and importance of mixing in the sbottom and stau sectors depend on $\tan \beta$. If $\tan \beta$ is not too large ($\lesssim 10$) the sbottoms and staus are not strongly effected by the mixing terms because m_b and m_τ are small. In this case the mass eigenstates are very nearly the same as the gauge eigenstates $\tilde{b}_L, \tilde{b}_R, \tilde{\tau}_L$ and $\tilde{\tau}_R$. while their masses can be calculated using Eqs. (31)-(37). For larger values of $\tan \beta$, the mixing effects are non-negligible, and the lightest sbottom and stau mass eigenstates can be significantly lighter than their first and second family counterparts.

4.2 The gluino

The gluino is a colour octet fermion. Therefore, it can not mix with any other particle in SUSY models. Since the gluino is strongly interacting, its running mass M_3 changes rather quickly with the renormalisation scale Q . Consequently, for an accurate estimate of the gluino mass one should use the scale-independent mass $M_{\tilde{g}}$ at which the renormalised gluino propagator has a pole. Including one-loop corrections to the gluino propagator that arise from gluon/gluino and quark/squark loops one finds that the gluino's pole mass is given in terms of the running mass in the $\overline{\text{DR}}$ scheme by

$$M_{\tilde{g}} = M_3(Q) \left[1 - \Delta_{\tilde{g}}(Q) \right]^{-1}, \quad (44)$$

where,

$$\Delta_{\tilde{g}}(Q) = \frac{g_3^2(Q)}{16\pi^2} \left\{ 9 \ln \left(\frac{Q^2}{M_3^2} \right) + 15 - \sum_{q'} \sum_{i=1}^2 B_1(M_3, m_{q'}, m_{\tilde{q}'_i}) \right. \\ \left. - \sum_q \frac{m_q}{M_3} \sin(2\theta_q) \left[B_0(M_3, m_q, m_{\tilde{q}_1}) - B_0(M_3, m_q, m_{\tilde{q}_2}) \right] \right\}, \quad (45)$$

and,

$$B_1(p, m_1, m_2) = \frac{1}{2p^2} \left[A_0(m_2) - A_0(m_1) + (p^2 + m_1^2 - m_2^2) B_0(p, m_1, m_2) \right], \quad (46)$$

$$A_0(m) = m^2 \left[1 - \ln \frac{m^2}{Q^2} \right], \quad (47)$$

$$B_0(p, m_1, m_2) = -\ln \left(\frac{p^2}{Q^2} \right) - f_B(x_+) - f_B(x_-), \quad (48)$$

with,

$$f_B(x) = \ln(1-x) - x \ln(1-x^{-1}) - 1, \quad x_{\pm} = \frac{s \pm \sqrt{s^2 - 4p^2(m_1^2 - i\varepsilon)}}{2p^2},$$

and $s = p^2 - m_2^2 + m_1^2$. This expression for the gluino's pole mass (44) automatically incorporates the one-loop renormalisation group resummation. The first two terms in the right hand side of Eq. (45) correspond to the gluon/gluino one-loop contributions while other terms represent quark/squark one-loop corrections to the gluino mass. Indices q' and \tilde{q}' in Eq. (45) denote light quarks and their Superpartners. In the case of the light quarks we neglect the mixing between left-handed and right-handed squark states. The sum over q in the bottom line of Eq. (45) includes only heavy quarks for which mixing effects parametrised via the mixing angle θ_q can not be ignored. The corrections specified above can be as large as 20%–30% because the gluino is strongly interacting, with a large group theory factor due to its colour, and because it couples to all of the squark–quark pairs.

4.3 The charginos and neutralinos

After EWSB, all Superpartners of the gauge and Higgs bosons acquire non-zero masses. Since the Supermultiplets of the Z' boson and SM-singlet Higgs field S are electromagnetically neutral they do not contribute any extra particles to the chargino spectrum. Consequently the chargino mass matrix and its eigenvalues remain the same as in the MSSM, namely

$$m_{\chi_{1,2}^{\pm}}^2 = \frac{1}{2} \left[M_2^2 + \mu_{\text{eff}}^2 + 2M_W^2 \pm \sqrt{(M_2^2 + \mu_{\text{eff}}^2 + 2M_W^2)^2 - 4(M_2\mu_{\text{eff}} - M_W^2 \sin 2\beta)^2} \right], \quad (49)$$

where M_2 is the $SU(2)$ gaugino mass and $\mu_{\text{eff}} = \frac{\lambda_s}{\sqrt{2}}$. LEP searches for SUSY particles including data collected at \sqrt{s} between 90 GeV and 209 GeV set a 95% CL lower limit on the chargino mass of about 100 GeV [54]. This lower bound constrains the parameter space of the E_6 SUSM restricting the absolute values of the effective μ -term and M_2 from below, i.e. $|M_2|, |\mu_{\text{eff}}| \geq 90 - 100$ GeV.

In the neutralino sector there are two extra neutralinos besides the four MSSM ones. One is an extra gaugino coming from the Z' vector Supermultiplet. The other is an additional Higgsino \tilde{S} (singlino) which is a fermion component of the SM-singlet Superfield \hat{S} . The Higgsino mass terms in the Lagrangian are induced by the trilinear interaction $\lambda\hat{S}(\hat{H}_d\hat{H}_u)$ in the Superpotential (11) after the breakdown of the gauge symmetry, so that their contributions are determined by the coupling λ and VEVs of the Higgs fields. The mixing between gauginos and Higgsinos is proportional to the corresponding gauge coupling and the VEV of the Higgsino's scalar partner. Taking this into account one obtains a 6×6 neutralino mass matrix, which in the interaction basis $(\tilde{B}, \tilde{W}_3, \tilde{H}_1^0, \tilde{H}_2^0, \tilde{S}, \tilde{B}')$ is,

$$M_{\tilde{\chi}^0} = \begin{pmatrix} M_1 & 0 & -\frac{1}{2}g'v_1 & \frac{1}{2}g'v_2 & 0 & 0 \\ 0 & M_2 & \frac{1}{2}gv_1 & -\frac{1}{2}gv_2 & 0 & 0 \\ -\frac{1}{2}g'v_1 & \frac{1}{2}gv_1 & 0 & -\mu_{\text{eff}} & -\frac{\lambda v_2}{\sqrt{2}} & \tilde{Q}_1 g'_1 v_1 \\ \frac{1}{2}g'v_2 & -\frac{1}{2}gv_2 & -\mu_{\text{eff}} & 0 & -\frac{\lambda v_1}{\sqrt{2}} & \tilde{Q}_2 g'_1 v_2 \\ 0 & 0 & -\frac{\lambda v_2}{\sqrt{2}} & -\frac{\lambda v_1}{\sqrt{2}} & 0 & \tilde{Q}_S g'_1 s \\ 0 & 0 & \tilde{Q}_1 g'_1 v_1 & \tilde{Q}_2 g'_1 v_2 & \tilde{Q}_S g'_1 s & M'_1 \end{pmatrix}, \quad (50)$$

where M_1 , M_2 and M'_1 are the soft gaugino masses for \tilde{B} , \tilde{W}_3 and \tilde{B}' respectively. In Eq. (50) we neglect the Abelian gaugino mass mixing M_{11} between \tilde{B} and \tilde{B}' that arises at low energies as a result of the kinetic term mixing even if there is no mixing in the initial values of the soft SUSY-breaking gaugino masses near the GUT or Planck scale [50]. The top-left 4×4 block of the mass matrix (50) contains the neutralino mass matrix of the MSSM where the parameter μ is replaced by μ_{eff} . The lower right 2×2 submatrix represents the extra components of neutralinos. The neutralino sector in E_6 inspired SUSY models was studied recently in [23], [31]–[32], [35]–[36], [55]–[56].

As one can see from Eqs. (49)–(50) the masses of charginos and neutralinos depend on λ , s , $\tan\beta$, M_1 , M'_1 and M_2 . In SUGRA models with uniform gaugino masses at the GUT scale, the RGE flow yields a relationship between M_1 , M'_1 and M_2 at the EW scale:

$$M'_1 \simeq M_1 \simeq 0.5M_2. \quad (51)$$

Due to stringent constraints on the mass of the Z' boson, the VEV of the SM singlet field S has to be large ($s \gtrsim 2 \text{ TeV}$). This implies that $\tilde{Q}_S g'_1 s$ and μ_{eff} are much larger than other off-diagonal entries in the neutralino mass matrix (50). As a result the mass matrix (50) can be approximately diagonalised and the expressions for the chargino masses (49)

can be substantially simplified. In this case one chargino and two neutralinos are almost degenerate with mass $|\mu_{\text{eff}}|$, i.e.

$$|m_{\chi_2^\pm}| \simeq |m_{\chi_3^0}| \simeq |m_{\chi_4^0}| \simeq |\mu_{\text{eff}}|. \quad (52)$$

They are formed predominantly from the neutral and charged Superpartners of the Higgs bosons. Two other neutralinos are mixtures of the $U(1)_N$ gaugino \tilde{B}' and singlino \tilde{S} . Their masses are closely approximated by

$$|m_{\chi_{5,6}^0}| \simeq \frac{1}{2} \left[\sqrt{M_1'^2 + 4M_{Z'}^2} \mp M_1' \right]. \quad (53)$$

Since the masses of extra neutralino states are controlled by the Z' boson mass they tend to be heavy (~ 1 TeV) so that their direct observation is unlikely in the near future. The Superpartners of the $SU(2)$ gauge bosons compose another chargino and neutralino whose masses are governed by $|M_2|$. Finally, the mass of the neutralino state that is predominantly bino, \tilde{B} , is set by $|M_1|$.

4.4 The exotic particles

In addition to the NMSSM-like particle content, the E_6 SSM involves exotic matter that forms three families of down-type quark Superfields (\overline{D}_i and D_i), two generations of Inert Higgs Supermultiplets (H_α^d and H_α^u), two families of extra singlets S_α and a vector-like doublet Superfield associated with the survival components of the extra $27'$ and $\overline{27}'$ (H' and \overline{H}') which manifest themselves in the Yukawa interactions (10) as fields with lepton number $L = \pm 1$. The masses of the fermion and scalar components of this vector-like lepton Supermultiplet are set by μ' which is expected to be of the order of 10 TeV. Therefore these exotic lepton fields are normally very heavy and decouple from the rest of the particle spectrum. The masses of the fermion components of the exotic quark and Inert Higgs Supermultiplets are determined by the VEV of the SM-singlet field S and by the Yukawa couplings κ_i and λ_α . They are given by

$$\mu_{D_i} = \frac{\kappa_i}{\sqrt{2}} s, \quad \mu_{\tilde{H}_\alpha} = \frac{\lambda_\alpha}{\sqrt{2}} s, \quad (54)$$

where μ_{D_i} are exotic quark masses, while $\mu_{\tilde{H}_\alpha}$ are the masses of the Inert Higgsinos. The experiments at LEP, HERA and the Tevatron set stringent lower bounds on the masses of exotic quarks and new charged particles, so the Yukawa couplings κ_i and λ_α cannot be negligibly small.

Relatively large masses of exotic quarks give rise to a substantial mixing between the corresponding exotic squark states. Since we choose a field basis such that the Yukawa couplings of D_i and \overline{D}_i to S are flavour diagonal, the calculation of the exotic squark

masses reduces to the diagonalisation of three 2×2 matrices whose eigenvalues can be written as

$$M_{D_{i1}, D_{i2}}^2 = \frac{1}{2} \left\{ m_{D_i}^2 + m_{\bar{D}_i}^2 + 2\mu_{D_i}^2 + \Delta_D + \Delta_{\bar{D}} \right. \\ \left. \mp \sqrt{\left[m_{D_i}^2 - m_{\bar{D}_i}^2 + \frac{2}{3}M_Z^2 \cos 2\beta \sin^2 \theta_W + \Delta_D - \Delta_{\bar{D}} \right]^2 + 4\mu_{D_i}^2 X_{D_i}^2} \right\}, \quad (55)$$

where $X_{D_i} = A_{\kappa_i} - \frac{\lambda}{2\sqrt{2}s}v^2 \sin 2\beta$ and $\Delta_\phi = \frac{g_1'^2}{2}(\tilde{Q}_1 v_1^2 + \tilde{Q}_2 v_2^2 + \tilde{Q}_S s^2)\tilde{Q}_\phi$. Relatively heavy Inert Higgsinos also lead to significant mixing effects in the Inert Higgs boson sector. Once again, the flavour diagonal structure of the Yukawa couplings of H_α^d and H_α^u to the singlet field S , leads to mixing only between the Inert Higgs bosons from the same family. Diagonalising the appropriate 2×2 mass matrices one finds,

$$m_{H_{\alpha 1}^0, H_{\alpha 2}^0}^2 = \frac{1}{2} \left\{ m_{H_\alpha^d}^2 + m_{H_\alpha^u}^2 + 2\mu_{\tilde{H}_\alpha}^2 + \Delta_{H^d} + \Delta_{H^u} \right. \\ \left. \mp \sqrt{\left[m_{H_\alpha^d}^2 - m_{H_\alpha^u}^2 + M_Z^2 \cos 2\beta + \Delta_{H^d} - \Delta_{H^u} \right]^2 + 4\mu_{\tilde{H}_\alpha}^2 X_{H_\alpha}^2} \right\}, \quad (56)$$

$$m_{H_{\alpha 1}^\pm, H_{\alpha 2}^\pm}^2 = \frac{1}{2} \left\{ m_{H_\alpha^d}^2 + m_{H_\alpha^u}^2 + 2\mu_{\tilde{H}_\alpha}^2 + \Delta_{H^d} + \Delta_{H^u} \right. \\ \left. \mp \sqrt{\left[m_{H_\alpha^d}^2 - m_{H_\alpha^u}^2 - M_Z^2 \cos 2\beta \cos 2\theta_W + \Delta_{H^d} - \Delta_{H^u} \right]^2 + 4\mu_{\tilde{H}_\alpha}^2 X_{H_\alpha}^2} \right\}, \quad (57)$$

where $X_{H_\alpha} = A_{\lambda_\alpha} - \frac{\lambda}{2\sqrt{2}s}v^2 \sin 2\beta$. The magnitude of the mixing in the exotic squark and Inert Higgs sectors is governed by the mixing parameters X_{D_i} and X_{H_α} as well as by the Yukawa couplings κ_i and λ_α . As before the mixing between these scalar particles arises from the F-term contribution to the scalar potential (12) and the trilinear scalar interactions induced by the soft breakdown of SUSY. If the Yukawa couplings that determine the mixing of the exotic scalar fields are large, the mixing effects can be so substantial that the corresponding lightest exotic squarks and/or Inert Higgs bosons may be among the lightest SUSY particles in the spectrum of the E₆SSM. Additionally, when κ_i or λ_i are relatively small the appropriate exotic quarks or Inert Higgsinos may be sufficiently light that they can be discovered at the LHC.

Since we neglect the couplings $f_{\alpha\beta}$ and $\tilde{f}_{\alpha\beta}$ in the Superpotential (10), the scalar components of the SM-singlet Superfields S_α do not mix with other scalar fields. Their masses are given by

$$M_{S_\alpha}^2 = m_{S_\alpha}^2 + \Delta_S, \quad (58)$$

where $m_{S_\alpha}^2$ are soft scalar masses while Δ_S is a $U(1)_N$ D-term contribution. In the leading approximation, the $U(1)_N$ D-term contributions to the masses of the exotic scalars are set by $M_{Z'}^2$,

$$\Delta_D \simeq \Delta_{H^u} \simeq -\frac{1}{5}M_{Z'}^2, \quad \Delta_{\bar{D}} \simeq \Delta_{H^d} \simeq -\frac{3}{10}M_{Z'}^2, \quad \Delta_S \simeq \frac{1}{2}M_{Z'}^2. \quad (59)$$

We emphasise that in contrast with the ordinary squarks and sleptons, the $U(1)_N$ D-term gives negative contributions to the masses of exotic squarks and Inert Higgs bosons because the $U(1)_N$ charge of the SM-singlet Superfield S and the $U(1)_N$ charges of the exotic quarks and Inert Higgs Supermultiplets are opposite. The $U(1)_N$ D-term gives the largest contributions to the masses of the scalar components of the SM-singlet Superfields S_α , making these fields rather heavy.

4.5 The Higgs bosons

Due to electric charge conservation the charged components of the Higgs doublets do not mix with neutral Higgs fields. They form a separate sector whose spectrum is described by a 2×2 mass matrix. Its determinant has zero value leading to the appearance of two Goldstone states which are absorbed into the longitudinal degrees of freedom of the W^\pm gauge boson. Their orthogonal linear combination gains mass

$$m_{H^\pm}^2 = \frac{\sqrt{2}\lambda A_\lambda}{\sin 2\beta} s - \frac{\lambda^2}{2}v^2 + \frac{g^2}{2}v^2 + \Delta_\pm, \quad (60)$$

where Δ_\pm represents the contribution of loop corrections to the charged Higgs boson mass in the E_6 SSM.

The imaginary parts of the neutral components of the Higgs doublets and imaginary part of the SM-singlet field S compose the CP-odd Higgs sector of the model. This sector includes two Goldstone modes G_0, G' which are swallowed by the Z and Z' bosons after EWSB, leaving only one physical CP-odd Higgs state A which acquires mass

$$m_A^2 = \frac{\sqrt{2}\lambda A_\lambda}{\sin 2\varphi} v + \Delta_A, \quad \tan \varphi = \frac{v}{2s} \sin 2\beta, \quad (61)$$

where Δ_A is the contribution of loop corrections.

The CP-even Higgs sector involves $\text{Re } H_d^0, \text{Re } H_u^0$ and $\text{Re } S$. In the field space basis (h, H, N) rotated by an angle β with respect to the initial one

$$\begin{aligned} \text{Re } H_d^0 &= (h \cos \beta - H \sin \beta + v_1)/\sqrt{2}, \\ \text{Re } H_u^0 &= (h \sin \beta + H \cos \beta + v_2)/\sqrt{2}, \\ \text{Re } S &= (s + N)/\sqrt{2}, \end{aligned} \quad (62)$$

the mass matrix of the Higgs scalars takes the form [57]:

$$M^2 = \begin{pmatrix} \frac{\partial^2 V}{\partial v^2} & \frac{1}{v} \frac{\partial^2 V}{\partial v \partial \beta} & \frac{\partial^2 V}{\partial v \partial s} \\ \frac{1}{v} \frac{\partial^2 V}{\partial v \partial \beta} & \frac{1}{v^2} \frac{\partial^2 V}{\partial^2 \beta} & \frac{1}{v} \frac{\partial^2 V}{\partial s \partial \beta} \\ \frac{\partial^2 V}{\partial v \partial s} & \frac{1}{v} \frac{\partial^2 V}{\partial s \partial \beta} & \frac{\partial^2 V}{\partial^2 s} \end{pmatrix} = \begin{pmatrix} M_{11}^2 & M_{12}^2 & M_{13}^2 \\ M_{21}^2 & M_{22}^2 & M_{23}^2 \\ M_{31}^2 & M_{32}^2 & M_{33}^2 \end{pmatrix}. \quad (63)$$

Taking second derivatives of the Higgs boson effective potential and substituting m_1^2 , m_2^2 , m_S^2 from the minimisation conditions (17)–(19) one obtains,

$$\begin{aligned} M_{11}^2 &= \frac{\lambda^2}{2} v^2 \sin^2 2\beta + \frac{\bar{g}^2}{4} v^2 \cos^2 2\beta + g_1'^2 v^2 (\tilde{Q}_1 \cos^2 \beta + \tilde{Q}_2 \sin^2 \beta)^2 + \Delta_{11}, \\ M_{12}^2 &= M_{21}^2 = \left(\frac{\lambda^2}{4} - \frac{\bar{g}^2}{8} \right) v^2 \sin 4\beta \\ &\quad + \frac{g_1'^2}{2} v^2 (\tilde{Q}_2 - \tilde{Q}_1) (\tilde{Q}_1 \cos^2 \beta + \tilde{Q}_2 \sin^2 \beta) \sin 2\beta + \Delta_{12}, \\ M_{22}^2 &= \frac{\sqrt{2} \lambda A_\lambda}{\sin 2\beta} s + \left(\frac{\bar{g}^2}{4} - \frac{\lambda^2}{2} \right) v^2 \sin^2 2\beta + \frac{g_1'^2}{4} (\tilde{Q}_2 - \tilde{Q}_1)^2 v^2 \sin^2 2\beta + \Delta_{22}, \\ M_{23}^2 &= M_{32}^2 = -\frac{\lambda A_\lambda}{\sqrt{2}} v \cos 2\beta + \frac{g_1'^2}{2} (\tilde{Q}_2 - \tilde{Q}_1) \tilde{Q}_S v s \sin 2\beta + \Delta_{23}, \\ M_{13}^2 &= M_{31}^2 = -\frac{\lambda A_\lambda}{\sqrt{2}} v \sin 2\beta + \lambda^2 v s + g_1'^2 (\tilde{Q}_1 \cos^2 \beta + \tilde{Q}_2 \sin^2 \beta) \tilde{Q}_S v s + \Delta_{13}, \\ M_{33}^2 &= \frac{\lambda A_\lambda}{2\sqrt{2} s} v^2 \sin 2\beta + g_1'^2 \tilde{Q}_S^2 s^2 + \Delta_{33}. \end{aligned} \quad (64)$$

In Eqs. (64) the Δ_{ij} 's are loop corrections to the mass matrix of the CP–even Higgs bosons in the E_6 SSM. The explicit expressions for Δ_{ij} , calculated in the leading one–loop approximation, are given in Appendix A.

When the SUSY–breaking scale M_S and VEV of the singlet field are considerably larger than the EW scale, the mass matrix (63)–(64) has a hierarchical structure. Therefore the masses of the heaviest Higgs bosons are closely approximated by the diagonal entries M_{22}^2 and M_{33}^2 which are expected to be of the order of M_S^2 or even higher. All off–diagonal matrix elements are relatively small $\lesssim M_S M_Z$. As a result the mass of one CP–even Higgs boson (approximately given by H) is governed by m_A while the mass of another one (predominantly the N singlet field) is set by M_Z . Since the minimal eigenvalue of the mass matrix (63)–(64) is always less than its smallest diagonal element at least one Higgs scalar in the CP–even sector (approximately h) remains light even when the SUSY–breaking scale tends to infinity, i.e. $m_{h_1}^2 \lesssim M_{11}^2$.

5. Constructing realistic cE₆SSM scenarios

5.1 RG flow of couplings in the cE₆SSM

Below the GUT scale, the RG flow causes the gauge couplings and the soft SUSY-breaking parameters to split from the universal values g_0 , m_0^2 , $M_{1/2}$ and A_0 . This splitting is described by the RGEs of the model, presented in Appendix B. For the gauge and Yukawa couplings two-loop RGEs are given as well as two-loop RGEs for $M_a(\mu)$ and $A_i(\mu)$ and one-loop RGEs for $m_i^2(\mu)$.

This complete set of E₆SSM RGEs can be separated into two parts. The first describes the evolution of gauge and Yukawa coupling constants and is a nonlinear set of equations even in the one-loop approximation. Therefore it is extremely difficult or even impossible to find either exact or approximate solutions of these equations. The remaining subset of RGEs describes the running of fundamental parameters which break SUSY in a soft way. If the renormalisation group flow of the gauge and Yukawa couplings is known, this part of the RGEs can be considered as a set of linear differential equations for the soft SUSY-breaking terms. To solve them, first one integrates the equations for the gaugino masses M_i . In the one-loop approximation we find,

$$M_i(t) = \frac{g_i^2(t)}{g_0^2} M_{1/2}, \quad M_1'(t) = \frac{g_1'^2(t)}{g_0^2} M_{1/2}, \quad (65)$$

where the index i runs from 1 to 3 and $t = \ln \frac{Q}{M_X}$, with Q being the renormalisation scale at which Eq. (65) holds true.

Next one integrates the one-loop RGEs for the trilinear scalar couplings $A_i(t)$ which can be written as,

$$\frac{dA_i(t)}{dt} = S_{ij}(t)A_j(t) + F_i(t). \quad (66)$$

The dependence of F_i on t comes from the gaugino masses appearing in the one-loop RGE of the trilinears. One then finds the solution of this system of linear differential equations,

$$A_i(t) = \Phi_{ij}(t)A_j(0) + \Phi_{ik}(t) \int_0^t \Phi_{kj}^{-1}(t')F_j(t')dt', \quad (67)$$

where we have introduced $\Phi_{ij}(t)$, which is the solution of the homogeneous equation $d\Phi_{ij}(t)/dt = S_{ik}(t)\Phi_{kj}(t)$, with the boundary conditions $\Phi_{ij}(0) = \delta_{ij}$. From the universality constraint and exploiting Eq. (65) to write $F_i(t) \propto M_{1/2}$, the solution of the RGEs for the trilinear scalar couplings takes the form

$$A_i(t) = e_i(t)A_0 + f_i(t)M_{1/2}. \quad (68)$$

The obtained solution Eq. (68) can be substituted into the right-hand sides of the RGEs for the soft scalar masses which may be presented in the following form,

$$\frac{dm_i^2(t)}{dt} = \tilde{S}_{ij}(t)m_j^2(t) + \tilde{F}_i(t). \quad (69)$$

Due to the scalar mass universality constraints and the fact that the functions $\tilde{F}_i(t)$ contain terms which are proportional to A_0^2 , $A_0M_{1/2}$, and $M_{1/2}^2$ the solution of the linear system of differential Eq. (69) reduces to,

$$m_i^2(t) = a_i(t)m_0^2 + b_i(t)M_{1/2}^2 + c_i(t)A_0M_{1/2} + d_i(t)A_0^2. \quad (70)$$

Analytic expressions for $e_i(t)$, $f_i(t)$, $a_i(t)$, $b_i(t)$, $c_i(t)$, and $d_i(t)$, which determine the evolution of $A_i(t)$ and $m_i^2(t)$, are unknown, since an exact analytic solution of the E_6 SSM RGEs is not available.

The sensitivity of these functions to the Yukawa and gauge couplings at M_X is again very strong. In particular it is important to reiterate that the one-loop β -function for the gauge coupling of strong interactions is zero. So the running of g_3 and M_3 is dictated solely by the two-loop contributions and these two-loop β -functions can change the RG flow substantially. In this study the two-loop β -functions for the gaugino masses and trilinear couplings were included. The solution of two-loop RGEs for the $M_i(t)$ can be written as,

$$M_i(t) = p_i(t)A_0 + q_i(t)M_{1/2}. \quad (71)$$

One can see that in the two-loop approximation gaugino masses depend not only on the universal gaugino mass, $M_{1/2}$, but also on the trilinear scalar coupling, A_0 . The numerical calculations show that the dependence of $M_i(t)$ on A_0 is rather weak, i.e. $p_i(t_0) \ll 1$. However the change in the co-efficient $q_i(t)$ is substantial and at low-energies the gaugino masses change by 20–40%.

The general form of the solutions of RGEs for $m_i^2(t)$ and $A_i(t)$ remains intact after the inclusion of two-loop effects. At the same time some of the coefficient functions $f_i(t)$, $b_i(t)$ and $c_i(t)$ change significantly. The two-loop corrections to the β -functions have the strongest impact on the RG flow of the soft SUSY-breaking terms which are sensitive to strong interactions.

The RG flow of the gauge couplings, $g_i(t)$, is also quite sensitive to threshold effects. In Fig. 1 the running of $\alpha_i(t)$ is presented for two different sets of threshold scales, $T_{MSSM} = T_{ESSM} = 175$ GeV and $T_{MSSM} = 250$ GeV, $T_{ESSM} = 1500$ GeV. The threshold T_{MSSM} is a common scale for the sparticles of ordinary matter, while T_{ESSM} is a common mass scale for new exotic particles not present in the MSSM. The unified gauge coupling at M_X changes from 1.24 to 1.4 between the two threshold choices. This result and also

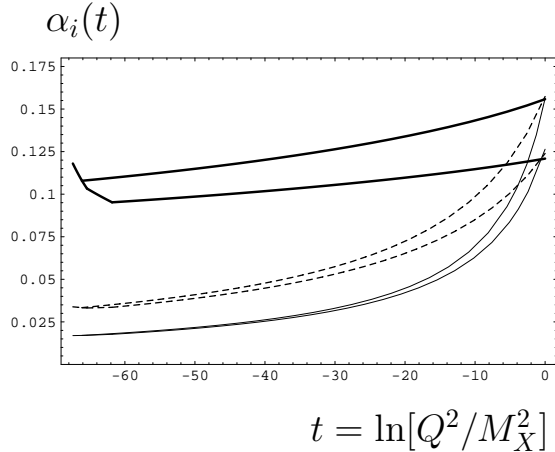


Figure 1: Two-loop RG flow of gauge couplings within the E_6 SSM for $T_{MSSM} = T_{ESSM} = M_t = 175$ GeV (upper lines) and $T_{MSSM} = 250$ GeV, $T_{ESSM} = 1500$ GeV (lower lines). Here we fix $\tan \beta = 10$ and $\alpha_3(M_Z) = 0.118$.

T_{MSSM} (GeV)	250	250	250	175	175	175
T_{ESSM} (GeV)	1500	800	250	1500	250	175
g_0^2	1.54	1.60	1.78	1.61	1.88	1.96
M_X (GeV)	$3.5 \cdot 10^{16}$	$3.3 \cdot 10^{16}$	$3.5 \cdot 10^{16}$	$3.7 \cdot 10^{16}$	$4 \cdot 10^{16}$	$4 \cdot 10^{16}$

Table 1: The dependence of g_0^2 and M_X on the threshold effects in the exceptional SUSY model. Here we fix $\tan \beta = 10$ and $\alpha_3(M_Z) = 0.118$.

the value of g_0^2 for several other threshold choices, T_{MSSM} and T_{ESSM} , are summarised in Tab. 1. Since soft SUSY-breaking terms depend very strongly on the values of the gauge couplings at the GUT scale, the uncertainty related to the choice of the threshold scales limits the accuracy of our calculations of the particle spectrum. The results of our numerical analysis presented in Tab. 1 and Fig. 1 indicate that it is unrealistic to expect an accuracy, in the calculation of the sparticle masses, better than 10%.

In our analysis thresholds are used only in the SUSY preserving sector where full two-loop RGE are employed and are neglected in the soft SUSY-breaking sector where only one-loop RGE are used for the scalar masses. The thresholds are chosen before the spectrum is determined and are therefore only an estimate. A more accurate analysis is left for a further study. We chose $T_{MSSM} = 600$ GeV and $T_{ESSM} = 3$ TeV to be the mass scale of the unobserved particles of the MSSM and the new exotic objects in the E_6 SSM respectively, based on preliminary studies where relatively heavy spectra were observed.

5.2 Procedure of our analysis

To calculate the particle spectrum within the eE_6 SSM one must find masses and couplings which are consistent with both the high scale universality constraints and the low scale EWSB constraints. To evolve between these two scales we use two-loop renormalisation group equations (RGEs), presented in Appendix B, in a modified version of SOFTSUSY

2.0.5 [58]. The details of the procedure we followed are summarized below.

1. The gauge and Yukawa couplings are determined independently of the soft SUSY breaking mass parameters as follows:

(i) We select values for $s = \sqrt{2}\langle S \rangle$ and $\tan \beta = v_2/v_1$.

(ii) We set the gauge couplings g_1 , g_2 and g_3 equal to the experimentally measured values at M_Z .

(iii) We fix the low energy Yukawa couplings h_t , h_b , and h_τ using the relations between the running masses of the fermions of the third generation and VEVs of the Higgs fields, i.e.

$$m_t(M_t) = \frac{h_t(M_t)v}{\sqrt{2}} \sin \beta, \quad m_b(M_t) = \frac{h_b(M_t)v}{\sqrt{2}} \cos \beta, \quad m_\tau(M_t) = \frac{h_\tau(M_t)v}{\sqrt{2}} \cos \beta. \quad (72)$$

(iv) The gauge and Yukawa couplings are then evolved up to the GUT scale M_X . Using the beta functions for QED and QCD, the gauge couplings are evolved up to m_t . Between m_t and T_{MSSM} we evolve the gauge and Yukawa couplings with SM RGEs and between T_{MSSM} and T_{ESSM} we employ the MSSM RGEs. At T_{ESSM} the values of E₆SSM gauge and Yukawa couplings, g_1 , g_2 , g_3 , h_t , h_b and h_τ , form a low energy boundary condition for what follows. Initial low energy estimates of the new E₆SSM Yukawa couplings, λ_i and κ_i are also input here, and all SUSY preserving couplings are evolved up to the unification scale using the two-loop E₆SSM RGEs.

(v) At the unification scale M_X we set $g'_1 = g_0$ and select values for $\kappa_i(M_X)$ and $\lambda_i(M_X)$, which are input parameters in our procedure. An iteration is then performed between M_X and the low energy scale to obtain the values of all the gauge and Yukawa couplings which are consistent with our input values for $\kappa_i(M_X)$, $\lambda_i(M_X)$, gauge coupling unification and our low scale boundary conditions, derived from experimental data.

2. Now that the values of the gauge and Yukawa couplings have been obtained, the coefficients $e_i(t)$, $f_i(t)$, $a_i(t)$, $b_i(t)$, $c_i(t)$, $d_i(t)$, $p_i(t)$ and $q_i(t)$, appearing in Eq. (68), Eq. (70) and Eq. (71), can be obtained for $t = \ln[T_{ESSM}/M_X^2]$. Low energy soft mass parameters are then functions of the GUT scale values of A_0 , $M_{1/2}$ and m_0 . These coefficients are determined numerically as follows:

(i) Set A_0 and $M_{1/2}$ to zero at M_X while giving m_0 a non-zero value and run the full set of E₆SSM parameters down to the low scale to yield the coefficients proportional to $a_i(t)$ in the expressions for each low energy scalar (mass)², m_i^2 .

(ii) Repeat for A_0 and $M_{1/2}$ to obtain coefficients $b_i(t)$ and $d_i(t)$ for each m_i^2 ; coefficients $e_i(t)$ and $f_i(t)$ for each low energy trilinear soft mass A_i and coefficients $p_i(t)$ and $q_i(t)$ for each low energy gaugino soft mass M_i .

(iii) The coefficients, $c_i(t)$, of the $A_0 M_{1/2}$ terms appearing in the semi-analytic expressions for each m_i^2 are then determined using non-zero values of both A_0 and $M_{1/2}$ at M_X ,

using the results in part (ii) to isolate this term.

3. The semi-analytic expressions for the soft masses from step 2 above provide the set of low energy constraints on the soft masses coming from our cE₆SSM universality conditions. These are then combined with the conditions for correct EWSB, appearing in Eqs. (17)-(19), at low energy and determine sets of m_0 , $M_{1/2}$ and A_0 which are consistent with EWSB, as follows:

(i) Working with the tree-level potential V_0 (to start with) we impose the minimisation conditions $\frac{\partial V_0}{\partial s} = \frac{\partial V_0}{\partial v_1} = \frac{\partial V_0}{\partial v_2} = 0$. In the tree-level approximation each of the EWSB conditions are quadratic functions of $\lambda_3(\mu)$, where μ is the energy scale at which the EWSB conditions are imposed. Using the semi-analytic approach described above to replace the third generation soft Higgs and Singlet masses and A_{λ_3} reveals that each EWSB condition also has quadratic dependence on the soft unification scale parameters m_0 , $M_{1/2}$ and A_0 . With three constraints and three soft mass parameters, the equations can be reduced to two second order equations with respect to A_0 and $M_{1/2}$, or equivalently one quartic equation with respect to A_0 . This equation is solved numerically, and the resulting value for A_0 is used to obtain $M_{1/2}$ and m_0 . For fixed values of gauge couplings, Yukawas and VEVs (determined from choices of $\tan\beta$ and s with v known from experiment) there are four sets of soft masses A_0 , $M_{1/2}$ and m_0 , though some or all can in principle be complex. Here we restrict our consideration to the scenarios with real values of fundamental parameters which do not induce any CP-violating effects. Therefore our routine deals with between 0 and 4 sets of real solutions to the soft masses.

(ii) For each solution m_0 , $M_{1/2}$ and A_0 the low energy stop soft mass parameters are determined and the one-loop Coleman-Weinberg Higgs effective potential V_1 is calculated. The new minimisation conditions for V_1 are then imposed, and new solutions for m_0 , $M_{1/2}$ and A_0 are obtained.

(iii) The procedure in (ii) is then iterated until we find stable solutions. For some values of $\tan\beta$, s and Yukawa couplings the solutions with real A_0 , $M_{1/2}$ and m_0 do not exist. There is a substantial part of the parameter space where there are only two solutions with real values of fundamental parameters. However, there are also some regions of the parameters where all four solutions of the non-linear algebraic equations are real.

Although correct EWSB is not guaranteed in the cE₆SSM, remarkably, there are always solutions with real A_0 , $M_{1/2}$ and m_0 for sufficiently large values of κ_i , which drive $m_{\mathcal{S}}^2$ negative. This is easy to understand since the κ_i couple the singlet to a large multiplicity of coloured fields, thereby efficiently driving its squared mass negative to trigger the breakdown of the gauge symmetry.

4. Using the obtained solutions we calculate the masses of all exotic and SUSY particles, using expressions given in section 4., for each set of fundamental parameters.

Finally, at the last stage of our analysis we vary Yukawa couplings, $\tan\beta$ and s to establish the qualitative pattern of the particle spectrum within the cE₆SSM. To avoid any conflict with present and former collider experiments as well as with recent cosmological observations we impose the set of constraints specified in the next section. We then demonstrate how these bounds restrict the allowed range of the parameter space in the cE₆SSM by performing scans over our input parameters.

5.3 Experimental and Theoretical Constraints

The experimental constraints applied in our analysis are: $m_h \geq 114$ GeV, all sleptons and charginos are heavier than 100 GeV, all squarks and gluinos have masses above 300 GeV and the Z' boson has a mass which is larger than 860 GeV [53]. We also impose the most conservative bound on the masses of exotic quarks and squarks that comes from the HERA experiments [59], by requiring that they are heavier than 300 GeV. Finally, we require that the Inert Higgs and Inert Higgsinos are heavier than 100 GeV to evade limits from LEP.

In addition to setting bounds from the non-observation of new particles in experiment, we impose some theoretical constraints. We require that the Lightest Supersymmetric Particle (LSP) should be a neutralino. We also restrict our consideration to the values of the Yukawa couplings $\lambda_i(M_X)$, $\kappa_i(M_X)$, $h_t(M_X)$, $h_b(M_X)$ and $h_\tau(M_X)$ less than 3 to ensure the applicability of perturbation theory up to the GUT scale.

In our exploration of the cE₆SSM parameter space we looked at scenarios with a universal coupling between exotic coloured Superfields and the third generation singlet field \hat{S} , $\kappa_{1,2,3}(M_X) = \kappa(M_X)$ and fixed the Inert Higgs couplings $\lambda_{1,2}(M_X) = 0.1$. In fixing $\lambda_{1,2}$ like this we are deliberately pre-selecting for relatively light Inert Higgsinos. The third generation Yukawa $\lambda = \lambda_3$ was allowed to vary along with κ . Splitting λ_3 from $\lambda_{1,2}$ seems reasonable since λ_3 plays a very special role in E₆SSM models in forming the effective μ -term when S develops a VEV.

The first results we found were for a very large singlet VEV, $s \approx 10 - 20$ TeV, and this leads to a very heavy particle spectrum where many of the new particles would be out of reach of current collider experiments. This can be seen in Fig. 2 where the dependencies of the soft mass parameters m_0 , $M_{1/2}$ and A_0 on λ for $s = 20$ TeV and a particular value of $\kappa = 0.25$ are plotted. One can see that for each value of λ there are two different values of each soft mass. This is because we find that for these points, of the four solutions to our quartic equation, two are complex, leaving only the two real solutions appearing in the plots. We find the existence of two real solutions and two complex solutions to be typical for the parameter space we have examined.

Notice also that the solutions presented above possess a certain symmetry. This is be-

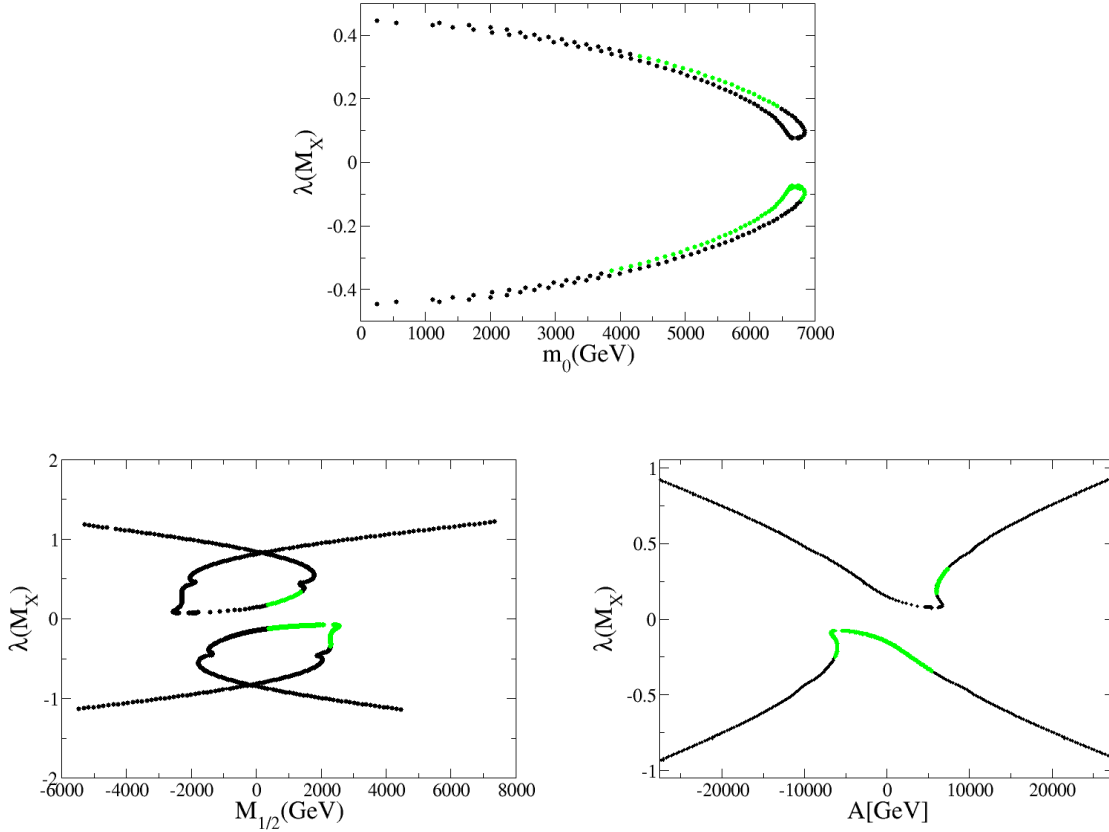


Figure 2: cE₆SSM solutions with $\tan\beta = 10$, $s = 20$ TeV and $\kappa_{1,2,3} = 0.25$, $\lambda_{1,2} = 0.1$ fixed showing the relationship between λ and m_0 (top), $M_{1/2}$ (bottom left) and A (bottom right). Points in green (light gray) satisfy all experimental constraints from LEP and Tevatron data, while points in black are ruled out.

cause there is an invariance under the transformation $A_0 \rightarrow -A_0$, $M_{1/2} \rightarrow -M_{1/2}$, $\lambda \rightarrow -\lambda$. However, we exploit this symmetry to adopt a convention whereby $M_{1/2} \geq 0$ is fixed, and therefore are only admitting physical solutions with $M_{1/2} \geq 0$, with the result that this symmetry is not apparent for our valid solutions shown in green (light gray).

After further study, we also discovered solutions that are allowed by all experimental constraints and have a significantly lighter s for a smaller range of λ_3 and our universal κ . This is illustrated in Fig. 3 where the soft mass dependencies on λ for $s = 5$ TeV and $\kappa = 0.25$ (which is within this narrow range allowing s to be relatively light). Since many particles in the cE₆SSM have their masses set by the singlet VEV it is of clear phenomenological interest to study the parameter space with low values of s .

To further explore this interesting region of the cE₆SSM parameter space, for different fixed values of $\tan\beta = 3, 10, 30$, we scan over s , κ_i and λ . From these input parameters, the sets of soft mass parameters, A_0 , $M_{1/2}$ and m_0 which are consistent with the correct

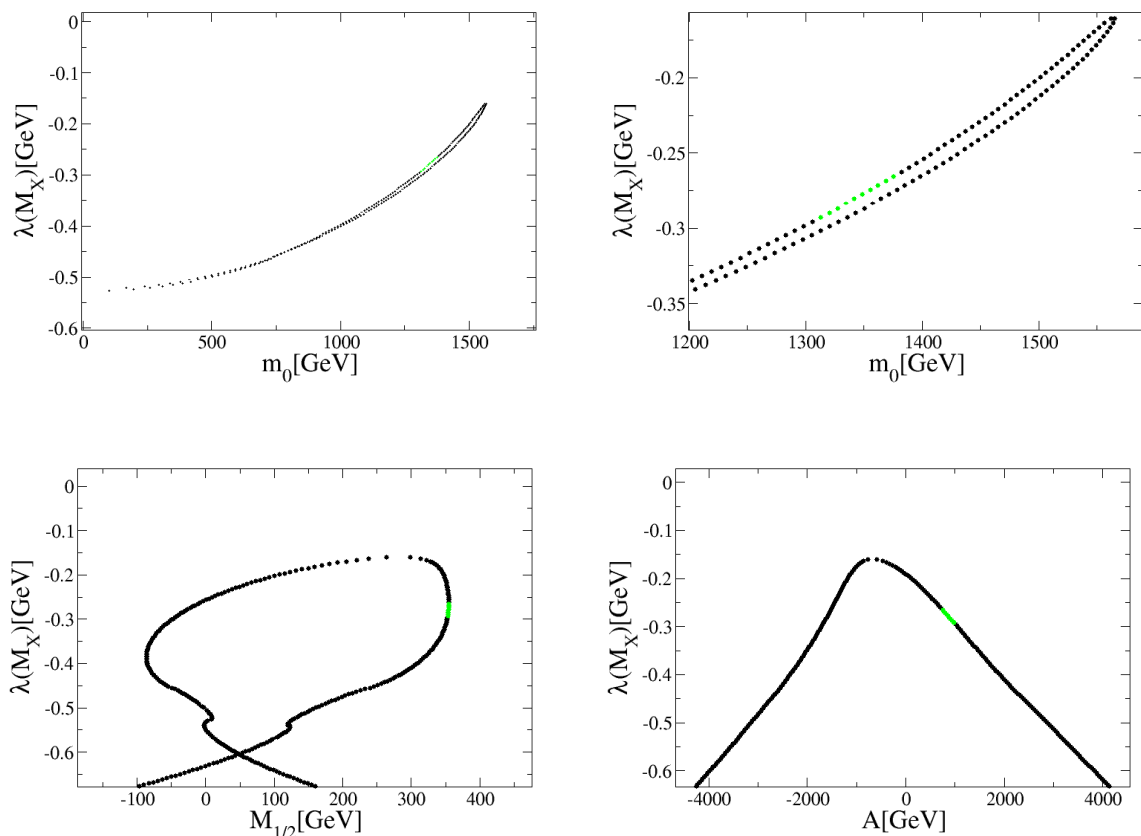


Figure 3: cE₆SSM solutions with $\tan\beta = 10$, $s = 5$ TeV and $\kappa_{1,2,3} = 0.25$, $\lambda_{1,2} = 0.1$ fixed showing the relationship between λ and m_0 (top left and magnified top right) $M_{1/2}$ (bottom left) and A (bottom right). Points in green (light gray) satisfy all experimental constraints from LEP and Tevatron data, while points in black are ruled out.

breakdown of the EW symmetry are found.

We find that for fixed values of the Yukawas the soft mass parameters scale with s , while if s and $\tan\beta$ are fixed, varying the Yukawas, λ and κ_i then produces a bounded region of allowed points.

The value of s determines the location and extent of the bounded regions. As s is increased the lowest values m_0 and $M_{1/2}$, consistent with experimental searches and EWSB requirements, increase. This is shown in Fig. 4 where the allowed regions for three different values of the singlet VEV, $s = 3$ TeV, 4 TeV and 5 TeV, are compared, with the allowed regions in red (dark grey), green (light grey), magenta (medium grey) respectively and the excluded regions in white. Note that these regions overlap since we are finding soft masses consistent with EWSB conditions that have a non-linear dependence on the VEVs and Yukawas.

Further scanning over s , leaving only $\tan\beta$ fixed, we find a lower limit on the ratio

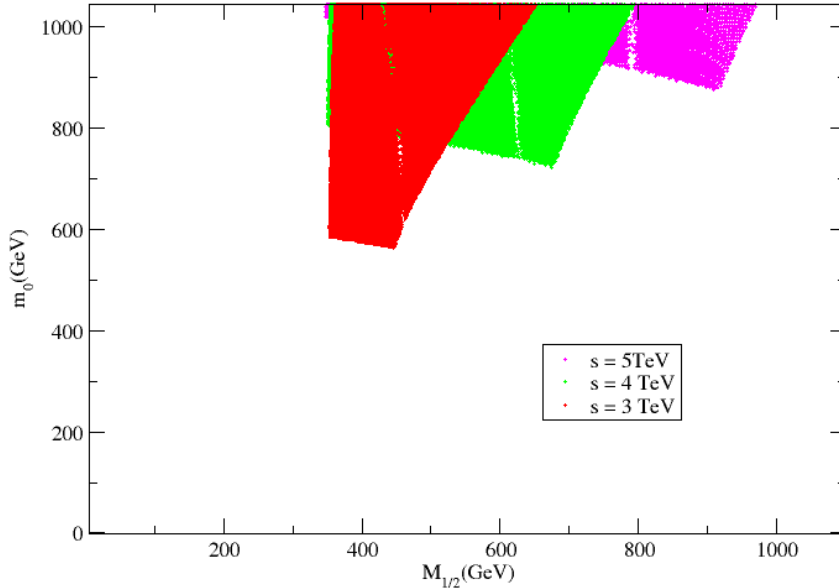


Figure 4: Physical solutions with $\tan \beta = 10$, $\lambda_{1,2} = 0.1$, $s = \{3, 4, 5\}$ TeV fixed and $\lambda \equiv \lambda_3$ and $\kappa \equiv \kappa_{1,2,3}$ varying, which pass experimental constraints from LEP and Tevatron data. On the left hand side of each allowed region the chargino mass is less than 100 GeV, while underneath the Inert Higgses are less than 100 GeV or becoming tachyonic. The region ruled out immediately to the right of the allowed points is due to $m_h < 114$ GeV.

$m_0/M_{1/2}$ which is a weak function of the singlet VEV s . For example, consider Fig. 5 (top, left). The region to the left of the allowed space is ruled out by the lightest chargino mass, $m_{\chi_{\pm 1}^{\pm}} < 100$ GeV, while the lower right region is ruled out by Inert Higgs bosons with masses below experimental bounds or tachyonic. This boundary implies that for $\tan \beta = 10$, over the allowed ranges shown, $m_0/M_{1/2}$ varies from ≈ 1.4 to ≈ 0.8 .

This boundary can be understood as follows. For fixed m_0 , maximizing $M_{1/2}$ requires the singlet VEV s to be increased, as well as varying the Yukawas, λ and κ . However, the squared masses of the Inert Higgs bosons receive a positive contribution from m_0^2 and a negative contribution from the auxiliary D-term which varies with s^2 (see Eqs. (56) and (57)). Due to this D-term contribution the mass of the lightest Inert Higgs boson decreases with s and at some point falls below experimental limits, bounding $M_{1/2}$ from above. The larger m_0 is, the larger the negative contribution must be in order to drive the Inert Higgs mass below its lower limit. Further, if one assumes that $m_0 \sim s$ and $A_\lambda \sim M_{1/2}$ then EWSB conditions imply $s \sim M_{1/2} \tan \beta$. This suggests not only the observed limit on $m_0/M_{1/2}$ but also that it will be more severe for large $\tan \beta$ and shallower for low $\tan \beta$.

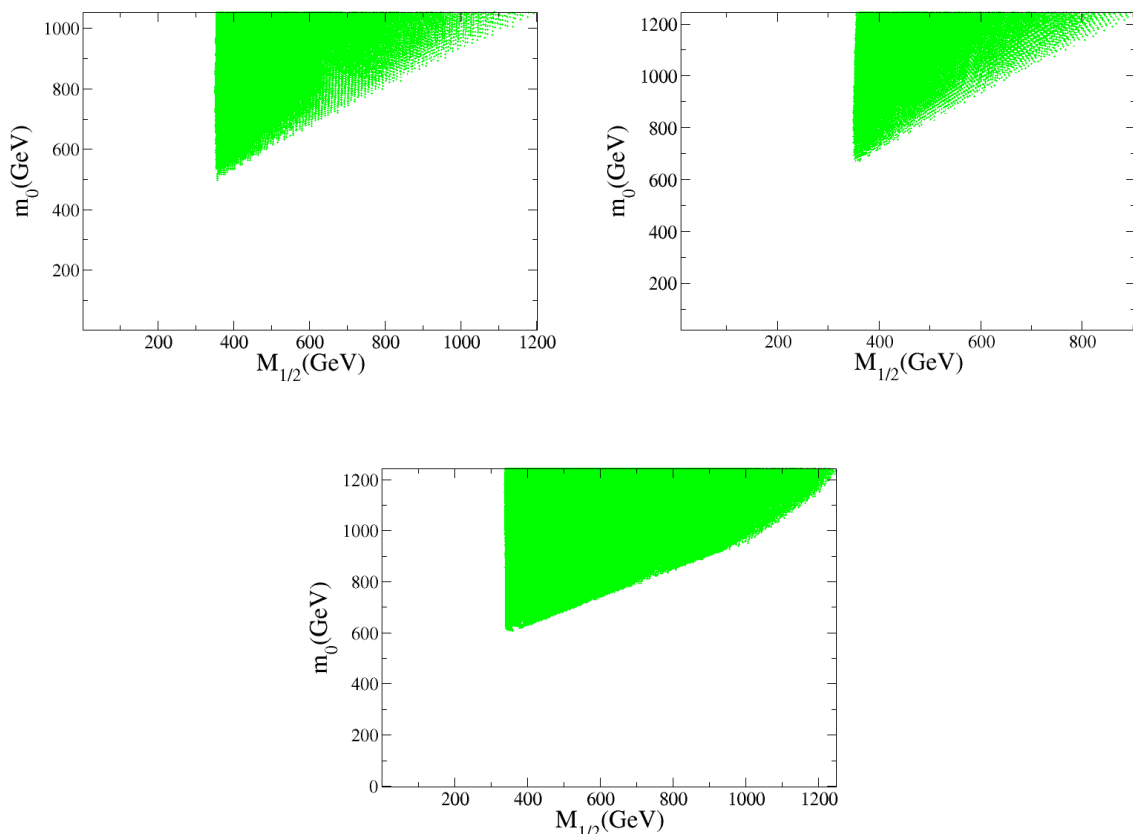


Figure 5: Physical solutions $\tan\beta = 10$ (top, left), $\tan\beta = 30$ (top, right) and $\tan\beta = 3$ (bottom) with $\lambda_{1,2} = 0.1$, fixed and $\lambda \equiv \lambda_3$ and $\kappa \equiv \kappa_{1,2,3}$ and s all varying, which pass experimental constraints from LEP and Tevatron data.

The allowed region for $\tan\beta = 30$ in Fig. 5 (top, right) has a similar shape but in this case $m_0/M_{1/2}$ varies from ≈ 1.9 to ≈ 1.4 , so for this larger $\tan\beta = 30$ the limit on ratio $m_0/M_{1/2}$ is enhanced. For $\tan\beta = 3$ in Fig. 5 (bottom) the situation is somewhat different. The region to the left of the allowed parameter space is still ruled out by experimental limits on the chargino mass. However the lower-right region is ruled out, not by the Inert Higgs masses, but by a light Higgs which is lower than the LEP limit. This change has two underlying reasons. Firstly the Inert Higgs bosons obtain positive contributions to their masses from m_0 (with a coefficient of ≈ 1) and $M_{1/2}$, while, due to the auxiliary D-term contribution, the Inert Higgs masses decrease with s . Since decreasing $\tan\beta$ reduces the hierarchy between s and $M_{1/2}$, this negative contribution to the mass of the Inert Higgs is smaller and does not decrease their mass as rapidly when m_0 is reduced. Secondly we observe that the lightest Higgs mass reduces with $\tan\beta$ as in the MSSM. At $\tan\beta = 3$ the maximal value of the mass of the lightest Higgs boson is rather close to the LEP bound. As a result the variations of parameters can result in the increase of the mixing in the

CP-even Higgs sector, which provides a negative contribution to the lightest Higgs boson mass, so that it becomes lower than the LEP limit of 114 GeV.

5.4 Benchmark Scenarios

A remarkable feature of the cE₆SSM is that the low energy gluino mass parameter M_3 is driven to be smaller than $M_{1/2}$ by RG running. The reason for this is that the E₆SSM has a much larger (super)field content than the MSSM (three 27's instead of three 16's) so much so that at one-loop order the QCD beta function (accidentally) vanishes in the E₆SSM, and at two loops it loses asymptotic freedom (though the gauge couplings remain perturbative at high energy). This implies that the low energy gaugino masses are all less than $M_{1/2}$ in the cE₆SSM, being given as roughly $M_3 \sim 0.7M_{1/2}$, $M_2 \sim 0.25M_{1/2}$, $M_1 \sim 0.15M_{1/2}$. These should be compared to the corresponding low energy values in the MSSM, $M_3 \sim 2.7M_{1/2}$, $M_2 \sim 0.8M_{1/2}$, $M_1 \sim 0.4M_{1/2}$.

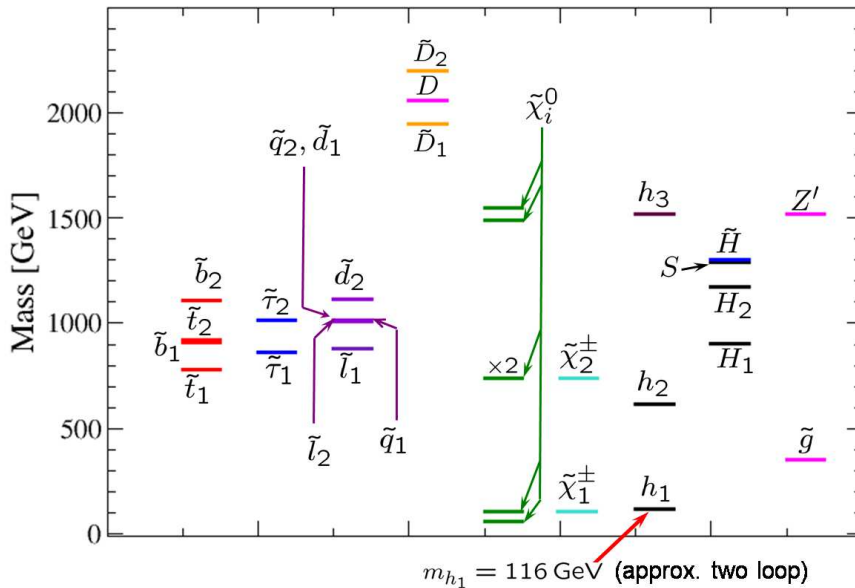


Figure 6: The particle mass spectra for cE₆SSM Benchmark Point 1, with $\tan\beta = 10$, $s = 4.0$ TeV, $M_{1/2} = 389$ GeV, $m_0 = 725$ GeV, $A = -1528$ GeV, $\lambda_{1,2}(M_X) = 2.6$, $\lambda_3(M_X) = -2.0$, $\lambda_3(\mu_S) = -0.259$, $\kappa_{1,2,3} = 2.5$, $\kappa_3(\mu_S) = 0.728$.

Thus, in the cE₆SSM, since the low energy gaugino masses M_i are driven by RG running to be small, the lightest SUSY states will generally consist of a light gluino of mass $\sim M_3$, a light wino-like neutralino and chargino pair of mass $\sim M_2$, and a light bino-like neutralino of mass $\sim M_1$, which are typically all much lighter than the Higgsino masses of order $\mu = \lambda s/\sqrt{2}$, where λ cannot be too small for correct EWSB.

The remaining neutralinos are mainly a superposition of the $U(1)_N$ gaugino and singlet Higgsino. Their masses are governed by $M_{Z'}$. The mass of the Z' is set by the singlet VEV, i.e. $M_{Z'} \approx g'_1 Q_{SS}$ ($g'_1 \approx g_1$) and therefore is also much heavier than gluino, lightest neutralino and chargino. The heaviest CP-even Higgs state is degenerate with the Z' while another CP-even Higgs, CP-odd and charged Higgs bosons have almost the same masses which are relatively close to the masses of charged and neutral Higgsinos. Since m_0 tends to be larger than $M_{1/2}$ for each value of s (as may be seen in Fig. 4) the Superpartners of ordinary quarks and leptons are considerably heavier than the light gauginos as well. This is a general prediction of the cE₆SSM. Moreover as follows from benchmark 1 (Fig. 6) all extra exotic particles in the cE₆SSM can be also relatively heavy so that the light sector of the sparticle spectrum includes only gluino, two light neutralinos and light chargino. Nonetheless, even the pessimistic scenario described by benchmark 1 leads to the striking collider signature. Indeed, because gluino, two light neutralinos and light chargino have relatively small masses in the considered case the pair production of $\chi_2^0 \chi_2^0$, $\chi_2^0 \chi_1^\pm$, $\chi_1^\pm \chi_1^\mp$ and $\tilde{g}\tilde{g}$ should be possible at the LHC.

With increasing VEV of the SM-singlet field the structure of the particle spectrum becomes more hierarchical. Due to the hierarchical spectrum the gluinos can be relatively narrow states because $\Gamma_{\tilde{g}} \propto M_{\tilde{g}}^5/m_{\tilde{q}}^4$. In particular their width can be comparable to that of W^\pm and Z bosons. They will decay through $\tilde{g} \rightarrow q\tilde{q}^* \rightarrow q\bar{q} + E_T^{\text{miss}}$, so gluino pair production will result in an appreciable enhancement of the cross section for $pp \rightarrow q\bar{q}q\bar{q} + E_T^{\text{miss}} + X$, where X refers, hereafter, to any number of light quark/gluon jets. The second lightest neutralino decays through $\chi_2^0 \rightarrow \chi_1^0 + \bar{l}l$ and so would produce an excess in $pp \rightarrow \bar{l}ll + E_T^{\text{miss}} + X$, which could be observed at the LHC.

Notice however that, while these are general predictions of the model, it is also possible that more exciting signatures could originate in the cE₆SSM. For example, when the Yukawa couplings κ_i of the exotic fermions D_i and \bar{D}_i have a hierarchical structure, some of them can be relatively light so that their production cross section at the LHC can be comparable with the cross section of $t\bar{t}$ production [33]. In the E₆SSM the D_i and \bar{D}_i fermions are SUSY particles with negative R -parity so they must be pair produced and decay into quark-squark (if diquarks) or quark-slepton, squark-lepton (if leptoquarks). Assuming that D_i and \bar{D}_i fermions couple most strongly to the third family (s)quarks and (s)leptons the presence of light exotic quarks in the particle spectrum can lead to a substantial enhancement of the cross section of either $pp \rightarrow t\bar{t}b\bar{b} + E_T^{\text{miss}} + X$ if exotic quarks are diquarks or $pp \rightarrow t\bar{t}\tau\bar{\tau} + E_T^{\text{miss}} + X$ and $pp \rightarrow b\bar{b} + E_T^{\text{miss}} + X$ if new quark states are leptoquarks. The scenarios with light exotic quarks, light stop and a TeV scale Z' , which have early discovery potential at the LHC, are considered in our companion paper [37].

In this work we concentrate on the various scenarios with universal κ couplings which have distinctive phenomenology and could provide interesting novel signatures at the LHC. In Tab. 2 we specify a set of benchmark points, which demonstrate different patterns of the particle spectrum that can be obtained in the considered case. The first block of Tab. 2 shows the input parameters which define the benchmark points. These benchmarks cover three different values of $\tan\beta = 3, 10, 30$. We deliberately restricted ourselves here to $s = 3.4 - 5.5$ TeV and $(m_0, M_{1/2}) < (1100, 950)$ GeV in order to get a relatively light particle spectrum that can be observed at the LHC. Since we focus on the solutions with $s = 3.4 - 5.5$ TeV, the allowed range of the cE₆SSM parameter space remains rather narrow and the lightest Higgs boson mass is always relatively close to the LEP limit of 114 GeV. Because we have taken the κ_i to be universal at the GUT scale these couplings have to be large enough to trigger EWSB. Since the κ_i 's control the exotic coloured fermion masses, this implies that all the D_i and \bar{D}_i fermions are all very heavy in the considered cases. For benchmarks presented in Tab. 2 the exotic coloured fermions have masses in the range 1.2 – 2.2 TeV.

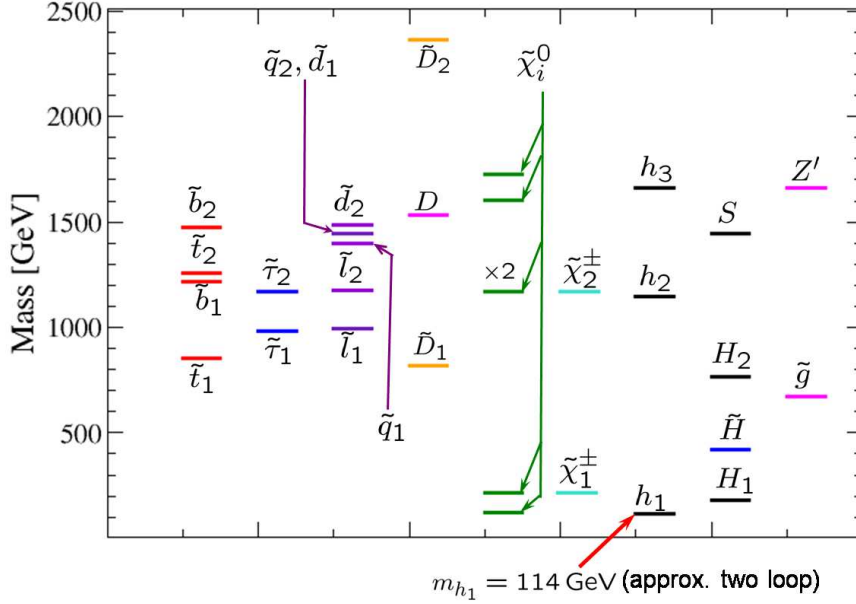


Figure 7: Benchmark point 2, with $\tan\beta = 10$, $s = 4.4$ TeV, $M_{1/2} = 775$ GeV, $m_0 = 799$ GeV, $A = 919$ GeV, $\lambda(M_X) = -0.3698$, $\lambda(\mu_S) = -0.3736$, $\lambda_{1,2}(M_X) = 0.1$, $\kappa_{1,2,3}(M_X) = 0.1780$, $\kappa_{1,2,3}(\mu_S) = 0.4935$.

In all of the scans carried out in the previous section and for the most of benchmark scenarios we have chosen $\lambda_{1,2}(M_X) = 0.1$ so that $|\lambda_3(M_X)| \gg \lambda_{1,2}(M_X)$. Low values of $\lambda_{1,2}(M_X)$ result in relatively light Inert Higgsinos (see benchmarks 2–6) because their masses are proportional to the corresponding couplings. For benchmarks 2–6 the Inert

Higgsinos are much lighter than squarks, sleptons and the exotic coloured fermions and have masses below 400 – 500 GeV. In contrast, the Inert Higgs bosons can be light or heavy depending on the free parameters.

Benchmark 2 (shown in Fig. 7) is a scenario with very light Inert Higgs bosons ($m_{H_{\alpha 1}} = 182$ GeV) and fairly light Inert Higgsinos ($\mu_{\tilde{H}} = 418$ GeV). The presence of light Inert Higgs bosons in the particle spectrum is caused by the large mixing effects in the Inert Higgs sector. The negative contributions from the $U(1)_N$ D-term to the diagonal entries of the Inert Higgs mass matrices also reduce masses of the corresponding mass eigenstates. The light Inert Higgs bosons decay via the Z_2^H violating terms $h_{i\alpha k}^N \hat{N}_i^c \hat{H}_\alpha^u \hat{L}_k$, $h_{i\alpha k}^U \hat{u}_i^c \hat{H}_\alpha^u \hat{Q}_k$, $h_{i\alpha k}^D \hat{d}_i^c \hat{H}_\alpha^d \hat{Q}_k$ and $h_{i\alpha k}^E \hat{e}_i^c \hat{H}_\alpha^d \hat{L}_k$, where the Inert Higgs Superfields are $SU(2)$ doublets with $\hat{H}_\alpha^d = (\hat{H}_\alpha^{d0}, \hat{H}_\alpha^{d-})$ and $\hat{H}_\alpha^u = (\hat{H}_\alpha^{u+}, \hat{H}_\alpha^{u0})$. These interactions are analogous to the Yukawa interactions of the Higgs Superfields, \hat{H}_u and \hat{H}_d . So the neutral Inert Higgs bosons decay predominantly into third generation fermion–anti-fermion pairs, like $H_{\alpha 1}^0 \rightarrow b\bar{b}$. The charged Inert Higgs bosons decays are also into fermion–anti-fermion pairs, but in this case it is the antiparticle of the fermions’ EW partner e.g. $H_{\alpha 1}^- \rightarrow \tau\bar{\nu}_\tau$.

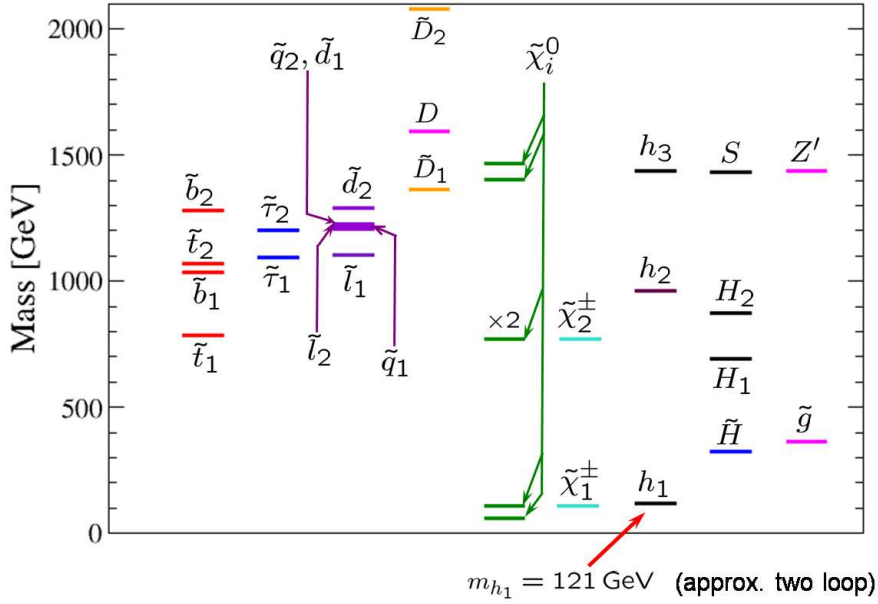


Figure 8: Benchmark point 3, with $\tan\beta = 10$, $s = 3.8$ TeV, $M_{1/2} = 390$ GeV, $m_0 = 998$ GeV, $A = 768$ GeV, $\lambda(M_X) = -0.3066$, $\lambda(\mu_S) = -0.2845$, $\lambda_{1,2}(M_X) = 0.1$, $\kappa_{1,2,3}(M_X) = 0.2463$, $\kappa_{1,2,3}(\mu_S) = 0.5935$.

The Inert Higgs bosons may also be quite heavy, so that the only light exotic particles are the Inert Higgsinos. Benchmark 3 (Fig. 8) is an example of this, emphasising the need to search for both the Inert Higgsinos as well as the Inert Higgs bosons at future colliders.

The Z_2^H symmetry violating couplings mentioned above also govern the decays of

the Inert Higgsinos. The electromagnetically neutral Higgsinos predominantly decay into fermion anti-sfermion pairs (e.g. $\tilde{H}_\alpha^0 \rightarrow t\tilde{t}^*$, $\tilde{H}_\alpha^0 \rightarrow \tau\tilde{\tau}^*$). The charged Higgsino decays are similar, but in this case the sfermion is the Supersymmetric partner of the EW partner of the fermion, (e.g. $\tilde{H}_\alpha^+ \rightarrow t\tilde{b}^*$, $\tilde{H}_\alpha^- \rightarrow \tau\tilde{\nu}_\tau^*$).

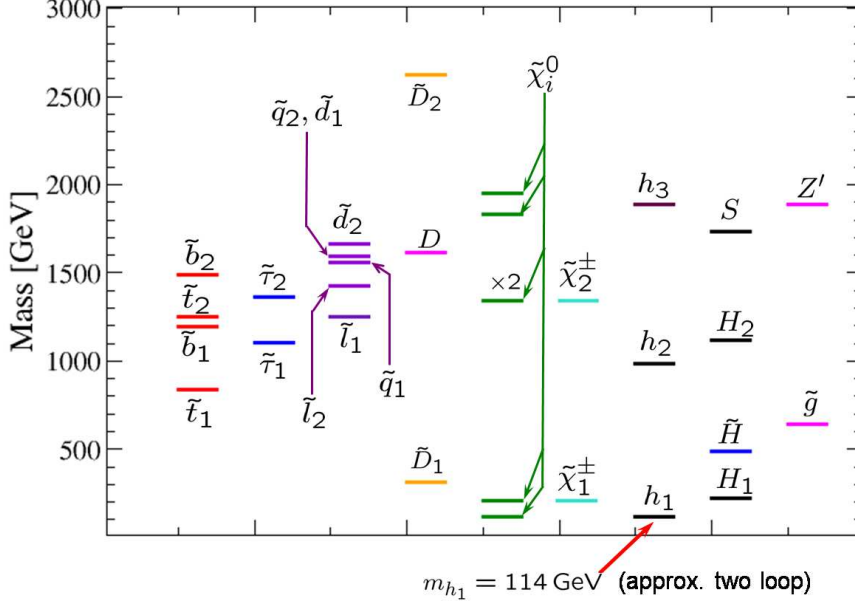


Figure 9: Benchmark point 4, with $\tan\beta = 30$, $s = 5.0$ TeV, $M_{1/2} = 725$ GeV, $m_0 = 1074$ GeV, $A = 1726$ GeV, $\lambda(M_X) = -0.3847$, $\lambda(\mu_S) = -0.3788$, $\lambda_{1,2}(M_X) = 0.1$, $\kappa_{1,2,3}(M_X) = 0.1579$, $\kappa_{1,2,3}(\mu_S) = 0.4559$.

Unfortunately the production cross sections of the Inert Higgs bosons and Inert Higgsinos at the LHC will not be large because they do not participate in strong interactions. In this context it is more interesting to study scenarios with light coloured particles. Benchmark 4 represents such a scenario (spectra shown in Fig. 9). In this case the lightest exotic squarks have masses 312 GeV and can be efficiently produced at the LHC. Once again the presence of light exotic squarks in the particle spectrum is caused by the mixing effects in the exotic squark sector. The RGEs for the soft SUSY-breaking masses, $m_{D_i}^2$ and $m_{\tilde{D}_i}^2$, are very similar with $\frac{d}{dt}(m_{D_i}^2 - m_{\tilde{D}_i}^2) = g_1^2 M_1'^2$, resulting in comparatively small splitting between these soft masses. Therefore, although the diagonal entries of the exotic squark mass matrices acquire large contributions proportional to s^2 that come from the F-term quartic interactions in the scalar potential⁶, mixing can be large even for moderate values of A_0 , leading to a large mass splitting between the two scalar partners of the exotic

⁶Note that in this case positive contributions to the diagonal entries of the exotic squark mass matrices from the F-terms dominate over negative contributions that originate from $U(1)_N$ D-term quartic interactions in the scalar potential.

coloured fermion. Recent, as yet unpublished, results from Tevatron searches for di-jet resonances [60] rule out scalar diquarks with a mass less than 630 GeV, however, scalar leptoquarks may be as light as 300 GeV since at hadron colliders they are pair produced through gluon fusion.

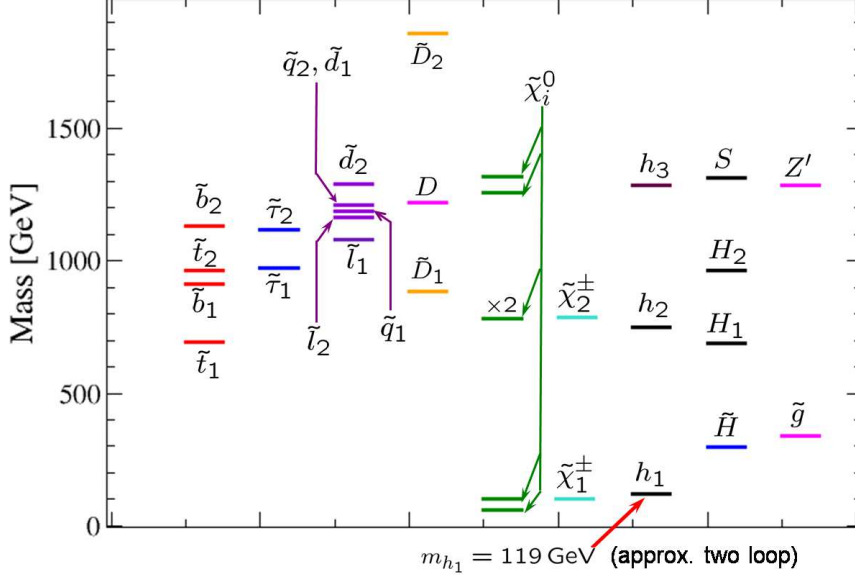


Figure 10: Benchmark point 5, with $\tan\beta = 30$, $s = 3.4$ TeV, $M_{1/2} = 361$ GeV, $m_0 = 993$ GeV, $A = 1121$ GeV, $\lambda(M_X) = -0.33$, $\lambda(\mu_S) = -0.32$, $\lambda_{1,2}(M_X) = 0.1$, $\kappa_{1,2,3}(M_X) = 0.18$, $\kappa_{1,2,3}(\mu_S) = 0.51$.

Scalar leptoquarks decay through Z_2^H violating terms, $g_{ijk}^N \hat{N}_i^c \hat{D}_j \hat{d}_k^c$, $g_{ijk}^E \hat{e}_i^c \hat{D}_j \hat{u}_k^c$ and $g_{ijk}^D (\hat{Q}_i \hat{L}_j) \hat{D}_k$. Thus in the cE₆SSM light scalar leptoquarks decay into quark–lepton final states. If the Z_2^H symmetry is mostly broken by the operators involving quarks and leptons of the third generation each scalar leptoquark gives one top quark and one τ –lepton in the final state. Since scalar leptoquarks can be pair produced through gluon fusion, light scalar leptoquarks should lead to an enhancement of $pp \rightarrow t\bar{t}l\bar{l} + X$ at the LHC [43]. Notice that SM production of $t\bar{t}\tau^+\tau^-$ is $(\alpha_W/\pi)^2$ suppressed in comparison to the light scalar leptoquark production cross section. Therefore light scalar leptoquark should produce a strong signal with low SM background at the LHC.

The decays of the lightest scalar diquarks are induced by the Z_2^H symmetry violating symmetry operators $g_{ijk}^Q \hat{D}_i (\hat{Q}_j \hat{Q}_k)$ and $g_{ijk}^q \hat{D}_i \hat{d}_j^c \hat{u}_k^c$ in the Superpotential. This results in the decays of \tilde{D}_{i1} into quark–quark final states. Assuming that exotic squarks couple most strongly to the third family quarks each \tilde{D}_{i1} gives t and b quarks in the final state. It is worth to emphasise here that exotic squarks are particles with positive R –parity. Therefore they can decay without missing energy from the LSP.

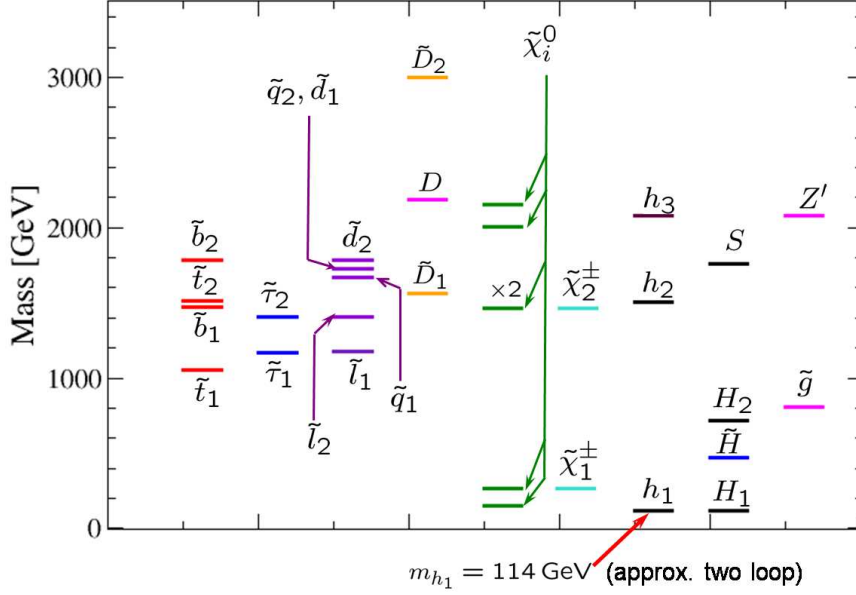


Figure 11: Benchmark point 6, with $\tan\beta = 3$, $s = 5.5$ TeV, $M_{1/2} = 931$ GeV, $m_0 = 918$ GeV, $A = 751$ GeV, $\lambda(M_X) = -0.434$, $\lambda(\mu_S) = -0.375$, $\lambda_{1,2}(M_X) = 0.1$, $\kappa_{1,2,3}(M_X) = 0.23$, $\kappa_{1,2,3}(\mu_S) = 0.56$.

Another very intriguing feature of the cE₆SSM is the presence of a $U(1)_N$ Z' gauge boson. In our benchmark point 5 (Fig. 10) this Z' is fairly light ($M_{Z'} = 1.285$ TeV) and within the reach of the LHC. Signatures for the Z' have already been discussed in [33] and are to be explored further in a follow up study [61]. However, the Z' mass can be significantly heavier, of order 2 TeV, as is shown in our final benchmark point 6 (Fig. 11). The spectrum for this point is rather heavy with even the lightest chargino being as heavy as $m_{\chi_1^\pm} = 262$ GeV and the lightest neutralino having $m_{\chi_1^0} = 148$ GeV.

The full spectrum for each of the benchmark points is given in Tab. 2. The Higgs spectrum for all the benchmark points contains a very light SM-like CP-even Higgs boson h_1 with a mass close to the LEP limit of 114 GeV. Other Higgs states have masses in the range 600–2100 GeV making them difficult to discover. The benchmark points all exhibit the characteristic SUSY spectrum described above containing a relatively light gluino, a light wino-like neutralino and chargino pair, and a light bino-like neutralino, with other sparticle masses being much heavier.

	BM 1	BM 2	BM 3	BM 4	BM 5	BM 6
$\tan\beta$	10	10	10	30	30	3
$\lambda_3(M_X)$	-2.0	-0.37	-0.31	-0.38	-0.33	-0.43
$\lambda_{1,2}(M_X)$	2.6	0.1	0.1	0.1	0.1	0.1
$\kappa_{1,2,3}(M_X)$	2.5	0.18	0.25	0.16	0.18	0.23
$s[\text{TeV}]$	4	4.4	3.8	5.0	3.4	5.5
$M_{1/2}[\text{GeV}]$	389	775	390	725	361	931
$m_0 [\text{GeV}]$	725	799	998	1074	993	918
$A[\text{GeV}]$	-1528	919	768	1726	1121	751
$m_{\tilde{D}_1}(1, 2, 3)[\text{GeV}]$	1948	821	1363	312	884	1567
$m_{\tilde{D}_2}(1, 2, 3)[\text{GeV}]$	2200	2363	2077	2623	1860	2997
$\mu_D(3)[\text{GeV}]$	2060	1535	1595	1612	1221	2187
$ m_{\chi_6^0} [\text{GeV}]$	1548	1727	1496	1950	1316	2155
$m_{h_3} \simeq M_{Z'}[\text{GeV}]$	1518	1664	1437	1890	1285	2079
$ m_{\chi_5^0} [\text{GeV}]$	1490	1603	1405	1832	1256	2006
$m_S(1, 2)[\text{GeV}]$	1290	1446	1430	1732	1351	1763
$m_{H^u}(1, 2)[\text{GeV}]$	1172	765	875	1117	966	714
$m_{H^d}(1, 2)[\text{GeV}]$	903	182	694	220	689	121
$\mu_{\tilde{H}}(1, 2)[\text{GeV}]$	1302	418	324	491	323	471
$m_{\tilde{u}_1}(1, 2)[\text{GeV}]$	1007	1398	1211	1557	1173	1666
$m_{\tilde{d}_1}(1, 2)[\text{GeV}]$	1023	1446	1225	1595	1186	1724
$m_{\tilde{u}_2}(1, 2)[\text{GeV}]$	1023	1446	1225	1595	1186	1724
$m_{\tilde{d}_2}(1, 2)[\text{GeV}]$	1113	1488	1292	1664	1241	1785
$m_{\tilde{e}_2}(1, 2)[\text{GeV}]$	1015	1176	1207	1427	1165	1409
$m_{\tilde{e}_1}(1, 2)[\text{GeV}]$	873	992	1105	1254	1080	1173
$m_{\tilde{\tau}_2}[\text{GeV}]$	1012	1172	1203	1363	1117	1409
$m_{\tilde{\tau}_1}[\text{GeV}]$	867	982	1095	1102	973	1172
$m_{\tilde{b}_2}[\text{GeV}]$	1108	1473	1282	1491	1133	1784
$m_{\tilde{b}_1}[\text{GeV}]$	907	1216	1036	1193	914	1472
$m_{\tilde{t}_2}[\text{GeV}]$	921	1259	1070	1248	964	1511
$m_{\tilde{t}_1}[\text{GeV}]$	777	853	787	837	694	1056
$ m_{\chi_3^0} \simeq m_{\chi_4^0} \simeq m_{\chi_{2,1}^\pm} [\text{GeV}]$	739	1168	771	1343	784	1463
$m_{h_2} \simeq m_A \simeq m_{H^\pm}[\text{GeV}]$	615	1145	963	998	748	1508
$m_{h_1}[\text{GeV}]$	116	114	121	114	119	114
$m_{\tilde{g}}[\text{GeV}]$	350	673	362	642	338	805
$ m_{\chi_1^\pm} \simeq m_{\chi_2^0} [\text{GeV}]$	106	217	110	206	102	262
$ m_{\chi_1^0} [\text{GeV}]$	59	122	62	116	58	148

Table 2: Particle spectra for our constrained E_6 SSM benchmark points.

6. Conclusions

In this paper we have considered the constrained version of the Exceptional Supersymmetric Standard Model (E₆SSM). The E₆SSM is based on the $SU(3)_C \times SU(2)_W \times U(1)_Y \times U(1)_N$ gauge group, which can originate from the breakdown of the E_6 symmetry at high energies. In this E_6 inspired SUSY model the right-handed neutrino does not participate in gauge interactions, allowing it to be used for both the see-saw mechanism and leptogenesis. To ensure anomaly cancellation and gauge coupling unification, the particle content of the E₆SSM includes three complete fundamental 27 representations of E_6 as well as the doublet H' and anti-doublet \overline{H}' from extra $27'$ and $\overline{27}'$ representations. Thus, in addition to a Z' corresponding to the $U(1)_N$ symmetry, the E₆SSM involves extra matter beyond the MSSM that form three families of new exotic charge 1/3 quarks and squarks, three generations of $SU(2)$ doublets of Inert Higgs bosons and Inert Higgsinos, as well as three SM-singlet bosons and their fermionic Superpartners, which carry $U(1)_N$ charges. The baryon number conservation requires exotic quarks and squarks to be either diquarks (E₆SSM Model I) or leptoquarks (E₆SSM Model II).

The extra $U(1)_N$ gauge symmetry forbids the term $\mu \hat{H}_d \hat{H}_u$ in the Superpotential. Nevertheless one of the SM-singlet bosons S develops a VEV $\langle S \rangle = s/\sqrt{2}$, breaking the extra $U(1)_N$ symmetry and providing the effective μ term for the Higgs doublets, as well as masses for exotic quarks, Inert Higgsinos and Z' . This solution of the μ problem is cosmologically safe because the Peccei–Quinn symmetry becomes embedded in the extra $U(1)_N$ gauge symmetry, i.e. troublesome axion is swallowed by the extra gauge boson via the Higgs mechanism resulting in a massive Z' at the TeV scale. Also there is no domain wall problem since there is no discrete Z_3 symmetry.

In general, the E_6 inspired SUSY models involves lots of new Yukawa couplings in comparison to the SM and MSSM. Some of these new couplings give rise to unacceptably large non-diagonal flavour transitions, which have not been observed. To suppress flavour changing processes, we have imposed an approximate Z_2^H symmetry under which only the Higgs Superfields H_u , H_d and S are even while all other Supermultiplets are odd. This discrete symmetry can only be an approximate one because it forbids all terms that allow the lightest exotic quarks to decay. To avoid large non-diagonal flavour transitions, we assumed that all Z_2^H symmetry violating Yukawas are rather small ($\lesssim 10^{-3} - 10^{-4}$) and therefore irrelevant for our analysis of the E₆SSM particle spectrum. We also imposed a certain hierarchical structure of the Z_2^H symmetry preserving Yukawa interactions to ensure the correct breakdown of gauge symmetry.

The number of new couplings is further reduced within the *constrained* E₆SSM (cE₆SSM). The cE₆SSM demands that all soft scalar masses, gaugino masses and tri-

linear scalar couplings are universal at the GUT scale. We analysed the RG flow of the gauge and Yukawa couplings, as well as soft SUSY breaking terms, using two-loop RGEs for the gauge and Yukawa couplings together with two-loop RGEs for the gaugino masses and trilinear scalar couplings and one-loop RGEs for the soft scalar masses. Since the E_6 SSM has a much larger Superfield content than the MSSM, the RG flow of the gauge and Yukawa couplings and soft SUSY breaking terms is entirely different from the minimal SUSY model. For example, due to the presence of three families of exotic quarks and squarks, the QCD beta function vanishes at one loop and at two loops it loses asymptotic freedom (though the gauge couplings remain perturbative at high energy). Thus, the E_6 SSM gauge couplings are considerably larger at high energies than in the MSSM, and the RG flows of gaugino and soft scalar masses are entirely different. For the same values of $M_{1/2}$, the gaugino masses in the cE_6 SSM are much smaller than in the c MSSM at low energies. One remarkable feature is that the low energy gluino mass parameter M_3 is driven to be smaller than $M_{1/2}$ by RG running.

For each set of $\tan\beta$ and SUSY preserving couplings we established semi-analytic relations between the soft SUSY breaking terms at the SUSY breaking scale and their values at the GUT scale. Then we imposed EWSB constraints, which can be considered as a system of non-linear algebraic equations with respect to A_0 , m_0 and $M_{1/2}$ and found the solutions of these equations for fixed $\tan\beta$, s and Yukawa couplings. We restricted our consideration to the scenarios with real values of fundamental parameters which do not induce any CP-violating effects. Remarkably, there are always solutions with real A_0 , $M_{1/2}$ and m_0 for sufficiently large values of exotic quark Yukawa couplings that facilitate the breakdown of the gauge symmetry in the cE_6 SSM. At the last stage of our analysis, we varied the Yukawa couplings, $\tan\beta$ and s to establish the qualitative pattern of the particle spectrum. To avoid any conflict with present and former collider experiments, as well as recent cosmological observations, we imposed a set of experimental and theoretical constraints which restrict the allowed region of parameter space.

The results of our analysis indicate that m_0 tends to be considerably larger than $M_{1/2}$ in the allowed region. As a consequence, the Superpartners of ordinary quarks and leptons are significantly heavier than the gluino and lightest neutralino and chargino, which are predominantly gaugino. Some of the exotic squarks can also be relatively light due to large mixing effects induced by the corresponding Yukawa couplings and A_0 . The substantial mixing and negative $U(1)_N$ D-term contributions can lead to the presence of light Inert Higgs bosons as well. The masses of exotic quarks and Inert Higgsinos which originate from complete 27 plets are controlled by the corresponding Yukawa couplings and can be relatively light if some of these couplings are small.

The mass terms of the right-handed neutrinos and survival components of $27'$ and $\overline{27}'$

are not forbidden by the gauge symmetry and therefore the scalar and fermion components of these Supermultiplets are expected to be rather heavy, so they decouple from the rest of the particle spectrum. The mass of the Z' is set by the singlet VEV, i.e. $M_{Z'} \approx g'_1 Q_S s$ where $Q_S \simeq 5/\sqrt{40}$ and $g'_1 \approx g_1$. As a result, the Z' is considerably heavier than the gluino, lightest neutralino and chargino. The lightest neutralino, χ_1^0 , is essentially pure bino, while the second lightest neutralino χ_2^0 and the lightest chargino χ_1^\pm are the degenerate components of the wino. The Higgsino states are degenerate and much heavier with the masses given by the effective μ term. The remaining neutralinos are mainly a superposition of the $U(1)_N$ gaugino and singlet Higgsino. Their masses are governed by $M_{Z'}$. The heaviest CP-even Higgs state is degenerate with the Z' while another CP-even Higgs, CP-odd and charged Higgs bosons have almost the same masses and are considerably heavier than the lightest SUSY particles. For $s = 3 - 5$ TeV, the lightest Higgs boson mass is rather close to the LEP limit of 114 GeV. In this work we specified a set of benchmark points that illustrate all the features of the particle spectrum discussed above and presented the allowed range of parameter space for different values of $\tan \beta$ and s . With increasing VEV of the SM-singlet field, the allowed region of parameter space grows, whereas the structure of the particle spectrum becomes more hierarchical.

Thus, throughout all cE₆SSM regions of parameter space, there is a general prediction that the lightest sparticles always include the gluino \tilde{g} , two lightest neutralinos χ_1^0, χ_2^0 , and the lightest chargino χ_1^\pm , which are considerably lighter than all the sfermions of ordinary matter. The corresponding hierarchical structure of the particle spectrum is caused by the RG flow. As a consequence, at the LHC one should observe pair production of $\chi_2^0 \chi_2^0, \chi_2^0 \chi_1^\pm, \chi_1^\pm \chi_1^\mp$ and $\tilde{g}\tilde{g}$. Due to the hierarchical spectrum, the gluinos can be relatively narrow states so their width can be comparable to that of W^\pm and Z bosons. Gluino pair production would result in an appreciable enhancement of the cross section for $pp \rightarrow q\bar{q}q\bar{q} + E_T^{\text{miss}} + X$. Since the second lightest neutralino decays through $\chi_2^0 \rightarrow \chi_1^0 + l\bar{l}$, its pair production would produce an excess in $pp \rightarrow l\bar{l}l\bar{l} + E_T^{\text{miss}} + X$, which can be also observed at the LHC.

Other possible manifestations of the E₆SSM at the LHC are related to the presence of a Z' and exotic multiplets of matter. A TeV scale Z' will provide an unmistakable signal that can be observed soon after the LHC starts. If exotic quarks are relatively light, their production cross sections can be comparable with the cross section of $t\bar{t}$ production. The lifetime and decays of light exotic quarks are determined by the Z_2^H violating Yukawa couplings. If D_i and \bar{D}_i couple most strongly to the third family of (s)quarks and (s)leptons, then light exotic quarks lead to a substantial enhancement of the cross section of either $pp \rightarrow t\bar{t}b\bar{b} + E_T^{\text{miss}} + X$ (if they are diquarks) or $pp \rightarrow t\bar{t}\tau\bar{\tau} + E_T^{\text{miss}} + X$ and $pp \rightarrow b\bar{b} + E_T^{\text{miss}} + X$ (if they are leptoquarks). When scalar exotic quarks are light, they can decay into quark-quark (if diquarks) or quark-lepton (if leptoquarks) without

missing energy from the LSP. As a result, their pair production leads to the enhancement of the cross section of either $pp \rightarrow t\bar{t}b\bar{b} + X$ or $pp \rightarrow t\bar{t}\tau\bar{\tau} + X$. Since the SM production cross sections of $pp \rightarrow t\bar{t}b\bar{b} + X$ or $pp \rightarrow t\bar{t}\tau\bar{\tau} + X$ are suppressed by many orders of magnitude compared to the cross section for $t\bar{t}$ production, the light exotic quarks and squarks should produce a strong signal with low SM background at the LHC.

The production cross sections of the Inert Higgs bosons and Inert Higgsinos will be much smaller at the LHC than the exotic (s)quark one. Nevertheless, their detection might also be possible if the corresponding states are light. Assuming that Inert Higgs bosons and Inert Higgsinos couple most strongly to the third family (s)quarks and (s)leptons, the lightest Inert Higgs bosons decay predominantly into third generation fermion–anti-fermion pairs like $H_{\alpha 1}^0 \rightarrow b\bar{b}$ and $H_{\alpha 1}^- \rightarrow \tau\bar{\nu}_\tau$, while Inert Higgsinos predominantly decay into third generation fermion-anti-fermion pairs. At an ILC the production rates of the light exotic (s)quarks and Inert Higgs bosons (Higgsinos) can be comparable, allowing their simultaneous observation.

We have not considered the question of cosmological cold dark matter (CDM) relic abundance due to the neutralino LSP and so one may be concerned that a bino-like lightest neutralino mass of around 100 GeV might give too large a contribution to Ω_{CDM} . Indeed a recent calculation of Ω_{CDM} in the USSM [62], which includes the effect of the MSSM states plus the extra Z' and the active singlet S , together with their superpartners, indicates that for the benchmarks considered here that Ω_{CDM} would be too large. However the USSM does not include the effect of the extra inert Higgs and Higgsinos that are present in the E_6 SSM. While we have considered the inert Higgsino masses given by $\mu_{\tilde{H}_\alpha} = \lambda_\alpha s/\sqrt{2}$, we have not considered the mass of the inert singlinos which are generated by mixing with the Higgs and inert Higgsinos, and are thus of order fv^2/s where their masses are controlled by additional Yukawa couplings f which we have not specified in our analysis. Since $s \gg v$ it is quite likely that the LSP neutralino in the cE_6 SSM will be an inert singlino with a mass lighter than 100 GeV. This would imply that the state χ_1^0 considered here is not cosmologically stable but would decay into lighter singlinos. The question of the calculation of the relic abundance of such an LSP singlino within the framework of the cE_6 SSM is beyond the scope of this article and will be considered elsewhere. In summary, it is clear that one should not regard the benchmark points with $|m_{\chi_1^0}| \approx 100$ GeV as being excluded by Ω_{CDM} .

The discovery of Z' and new exotic particles predicted by the E_6 SSM at future colliders will open a new era in elementary particle physics. It will represent a possible indirect signature of an underlying E_6 gauge structure at high energies and may provide a window into string theory.

Acknowledgements

We would like to thank A. Belyaev, C. D. Froggatt and D. Sutherland for fruitful discussions. RN is also grateful to E. Boos, D. I. Kazakov, M. Sher and P. M. Zerwas for valuable comments and remarks. PA would like to thank D. Stockinger for helpful discussions during the preparation of this manuscript. DJM acknowledges support from the STFC Advanced Fellowship Grant PP/C502722/1. RN acknowledges support from the SHEFC grant HR03020 SUPA 36878. SFK acknowledges partial support from the following grants: STFC Rolling Grant ST/G000557/1 (also SM); EU Network MRTN-CT-2004-503369; NATO grant PST.CLG.980066 (also SM); EU ILIAS RII3-CT-2004-506222. SM is also partially supported by the FP7 RTN MRTN-CT-2006-035505 and by the scheme ‘Visiting Professor - Azione D - Atto Integrativo tra la Regione Piemonte e gli Atenei Piemontesi’.

A One-loop corrections to the Higgs masses

Higgs masses are obtained by taking double derivatives of the effective potential with respect to the Higgs fields.

The tree-level Higgs masses for the CP-even Higgs sector were presented in section 4.5, Eq. (64). The expression for the one-loop contribution, $\Delta V^{(1)}$, to the effective potential also appears in Eq. (15) and the physical masses of the stops, appearing in this equation, are calculated in the tree-level approximation,

$$m_{\tilde{t}_{1,2}}^2 = \frac{1}{2} \left\{ m_{Q_3}^2 + m_{u_3}^2 + \frac{1}{2} M_Z^2 \cos 2\beta + \Delta_Q + \Delta_{u^c} + 2m_t^2 \mp \sqrt{M_{Q_Q}^4 + 4m_t^2 X_t^2} \right\}, \quad (\text{A.1})$$

where

$$\Delta_Q = \frac{g_1'}{80}(-3v_1^2 - 2v_2^2 + 5s^2), \quad \Delta_{u^c} = \frac{g_1'}{80}(-3v_1^2 - 2v_2^2 + 5s^2), \quad (\text{A.2})$$

$$M_{Q_Q}^2 = m_{Q_3}^2 - m_{u_3}^2 + \left[\frac{1}{2} - \frac{4}{3} \sin^2 \theta_W \right] M_Z^2 \cos 2\beta + \Delta_Q - \Delta_U, \quad (\text{A.3})$$

$$X_t = A_t - \frac{\lambda s}{\sqrt{2} \tan \beta}, \quad (\text{A.4})$$

and for further convenience defining,

$$r_t \equiv M_{Q_Q}^4 + 4m_t^2 X_t^2 \quad \text{and} \quad R_{Q_Q} \equiv M_{Q_Q}^2 (g_2^2 - g_1^2), \quad (\text{A.5})$$

$$\mu_{eff} \equiv \frac{\lambda s}{\sqrt{2}} \quad \text{and} \quad \bar{g} \equiv \sqrt{g_2^2 + \frac{3g_1^2}{5}} \quad (\text{A.6})$$

Including only stop/top contributions we find,

$$\frac{\partial \Delta V}{\partial x} = \frac{3}{32\pi^2} \left[2a_0(m_{\tilde{t}_1}) \frac{\partial}{\partial x} m_{\tilde{t}_1}^2 + 2a_0(m_{\tilde{t}_2}) \frac{\partial}{\partial x} m_{\tilde{t}_2}^2 - 4a_0(m_t) \frac{\partial}{\partial x} m_t^2 \right], \quad (\text{A.7})$$

where

$$a_0(m) \equiv m^2 \left[\ln \frac{m^2}{Q^2} - 1 \right]. \quad (\text{A.8})$$

Now, defining

$$\Delta_x m_i \equiv a_0(m_i) \frac{\partial}{\partial x} m_i^2, \quad (\text{A.9})$$

it follows that

$$\frac{\partial^2 \Delta V}{\partial y \partial x} = \frac{3}{32\pi^2} \left[2 \frac{\partial}{\partial y} \Delta_x m_{\tilde{t}_1} + 2 \frac{\partial}{\partial y} \Delta_x m_{\tilde{t}_2} - 4 \frac{\partial}{\partial y} \Delta_x m_t \right], \quad (\text{A.10})$$

$$\frac{\partial}{\partial x} \Delta_x m = \left(\frac{\partial}{\partial x} m^2 \right)^2 \ln \frac{m^2}{Q^2} + a_0(m) \frac{\partial^2}{\partial x^2} m^2, \quad (\text{A.11})$$

$$\frac{\partial}{\partial y} \Delta_x m = \left(\frac{\partial}{\partial y} m^2 \right) \left(\frac{\partial}{\partial x} m^2 \right) \ln \frac{m^2}{Q^2} + a_0(m) \frac{\partial^2}{\partial y \partial x} m^2. \quad (\text{A.12})$$

Here we present the corrections in the basis $(v_1, v_2, v_3 \equiv s)$, with $\Delta'_{ij} = \frac{\partial^2}{\partial v_i \partial v_j} \Delta V$ such that $\Delta'_{11} = \frac{\partial^2}{\partial v_1^2} \Delta V$ etc. The corrections, Δ_{ij} appearing in Eq. (64) can be obtained from these using the relations,

$$\Delta_{11} = \cos^2 \beta \Delta'_{11} - 2 \sin \beta \cos \beta \Delta'_{12} + \sin^2 \beta \Delta'_{22} \quad (\text{A.13})$$

$$\Delta_{22} = \sin^2 \beta \Delta'_{11} - 2 \sin \beta \cos \beta \Delta'_{12} + \cos^2 \beta \Delta'_{22} \quad (\text{A.14})$$

$$\Delta_{33} = \Delta'_{33} \quad (\text{A.15})$$

$$\Delta_{12} = (\cos^2 \beta - \sin^2 \beta) \Delta'_{12} + \sin \beta \cos \beta (\Delta'_{22} - \Delta'_{11}) \quad (\text{A.16})$$

$$\Delta_{31} = \cos \beta \Delta'_{13} + \sin \beta \Delta'_{23} \quad (\text{A.17})$$

$$\Delta_{32} = \cos \beta \Delta'_{23} - \sin \beta \Delta'_{13} \quad (\text{A.18})$$

$$\begin{aligned} \Delta'_{11} = & \frac{3}{16\pi^2} \left\{ \left[\left(\frac{\bar{g}^2}{8} - \frac{3g_1'^2}{40} \right)^2 v_1^2 + \frac{1}{r_t} \left(\frac{v_1 R_{QQ} - 2m_t^2 X_t \frac{s\lambda}{\sqrt{2}v_2}}{8} \right)^2 \right] \ln \frac{m_{\tilde{t}_1}^2 m_{\tilde{t}_2}^2}{Q^4} \right. \\ & + \frac{v_1}{32} \left(\bar{g}^2 - \frac{3}{5} g_1'^2 \right) r_t^{-\frac{1}{2}} \left(v_1 R_{QQ} - 16m_t^2 X_t \frac{s\lambda}{\sqrt{2}v_2} \right) \ln \frac{m_{\tilde{t}_2}^2}{m_{\tilde{t}_1}^2} \\ & + \left(\frac{\bar{g}^2}{8} - \frac{3g_1'^2}{40} \right) (a_0(m_{\tilde{t}_1}) + a_0(m_{\tilde{t}_2})) + \frac{1}{32} \left[r_t^{-\frac{1}{2}} (4R_{QQ} + (g_2^2 - g_1^2)^2 v_1^2 \right. \\ & \left. \left. + 16y_t^2 s^2 \lambda^2) - \left(v_1 R_{QQ} - 16m_t^2 X_t \frac{s\lambda}{\sqrt{2}v_2} \right)^2 r_t^{-\frac{3}{2}} \right] (a_0(m_{\tilde{t}_2}) - a_0(m_{\tilde{t}_1})) \right\} \quad (\text{A.19}) \end{aligned}$$

$$\begin{aligned} \Delta'_{22} = & \frac{3}{16\pi^2} \left\{ \left[\left(y_t^2 - \frac{\bar{g}^2}{8} - \frac{g_1'^2}{20} \right)^2 + \frac{(8X_t A_t y_t^2 - R_{QQ})^2}{64r_t} \right] v_2^2 \ln \frac{m_{\tilde{t}_1}^2 m_{\tilde{t}_2}^2}{Q^4} \right. \\ & + \frac{v_2^2}{4\sqrt{r_t}} \left(y_t^2 - \frac{\bar{g}^2}{8} - \frac{g_1'^2}{20} \right) (8y_t^2 X_t A_t - R_{QQ}) \ln \frac{m_{\tilde{t}_2}^2}{m_{\tilde{t}_1}^2} \\ & + \left(y_t^2 - \frac{\bar{g}^2}{8} - \frac{g_1'^2}{20} \right) (a_0(m_{\tilde{t}_1}) + a_0(m_{\tilde{t}_2})) + \frac{1}{\sqrt{r_t}} \left[\frac{(g_2^2 - g_1^2)^2 v_2^2}{32} - \frac{R_{QQ}}{8} + y_t^2 A_t^2 \right. \\ & \left. \left. - \frac{(8X_t A_t y_t^2 - R_{QQ})^2 v_2^2}{32r_t} \right] (a_0(m_{\tilde{t}_1}) - a_0(m_{\tilde{t}_2})) - 2y_t^4 v_2^2 \ln \frac{m_{\tilde{t}_2}^2}{Q^2} - 2y_t^2 a_0(m_t) \right\} \quad (\text{A.20}) \end{aligned}$$

$$\begin{aligned} \Delta'_{33} = & \frac{3}{16\pi^2} \left\{ \left[\frac{g_1'^4 s^2}{64} + \frac{2m_t^4 X_t^2 \lambda^2}{r_t \tan^2 \beta} \right] \ln \frac{m_{\tilde{t}_1}^2 m_{\tilde{t}_2}^2}{Q^4} - \frac{g_1'^2 m_t^2 X_t \mu_{eff}}{2\sqrt{r_t} \tan \beta} \ln \frac{m_{\tilde{t}_2}^2}{m_{\tilde{t}_1}^2} \right. \\ & \left. + \frac{g_1'^2}{8} (a_0(m_{\tilde{t}_1}) + a_0(m_{\tilde{t}_2})) + \frac{\lambda^2 m_t^2}{\sqrt{r_t} \tan^2 \beta} \left[1 - \frac{4X_t^2 m_t^2}{r_t} \right] (a_0(m_{\tilde{t}_2}) - a_0(m_{\tilde{t}_1})) \right\} \quad (\text{A.21}) \end{aligned}$$

$$\begin{aligned}
\Delta'_{12} = & \frac{3}{16\pi^2} \left\{ \left[\left(\frac{\bar{g}^2}{8} - \frac{3}{40} g_1'^2 \right) \left(y_t^2 - \frac{\bar{g}^2}{8} - \frac{g_1'^2}{20} \right) + \left(\frac{R_{QQ}}{8} - y_t^2 X_t \mu_{eff} \tan \beta \right) \frac{1}{r_t} \right. \right. \\
& \times \left. \left(y_t^2 X_t A_t - \frac{R_{QQ}}{8} \right) \right] v_1 v_2 \ln \frac{m_{\bar{t}_1}^2 m_{\bar{t}_2}^2}{Q^4} + \left[\left(\frac{\bar{g}^2}{8} - \frac{3g_1'^2}{40} \right) \left(y_t^2 X_t A_t - \frac{R_{QQ}}{8} \right) \right. \\
& + \left. \left. \left(\frac{R_{QQ}}{8} - y_t^2 X_t \mu_{eff} \tan \beta \right) \left(y_t^2 - \frac{1}{8} \bar{g}^2 - \frac{1}{20} g_1'^2 \right) \right] \frac{v_1 v_2}{\sqrt{r_t}} \ln \frac{m_{\bar{t}_2}^2}{m_{\bar{t}_1}^2} \right. \\
& - \left[\left(\frac{g_2^2 - g_1^2}{32} v_1 v_2 + A_t y_t^2 \mu_{eff} \right) + \left(\frac{R_{QQ}}{8} - y_t^2 X_t \mu_{eff} \tan \beta \right) (2y_t^2 X_t A_t \right. \\
& \left. \left. - \frac{R_{QQ}}{4} \right) \frac{v_1 v_2}{r_t} \right] \left(\frac{a_0(m_{\bar{t}_2}) - a_0(m_{\bar{t}_1})}{\sqrt{r_t}} \right) \left. \right\} \quad (\text{A.22})
\end{aligned}$$

$$\begin{aligned}
\Delta'_{13} = & \frac{3}{16\pi^2} \left\{ \left[\left(\frac{\bar{g}^2}{8} - \frac{3g_1'^2}{40} \right) \frac{g_1'^2}{8} s v_1 - \left(\frac{R_{QQ}}{8} v_1 - y_t^2 X_t \mu_{eff} v_2 \right) \frac{2m_{\bar{t}_1}^2 X_t \lambda}{r_t \sqrt{2} \tan \beta} \right] \ln \frac{m_{\bar{t}_1}^2 m_{\bar{t}_2}^2}{Q^4} \right. \\
& - \left[\left(\frac{\bar{g}^2}{8} - \frac{3g_1'^2}{40} \right) \frac{2v_1 m_{\bar{t}_1}^2 X_t \lambda}{\sqrt{2} \tan \beta \sqrt{r_t}} - \frac{g_1'^2 s}{8\sqrt{r_t}} \left(\frac{R_{QQ}}{8} v_1 - 2m_{\bar{t}_1}^2 X_t \frac{s\lambda}{\sqrt{2} v_2} \right) \right] \ln \frac{m_{\bar{t}_2}^2}{m_{\bar{t}_1}^2} \\
& \left. + \frac{y_t^2 v_1 \lambda \mu_{eff}}{\sqrt{2} r_t} \left[1 - \frac{X_t \tan \beta}{\mu_{eff}} - \frac{4X_t^2 m_{\bar{t}_1}^2}{r_t} + \frac{v_1 v_2 R_{QQ} X_t}{4\mu_{eff} r_t} \right] (a_0(m_{\bar{t}_2}) - a_0(m_{\bar{t}_1})) \right\} \quad (\text{A.23})
\end{aligned}$$

$$\begin{aligned}
\Delta'_{23} = & \frac{3}{16\pi^2} \left\{ \left[\frac{g_1'^2}{8} \left(y_t^2 - \frac{\bar{g}^2}{8} - \frac{g_1'^2}{20} \right) s - \frac{2m_{\bar{t}_1}^2 X_t \lambda}{r_t \sqrt{2} \tan \beta} \left(y_t^2 X_t A_t - \frac{R_{QQ}}{8} \right) \right] v_2 \ln \frac{m_{\bar{t}_1}^2 m_{\bar{t}_2}^2}{Q^4} \right. \\
& + r_t^{-\frac{1}{2}} \left[\frac{g_1'^2}{8} s \left(y_t^2 X_t A_t - \frac{R_{QQ}}{8} \right) - \frac{2m_{\bar{t}_1}^2 X_t \lambda}{\sqrt{2} \tan \beta} \left(y_t^2 - \frac{\bar{g}^2}{8} - \frac{g_1'^2}{20} \right) \right] v_2 \ln \frac{m_{\bar{t}_2}^2}{m_{\bar{t}_1}^2} \\
& \left. - \frac{y_t^2 \lambda v_1 A_t}{\sqrt{2} r_t} \left[1 - \frac{4m_{\bar{t}_1}^2 X_t^2}{r_t} + \frac{v_2^2 X_t R_{QQ}}{4A_t r_t} \right] (a_0(m_{\bar{t}_2}) - a_0(m_{\bar{t}_1})) \right\} \quad (\text{A.24})
\end{aligned}$$

These complicated expressions can be simplified by keeping only the dominant contributions. Neglecting those auxiliary D-term contributions to the stop masses which are proportional to v_1^2 and v_2^2 we obtain the following simpler expressions,

$$\Delta'_{11} \approx \frac{3y_t^2}{16\pi^2} \left\{ \frac{m_{\bar{t}_1}^2 X_t^2 s^2 \lambda^2}{r_t} \ln \frac{m_{\bar{t}_1}^2 m_{\bar{t}_2}^2}{Q^4} + \frac{\mu_{eff}^2}{\sqrt{r_t}} \left[1 - \frac{4m_{\bar{t}_1}^2 X_t^2}{r_t} \right] (a_0(m_{\bar{t}_2}) - a_0(m_{\bar{t}_1})) \right\} \quad (\text{A.25})$$

$$\begin{aligned}
\Delta'_{22} \approx & \frac{3y_t^2}{16\pi^2} \left\{ 2m_{\bar{t}_1}^2 \left(1 + \frac{X_t^2 A_t^2}{r_t} \right) \ln \frac{m_{\bar{t}_1}^2 m_{\bar{t}_2}^2}{Q^4} + \frac{A_t^2}{\sqrt{r_t}} \left[1 - \frac{4m_{\bar{t}_1}^2 X_t^2}{r_t} \right] (a_0(m_{\bar{t}_1}) - a_0(m_{\bar{t}_2})) \right. \\
& \left. + (a_0(m_{\bar{t}_1}) + a_0(m_{\bar{t}_2}) - 2a_0(m_t)) + \frac{4m_{\bar{t}_1}^2}{\sqrt{r_t}} X_t A_t \ln \frac{m_{\bar{t}_2}^2}{m_{\bar{t}_1}^2} - 4m_{\bar{t}_1}^2 \ln \frac{m_{\bar{t}_1}^2}{Q^2} \right\} \quad (\text{A.26})
\end{aligned}$$

$$\begin{aligned} \Delta'_{33} \approx & \frac{3}{16\pi^2} \left\{ \left[\frac{g_1'^4 s^2}{64} + \frac{2m_t^4 X_t^2 \lambda^2}{r_t \tan^2 \beta} \right] \ln \frac{m_{\tilde{t}_1}^2 m_{\tilde{t}_2}^2}{Q^4} - \frac{g_1'^2 m_t^2 X_t \mu_{eff}}{2\sqrt{r_t} \tan \beta} \ln \frac{m_{\tilde{t}_2}^2}{m_{\tilde{t}_1}^2} \right. \\ & \left. + \frac{g_1'^2}{8} (a_0(m_{\tilde{t}_1}) + a_0(m_{\tilde{t}_2})) + \frac{\lambda^2 m_t^2}{\sqrt{r_t} \tan^2 \beta} \left[1 - \frac{4X_t^2 m_t^2}{r_t} \right] (a_0(m_{\tilde{t}_2}) - a_0(m_{\tilde{t}_1})) \right\} \quad (\text{A.27}) \end{aligned}$$

$$\begin{aligned} \Delta'_{12} \approx & \frac{3y_t^2}{16\pi^2} \left\{ -\frac{2m_t^2 \mu_{eff} A_t X_t^2}{r_t} \ln \frac{m_{\tilde{t}_1}^2 m_{\tilde{t}_2}^2}{Q^4} - \frac{2m_t^2 X_t \mu_{eff}}{\sqrt{r_t}} \ln \frac{m_{\tilde{t}_2}^2}{m_{\tilde{t}_1}^2} \right. \\ & \left. - \frac{\mu_{eff} A_t}{\sqrt{r_t}} \left[1 - \frac{4m_t^2 X_t^2}{r_t} \right] (a_0(m_{\tilde{t}_2}) - a_0(m_{\tilde{t}_1})) \right\} \quad (\text{A.28}) \end{aligned}$$

$$\begin{aligned} \Delta'_{13} \approx & \frac{3}{16\pi^2} \left\{ \frac{2m_t^4 X_t^2 \lambda^2 s}{r_t \tan \beta v_2} \ln \frac{m_{\tilde{t}_1}^2 m_{\tilde{t}_2}^2}{Q^4} - \frac{g_1'^2 s^2 m_t^2 X_t \lambda}{4v_2 \sqrt{2r_t}} \ln \frac{m_{\tilde{t}_2}^2}{m_{\tilde{t}_1}^2} \right. \\ & \left. + \frac{y_t^2 v_1 \lambda \mu_{eff}}{\sqrt{2r_t}} \left[1 - \frac{X_t \tan \beta}{\mu_{eff}} - \frac{4X_t^2 m_t^2}{r_t} \right] (a_0(m_{\tilde{t}_2}) - a_0(m_{\tilde{t}_1})) \right\} \quad (\text{A.29}) \end{aligned}$$

$$\begin{aligned} \Delta'_{23} \approx & \frac{3y_t^2}{16\pi^2} \left\{ \left(\frac{g_1'^2 s v_2}{8} - \frac{2m_t^2 X_t^2 \lambda v_2}{r_t \sqrt{2} \tan \beta} A_t \right) \ln \frac{m_{\tilde{t}_1}^2 m_{\tilde{t}_2}^2}{Q^4} + \frac{(g_1'^2 A_t v_2 s - 8\sqrt{2} m_t^2 \lambda v_1) X_t}{8\sqrt{r_t}} \ln \frac{m_{\tilde{t}_2}^2}{m_{\tilde{t}_1}^2} \right. \\ & \left. - \frac{\lambda v_1 A_t}{\sqrt{2r_t}} \left[1 - \frac{4m_t^2 X_t^2}{r_t} \right] (a_0(m_{\tilde{t}_2}) - a_0(m_{\tilde{t}_1})) \right\} \quad (\text{A.30}) \end{aligned}$$

B RGEs

The running of the gauge couplings from the GUT scale to the EW scale is determined by a set of RGEs. In our analysis, we use two-loop RGEs for the gauge and Yukawa couplings together with two-loop RGEs for the gaugino masses $M_a(\mu)$ and trilinear scalar couplings $A_i(\mu)$, as well as one-loop RGEs for the soft scalar masses $m_i^2(\mu)$. A simplified set of one-loop RG equations may be found in [23]. The two-loop RGEs can be derived using general results presented in [63].

In the E₆SSM the RGEs for the gauge couplings can be written,

$$\frac{dG}{dt} = G \times B, \quad \frac{dg_2}{dt} = \frac{\beta_2 g_2^3}{(4\pi)^2}, \quad \frac{dg_3}{dt} = \frac{\beta_3 g_3^3}{(4\pi)^2}, \quad (\text{B.1})$$

where $t = \ln[Q/M_X]$, while B and G are 2×2 matrices describing the RG flow of the Abelian gauge couplings, which is affected by the kinetic term mixing,

$$G = \begin{pmatrix} g_1 & g_{11} \\ 0 & g'_1 \end{pmatrix}, \quad B = \begin{pmatrix} B_1 & B_{11} \\ 0 & B'_1 \end{pmatrix} = \frac{1}{(4\pi)^2} \begin{pmatrix} \beta_1 g_1^2 & 2g_1 g'_1 \beta_{11} + 2g_1 g_{11} \beta_1 \\ 0 & g_1'^2 \beta'_1 + 2g'_1 g_{11} \beta_{11} + g_{11}^2 \beta_1 \end{pmatrix}. \quad (\text{B.2})$$

In the one-loop approximation $\beta_{11} = \frac{\sqrt{6}}{5}$. The two-loop diagonal β -functions of the gauge couplings are given by

$$\begin{aligned} \beta_3 &= -9 + 3N_g + \frac{1}{16\pi^2} \left[g_3^2(-54 + 34N_g) + 3N_g g_2^2 + N_g g_1^2 \right. \\ &\quad \left. + N_g g_1'^2 - 4h_t^2 - 4h_b^2 - 2\Sigma_\kappa \right], \\ \beta_2 &= -5 + 3N_g + \frac{1}{16\pi^2} \left[8N_g g_3^2 + (-17 + 21N_g)g_2^2 + \left(\frac{3}{5} + N_g\right) g_1^2 \right. \\ &\quad \left. + \left(\frac{2}{5} + N_g\right) g_1'^2 - 6h_t^2 - 6h_b^2 - 2h_\tau^2 - 2\Sigma_\lambda \right], \\ \beta_1 &= \frac{3}{5} + 3N_g + \frac{1}{16\pi^2} \left[8N_g g_3^2 + \left(\frac{9}{5} + 3N_g\right) g_2^2 + \left(\frac{9}{25} + 3N_g\right) g_1^2 \right. \\ &\quad \left. + \left(\frac{6}{25} + N_g\right) g_1'^2 - \frac{26}{5}h_t^2 - \frac{14}{5}h_b^2 - \frac{18}{5}h_\tau^2 - \frac{6}{5}\Sigma_\lambda - \frac{4}{5}\Sigma_\kappa \right], \\ \beta'_1 &= \frac{2}{5} + 3N_g + \frac{1}{16\pi^2} \left[8N_g g_3^2 + \left(\frac{6}{5} + 3N_g\right) g_2^2 + \left(\frac{6}{25} + N_g\right) g_1^2 \right. \\ &\quad \left. + \left(\frac{4}{25} + 3N_g\right) g_1'^2 - \frac{9}{5}h_t^2 - \frac{21}{5}h_b^2 - \frac{7}{5}h_\tau^2 - \frac{19}{5}\Sigma_\lambda - \frac{57}{10}\Sigma_\kappa \right], \\ \Sigma_\lambda &= \lambda_1^2 + \lambda_2^2 + \lambda_3^2, \quad \Sigma_\kappa = \kappa_1^2 + \kappa_2^2 + \kappa_3^2. \end{aligned} \quad (\text{B.3})$$

The Yukawa couplings appearing in the Superpotential of the cE₆SSM obey the following system of two-loop RGEs:

$$\begin{aligned}
\frac{d\lambda_i}{dt} &= \frac{\lambda_i}{(4\pi)^2} \left[2\lambda_i^2 + 2\Sigma_\lambda + 3\Sigma_\kappa + \left(3h_t^2 + 3h_b^2 + h_\tau^2 \right) \delta_{i3} \right. \\
&\quad \left. - 3g_2^2 - \frac{3}{5}g_1^2 - \frac{19}{10}g_1'^2 + \frac{\beta_{\lambda_i}^{(2)}}{(4\pi)^2} \right], \\
\frac{d\kappa_i}{dt} &= \frac{\kappa_i}{(4\pi)^2} \left[2\kappa_i^2 + 2\Sigma_\lambda + 3\Sigma_\kappa - \frac{16}{3}g_3^2 - \frac{4}{15}g_1^2 - \frac{19}{10}g_1'^2 + \frac{\beta_{\kappa_i}^{(2)}}{(4\pi)^2} \right], \\
\frac{dh_t}{dt} &= \frac{h_t}{(4\pi)^2} \left[\lambda^2 + 6h_t^2 + h_b^2 - \frac{16}{3}g_3^2 - 3g_2^2 - \frac{13}{15}g_1^2 - \frac{3}{10}g_1'^2 + \frac{\beta_{h_t}^{(2)}}{(4\pi)^2} \right], \\
\frac{dh_b}{dt} &= \frac{h_b}{(4\pi)^2} \left[\lambda^2 + h_t^2 + 6h_b^2 + h_\tau^2 - \frac{16}{3}g_3^2 - 3g_2^2 - \frac{7}{15}g_1^2 - \frac{7}{10}g_1'^2 + \frac{\beta_{h_b}^{(2)}}{(4\pi)^2} \right], \\
\frac{dh_\tau}{dt} &= \frac{h_\tau}{(4\pi)^2} \left[\lambda^2 + 3h_b^2 + 4h_\tau^2 - 3g_2^2 - \frac{9}{5}g_1^2 - \frac{7}{10}g_1'^2 + \frac{\beta_{h_\tau}^{(2)}}{(4\pi)^2} \right],
\end{aligned} \tag{B.4}$$

where the two-loop contributions to the corresponding β -functions are given by

$$\begin{aligned}
\beta_{\lambda_i}^{(2)} &= -2\lambda_i^2 \left(\lambda_i^2 + 2\Sigma_\lambda + 3\Sigma_\kappa \right) - 4\Pi_\lambda - 6\Pi_\kappa \\
&\quad - \lambda^2 \left(3h_t^2 + 3h_b^2 + h_\tau^2 \right) (2 + \delta_{i3}) - \left[9h_t^4 + 9h_b^4 + 6h_t^2h_b^2 + 3h_\tau^4 \right] \delta_{i3} \\
&\quad + 16g_3^2\Sigma_\kappa + 6g_2^2\Sigma_\lambda + g_1^2 \left(\frac{4}{5}\Sigma_\kappa + \frac{6}{5}\Sigma_\lambda \right) + g_1'^2 \left(\frac{5}{2}\lambda_i^2 - \frac{9}{5}\Sigma_\kappa - \frac{6}{5}\Sigma_\lambda \right) \\
&\quad + \left[16g_3^2 \left(h_t^2 + h_b^2 \right) + g_1^2 \left(\frac{4}{5}h_t^2 - \frac{2}{5}h_b^2 + \frac{6}{5}h_\tau^2 \right) \right. \\
&\quad \left. + g_1'^2 \left(-\frac{3}{10}h_t^2 - \frac{1}{5}h_b^2 - \frac{1}{5}h_\tau^2 \right) \right] \delta_{i3} + 3g_2^4 \left(3N_g - \frac{7}{2} \right) \\
&\quad + \frac{3}{5}g_1^4 \left(3N_g + \frac{9}{10} \right) + \frac{19}{10}g_1'^4 \left(3N_g + \frac{27}{20} \right) + \frac{9}{5}g_2^2g_1^2 \\
&\quad + \frac{39}{20}g_2^2g_1'^2 + \frac{39}{100}g_1^2g_1'^2,
\end{aligned} \tag{B.5}$$

$$\begin{aligned}
\beta_{\kappa_i}^{(2)} &= -2\kappa_i^2 \left(\kappa_i^2 + 2\Sigma_\lambda + 3\Sigma_\kappa \right) - 4\Pi_\lambda - 6\Pi_\kappa - 2\lambda^2 \left(3h_t^2 + 3h_b^2 + h_\tau^2 \right) \\
&\quad + 16g_3^2\Sigma_\kappa + 6g_2^2\Sigma_\lambda + g_1^2 \left(\frac{4}{5}\Sigma_\kappa + \frac{6}{5}\Sigma_\lambda \right) + g_1'^2 \left(\frac{5}{2}\kappa_i^2 - \frac{9}{5}\Sigma_\kappa - \frac{6}{5}\Sigma_\lambda \right) \\
&\quad + \frac{16}{3}g_3^4 \left(3N_g - \frac{19}{3} \right) + \frac{4}{15}g_1^4 \left(3N_g + \frac{11}{15} \right) + \frac{19}{10}g_1'^4 \left(3N_g + \frac{27}{20} \right) \\
&\quad + \frac{64}{45}g_3^2g_1^2 + \frac{52}{15}g_3^2g_1'^2 + \frac{13}{75}g_1^2g_1'^2,
\end{aligned}$$

$$\begin{aligned}
\beta_{h_t}^{(2)} &= -22h_t^4 - 5h_b^4 - 5h_t^2h_b^2 - h_b^2h_\tau^2 - \lambda^2 \left(\lambda^2 + 3h_t^2 \right. \\
&\quad \left. + 4h_b^2 + h_\tau^2 + 2\Sigma_\lambda + 3\Sigma_\kappa \right) + 16g_3^2h_t^2 + 6g_2^2h_t^2 + g_1^2 \left(\frac{6}{5}h_t^2 + \frac{2}{5}h_b^2 \right) \\
&\quad + g_1'^2 \left(\frac{3}{2}\lambda^2 + \frac{3}{10}h_t^2 + \frac{3}{5}h_b^2 \right) + \frac{16}{3}g_3^4 \left(3N_g - \frac{19}{3} \right) + 3g_2^4 \left(3N_g - \frac{7}{2} \right) \\
&\quad + \frac{13}{15}g_1^4 \left(3N_g + \frac{31}{30} \right) + \frac{3}{10}g_1'^4 \left(3N_g + \frac{11}{20} \right) + 8g_3^2g_2^2 + \frac{136}{45}g_3^2g_1^2 \\
&\quad + \frac{8}{15}g_3^2g_1'^2 + g_2^2g_1^2 + \frac{3}{4}g_2^2g_1'^2 + \frac{53}{300}g_1^2g_1'^2, \\
\beta_{h_b}^{(2)} &= -5h_t^4 - 22h_b^4 - 5h_t^2h_b^2 - 3h_b^2h_\tau^2 - 3h_\tau^4 - \lambda^2 \left(\lambda^2 + 4h_t^2 \right. \\
&\quad \left. + 3h_b^2 + 2\Sigma_\lambda + 3\Sigma_\kappa \right) + 16g_3^2h_b^2 + 6g_2^2h_b^2 + g_1^2 \left(\frac{4}{5}h_t^2 + \frac{2}{5}h_b^2 + \frac{6}{5}h_\tau^2 \right) \\
&\quad + g_1'^2 \left(\lambda^2 + \frac{1}{5}h_t^2 + h_b^2 - \frac{1}{5}h_\tau^2 \right) + \frac{16}{3}g_3^4 \left(3N_g - \frac{19}{3} \right) + 3g_2^4 \left(3N_g - \frac{7}{2} \right) \\
&\quad + \frac{7}{15}g_1^4 \left(3N_g + \frac{5}{6} \right) + \frac{7}{10}g_1'^4 \left(3N_g + \frac{3}{4} \right) + 8g_3^2g_2^2 + \frac{8}{9}g_3^2g_1^2 + \frac{4}{3}g_3^2g_1'^2 \\
&\quad + g_2^2g_1^2 + \frac{3}{2}g_2^2g_1'^2 + \frac{49}{150}g_1^2g_1'^2, \\
\beta_{h_\tau}^{(2)} &= -9h_b^4 - 3h_t^2h_b^2 - 9h_b^2h_\tau^2 - 10h_\tau^4 - \lambda^2 \left(\lambda^2 + 3h_t^2 \right. \\
&\quad \left. + 3h_\tau^2 + 2\Sigma_\lambda + 3\Sigma_\kappa \right) + 16g_3^2h_b^2 + 6g_2^2h_\tau^2 + g_1^2 \left(-\frac{2}{5}h_b^2 + \frac{6}{5}h_\tau^2 \right) \\
&\quad + g_1'^2 \left(\lambda^2 - \frac{1}{5}h_b^2 + \frac{13}{10}h_\tau^2 \right) + 3g_2^4 \left(3N_g - \frac{7}{2} \right) + \frac{9}{5}g_1^4 \left(3N_g + \frac{3}{2} \right) \\
&\quad + \frac{7}{10}g_1'^4 \left(3N_g + \frac{3}{4} \right) + \frac{9}{5}g_2^2g_1^2 + \frac{39}{20}g_2^2g_1'^2 + \frac{51}{100}g_1^2g_1'^2,
\end{aligned}$$

and

$$\Pi_\lambda = \lambda_1^4 + \lambda_2^4 + \lambda_3^4, \quad \Pi_\kappa = \kappa_1^4 + \kappa_2^4 + \kappa_3^4.$$

Using the two-loop β -functions for the gauge and Yukawa couplings and a method proposed in [64], one can obtain the two-loop RGEs for the gaugino masses and trilinear scalar couplings:

$$\begin{aligned}
\frac{dM_3}{dt} &= \frac{g_3^2}{16\pi^2} \left[(-18 + 6N_g)M_3 + \frac{1}{16\pi^2} \left((-216 + 136N_g)g_3^2M_3 + 6N_gg_2^2(M_2 + M_3) \right. \right. \\
&\quad \left. \left. + 2N_gg_1^2(M_1 + M_3) + 2N_gg_1'^2(M_1' + M_3) - 8h_t^2(A_t + M_3) - 8h_b^2(A_b + M_3) \right. \right. \\
&\quad \left. \left. - 4\Sigma_{A_\kappa} - 4\Sigma_\kappa M_3 \right) \right], \\
\frac{dM_2}{dt} &= \frac{g_2^2}{16\pi^2} \left[(-10 + 6N_g)M_2 + \frac{1}{16\pi^2} \left(16N_gg_3^2(M_3 + M_2) + (-68 + 84N_g)g_2^2M_2 \right. \right. \\
&\quad \left. \left. + \left(\frac{6}{5} + 2N_g \right) g_1^2(M_1 + M_2) + \left(\frac{4}{5} + 2N_g \right) g_1'^2(M_1' + M_2) - 12h_t^2(A_t + M_2) \right. \right. \\
&\quad \left. \left. - 12h_b^2(A_b + M_2) - 4h_\tau^2(A_\tau + M_2) - 4\Sigma_{A_\lambda} - 4\Sigma_\lambda M_2 \right) \right],
\end{aligned}$$

$$\begin{aligned}
\frac{dM_1}{dt} &= \frac{g_1^2}{16\pi^2} \left[\left(\frac{6}{5} + 6N_g \right) M_1 + \frac{1}{16\pi^2} \left(16N_g g_3^2 (M_3 + M_1) \right. \right. \\
&+ \left. \left(\frac{18}{5} + 6N_g \right) g_2^2 (M_2 + M_1) + \left(\frac{36}{25} + 12N_g \right) g_1^2 M_1 \right. \\
&+ \left. \left(\frac{12}{25} + 2N_g \right) g_1'^2 (M_1' + M_1) - \frac{52}{5} h_t^2 (A_t + M_1) - \frac{28}{5} h_b^2 (A_b + M_1) \right. \\
&\left. - \frac{36}{5} h_\tau^2 (A_\tau + M_1) - \frac{12}{5} \Sigma_{A_\lambda} - \frac{12}{5} \Sigma_\lambda M_1 - \frac{8}{5} \Sigma_{A_\kappa} - \frac{8}{5} \Sigma_\kappa M_1 \right), \tag{B.6} \\
\frac{dM_1'}{dt} &= \frac{g_1'^2}{16\pi^2} \left[\left(\frac{4}{5} + 6N_g \right) M_1' + \frac{1}{16\pi^2} \left(16N_g g_3^2 (M_3 + M_1') \right. \right. \\
&+ \left. \left(\frac{12}{5} + 6N_g \right) g_2^2 (M_2 + M_1') + \left(\frac{12}{25} + 2N_g \right) g_1^2 (M_1 + M_1') \right. \\
&+ \left. \left(\frac{16}{25} + 12N_g \right) g_1'^2 M_1' - \frac{18}{5} h_t^2 (A_t + M_1') - \frac{42}{5} h_b^2 (A_b + M_1') \right. \\
&\left. - \frac{14}{5} h_\tau^2 (A_\tau + M_1') - \frac{38}{5} \Sigma_{A_\lambda} - \frac{38}{5} \Sigma_\lambda M_1' - \frac{57}{5} \Sigma_{A_\kappa} - \frac{57}{5} \Sigma_\kappa M_1' \right),
\end{aligned}$$

$$\begin{aligned}
\frac{dA_{\lambda_i}}{dt} &= \frac{1}{(4\pi)^2} \left[4\lambda_i^2 A_{\lambda_i} + 4\Sigma_{A_\lambda} + 6\Sigma_{A_\kappa} + (6h_t^2 A_t + 6h_b^2 A_b + 2h_\tau^2 A_\tau) \delta_{i3} \right. \\
&\left. - 6g_2^2 M_2 - \frac{6}{5} g_1^2 M_1 - \frac{19}{5} g_1'^2 M_1' + \frac{\beta_{A_{\lambda_i}}^{(2)}}{(4\pi)^2} \right], \\
\frac{dA_{\kappa_i}}{dt} &= \frac{1}{(4\pi)^2} \left[4\kappa_i^2 A_{\kappa_i} + 4\Sigma_{A_\lambda} + 6\Sigma_{A_\kappa} - \frac{32}{3} g_3^2 M_3 - \frac{8}{15} g_1^2 M_1 \right. \\
&\left. - \frac{19}{5} g_1'^2 M_1' + \frac{\beta_{A_{\kappa_i}}^{(2)}}{(4\pi)^2} \right], \\
\frac{dA_t}{dt} &= \frac{1}{(4\pi)^2} \left[2\lambda^2 A_\lambda + 12h_t^2 A_t + 2h_b^2 A_b - \frac{32}{3} g_3^2 M_3 - 6g_2^2 M_2 \right. \\
&\left. - \frac{26}{15} g_1^2 M_1 - \frac{3}{5} g_1'^2 M_1' + \frac{\beta_{A_t}^{(2)}}{(4\pi)^2} \right], \tag{B.7} \\
\frac{dA_b}{dt} &= \frac{1}{(4\pi)^2} \left[2\lambda^2 A_\lambda + 2h_t^2 A_t + 12h_b^2 A_b + 2h_\tau^2 A_\tau - \frac{32}{3} g_3^2 M_3 - 6g_2^2 M_2 \right. \\
&\left. - \frac{14}{15} g_1^2 M_1 - \frac{7}{5} g_1'^2 M_1' + \frac{\beta_{A_b}^{(2)}}{(4\pi)^2} \right], \\
\frac{dA_\tau}{dt} &= \frac{1}{(4\pi)^2} \left[2\lambda^2 A_\lambda + 6h_b^2 A_b + 8h_\tau^2 A_\tau - 6g_2^2 M_2 - \frac{18}{5} g_1^2 M_1 - \frac{7}{5} g_1'^2 M_1' + \frac{\beta_{A_\tau}^{(2)}}{(4\pi)^2} \right],
\end{aligned}$$

where the two-loop contributions to the β -functions of trilinear scalar couplings are given

by

$$\begin{aligned}
\beta_{A_{\lambda_i}}^{(2)} &= -4\lambda_i^2 \left(\lambda_i^2 + 2\Sigma_\lambda + 3\Sigma_\kappa \right) A_{\lambda_i} - 4\lambda_i^2 \left(\lambda_i^2 A_{\lambda_i} + 2\Sigma_{A_\lambda} + 3\Sigma_{A_\kappa} \right) - 16\Pi_{A_\lambda} - 24\Pi_{A_\kappa} \\
&\quad - 2\lambda^2 \left(3h_t^2 + 3h_b^2 + h_\tau^2 \right) (2 + \delta_{i3}) A_\lambda - 2\lambda^2 \left(3h_t^2 A_t + 3h_b^2 A_b + h_\tau^2 A_\tau \right) (2 + \delta_{i3}) \\
&\quad - 12 \left[3h_t^4 A_t + 3h_b^4 A_b + h_t^2 h_b^2 (A_t + A_b) + h_\tau^4 A_\tau \right] \delta_{i3} + 32g_3^2 \left(\Sigma_\kappa M_3 + \Sigma_{A_\kappa} \right) \\
&\quad + 12g_2^2 \left(\Sigma_\lambda M_2 + \Sigma_{A_\lambda} \right) + 2g_1^2 \left[\left(\frac{4}{5}\Sigma_\kappa + \frac{6}{5}\Sigma_\lambda \right) M_1 + \frac{4}{5}\Sigma_{A_\kappa} + \frac{6}{5}\Sigma_{A_\lambda} \right] \\
&\quad + 2g_1'^2 \left[\left(\frac{5}{2}\lambda_i^2 - \frac{9}{5}\Sigma_\kappa - \frac{6}{5}\Sigma_\lambda \right) M_1' + \frac{5}{2}\lambda_i^2 A_{\lambda_i} - \frac{9}{5}\Sigma_{A_\kappa} - \frac{6}{5}\Sigma_{A_\lambda} \right] \\
&\quad + 32g_3^2 \left[\left(h_t^2 + h_b^2 \right) M_3 + h_t^2 A_t + h_b^2 A_b \right] \delta_{i3} + 2g_1^2 \left[\left(\frac{4}{5}h_t^2 - \frac{2}{5}h_b^2 + \frac{6}{5}h_\tau^2 \right) M_1 + \frac{4}{5}h_t^2 A_t \right. \\
&\quad \left. - \frac{2}{5}h_b^2 A_b + \frac{6}{5}h_\tau^2 A_\tau \right] \delta_{i3} + g_1'^2 \left[\left(-\frac{3}{5}h_t^2 - \frac{2}{5}h_b^2 - \frac{2}{5}h_\tau^2 \right) M_1' - \frac{3}{5}h_t^2 A_t - \frac{2}{5}h_b^2 A_b \right. \\
&\quad \left. - \frac{2}{5}h_\tau^2 A_\tau \right] \delta_{i3} + 12g_2^4 \left(3N_g - \frac{7}{2} \right) M_2 + \frac{12}{5}g_1^4 \left(3N_g + \frac{9}{10} \right) M_1 + \frac{38}{5}g_1'^4 \left(3N_g + \frac{27}{20} \right) M_1' \\
&\quad + \frac{18}{5}g_2^2 g_1^2 \left(M_2 + M_1 \right) + \frac{39}{10}g_2^2 g_1'^2 \left(M_2 + M_1' \right) + \frac{39}{50}g_1^2 g_1'^2 \left(M_1 + M_1' \right),
\end{aligned}$$

$$\begin{aligned}
\beta_{A_{\kappa_i}}^{(2)} &= -4\kappa_i^2 \left(\kappa_i^2 + 2\Sigma_\lambda + 3\Sigma_\kappa \right) A_{\kappa_i} - 4\kappa_i^2 \left(\kappa_i^2 A_{\kappa_i} + 2\Sigma_{A_\lambda} + 3\Sigma_{A_\kappa} \right) - 16\Pi_{A_\lambda} - 24\Pi_{A_\kappa} \\
&\quad - 4\lambda^2 \left(3h_t^2 + 3h_b^2 + h_\tau^2 \right) A_\lambda - 4\lambda^2 \left(3h_t^2 A_t + 3h_b^2 A_b + h_\tau^2 A_\tau \right) + 32g_3^2 \left(\Sigma_\kappa M_3 + \Sigma_{A_\kappa} \right) \\
&\quad + 12g_2^2 \left(\Sigma_\lambda M_2 + \Sigma_{A_\lambda} \right) + 2g_1^2 \left[\left(\frac{4}{5}\Sigma_\kappa + \frac{6}{5}\Sigma_\lambda \right) M_1 + \frac{4}{5}\Sigma_{A_\kappa} + \frac{6}{5}\Sigma_{A_\lambda} \right] \\
&\quad + 2g_1'^2 \left[\left(\frac{5}{2}\kappa_i^2 - \frac{9}{5}\Sigma_\kappa - \frac{6}{5}\Sigma_\lambda \right) M_1' + \frac{5}{2}\kappa_i^2 A_{\kappa_i} - \frac{9}{5}\Sigma_{A_\kappa} - \frac{6}{5}\Sigma_{A_\lambda} \right] \\
&\quad + \frac{64}{3}g_3^4 \left(3N_g - \frac{19}{3} \right) M_3 + \frac{16}{15}g_1^4 \left(3N_g + \frac{11}{15} \right) M_1 + \frac{38}{5}g_1'^4 \left(3N_g + \frac{27}{20} \right) M_1' \\
&\quad + \frac{128}{45}g_3^2 g_1^2 \left(M_3 + M_1 \right) + \frac{104}{15}g_3^2 g_1'^2 \left(M_3 + M_1' \right) + \frac{26}{75}g_1^2 g_1'^2 \left(M_1 + M_1' \right),
\end{aligned}$$

$$\begin{aligned}
\beta_{A_t}^{(2)} &= -88h_t^4 A_t - 20h_b^4 A_b - 10h_t^2 h_b^2 \left(A_t + A_b \right) - 2h_b^2 h_\tau^2 \left(A_b + A_\tau \right) - 2\lambda^2 \left[\left(2\lambda^2 + 3h_t^2 \right. \right. \\
&\quad \left. \left. + 4h_b^2 + h_\tau^2 + 2\Sigma_\lambda + 3\Sigma_\kappa \right) A_\lambda + 3h_t^2 A_t + 4h_b^2 A_b + h_\tau^2 A_\tau + 2\Sigma_{A_\lambda} + 3\Sigma_{A_\kappa} \right] \\
&\quad + 32g_3^2 h_t^2 \left(M_3 + A_t \right) + 12g_2^2 h_t^2 \left(M_2 + A_t \right) + 2g_1^2 \left[\left(\frac{6}{5}h_t^2 + \frac{2}{5}h_b^2 \right) M_1 + \frac{6}{5}h_t^2 A_t \right. \\
&\quad \left. + \frac{2}{5}h_b^2 A_b \right] + 2g_1'^2 \left[\left(\frac{3}{2}\lambda^2 + \frac{3}{10}h_t^2 + \frac{3}{5}h_b^2 \right) M_1' + \frac{3}{2}\lambda^2 A_\lambda + \frac{3}{10}h_t^2 A_t + \frac{3}{5}h_b^2 A_b \right] \\
&\quad + \frac{64}{3}g_3^4 \left(3N_g - \frac{19}{3} \right) M_3 + 12g_2^4 \left(3N_g - \frac{7}{2} \right) M_2 + \frac{52}{15}g_1^4 \left(3N_g + \frac{31}{30} \right) M_1 \\
&\quad + \frac{6}{5}g_1'^4 \left(3N_g + \frac{11}{20} \right) M_1' + 16g_3^2 g_2^2 \left(M_3 + M_2 \right) + \frac{272}{45}g_3^2 g_1^2 \left(M_3 + M_1 \right) \\
&\quad + \frac{16}{15}g_3^2 g_1'^2 \left(M_3 + M_1' \right) + 2g_2^2 g_1^2 \left(M_2 + M_1 \right) + \frac{3}{2}g_2^2 g_1'^2 \left(M_2 + M_1' \right) + \frac{53}{150}g_1^2 g_1'^2 \left(M_1 + M_1' \right),
\end{aligned}$$

$$\begin{aligned}
\beta_{A_b}^{(2)} &= -20h_t^4 A_t - 88h_b^4 A_b - 10h_t^2 h_b^2 (A_t + A_b) - 6h_b^2 h_\tau^2 (A_b + A_\tau) - 12h_\tau^4 A_\tau \\
&\quad - 2\lambda^2 \left[\left(2\lambda^2 + 4h_t^2 + 3h_b^2 + 2\Sigma_\lambda + 3\Sigma_\kappa \right) A_\lambda + 4h_t^2 A_t + 3h_b^2 A_b + 2\Sigma_{A_\lambda} + 3\Sigma_{A_\kappa} \right] \\
&\quad + 32g_3^2 h_b^2 (M_3 + A_b) + 12g_2^2 h_b^2 (M_2 + A_b) + 4g_1^2 \left[\left(\frac{2}{5}h_t^2 + \frac{1}{5}h_b^2 + \frac{3}{5}h_\tau^2 \right) M_1 \right. \\
&\quad \left. + \frac{2}{5}h_t^2 A_t + \frac{1}{5}h_b^2 A_b + \frac{3}{5}h_\tau^2 A_\tau \right] + 2g_1'^2 \left[\left(\lambda^2 + \frac{1}{5}h_t^2 + h_b^2 - \frac{1}{5}h_\tau^2 \right) M_1' + \lambda^2 A_\lambda \right. \\
&\quad \left. + \frac{1}{5}h_t^2 A_t + h_b^2 A_b - \frac{1}{5}h_\tau^2 A_\tau \right] + \frac{64}{3}g_3^4 \left(3N_g - \frac{19}{3} \right) M_3 + 12g_2^4 \left(3N_g - \frac{7}{2} \right) M_2 \\
&\quad + \frac{28}{15}g_1^4 \left(3N_g + \frac{5}{6} \right) M_1 + \frac{14}{5}g_1'^4 \left(3N_g + \frac{3}{4} \right) M_1' + 16g_3^2 g_2^2 (M_3 + M_2) \\
&\quad + \frac{16}{9}g_3^2 g_1^2 (M_3 + M_1) + \frac{8}{3}g_3^2 g_1'^2 (M_3 + M_1') + 2g_2^2 g_1^2 (M_2 + M_1) \\
&\quad + 3g_2^2 g_1'^2 (M_2 + M_1') + \frac{49}{75}g_1^2 g_1'^2 (M_1 + M_1'), \\
\beta_{A_\tau}^{(2)} &= -36h_b^4 A_b - 6h_t^2 h_b^2 (A_t + A_b) - 18h_b^2 h_\tau^2 (A_b + A_\tau) - 40h_\tau^4 A_\tau - 2\lambda^2 \left[\left(2\lambda^2 + 3h_t^2 \right. \right. \\
&\quad \left. \left. + 3h_b^2 + 2\Sigma_\lambda + 3\Sigma_\kappa \right) A_\lambda + 3h_t^2 A_t + 3h_b^2 A_b + 2\Sigma_{A_\lambda} + 3\Sigma_{A_\kappa} \right] + 32g_3^2 h_b^2 (M_3 + A_b) \\
&\quad + 12g_2^2 h_\tau^2 (M_2 + A_\tau) + 4g_1^2 \left[\left(-\frac{1}{5}h_b^2 + \frac{3}{5}h_\tau^2 \right) M_1 - \frac{1}{5}h_b^2 A_b + \frac{3}{5}h_\tau^2 A_\tau \right] \\
&\quad + 2g_1'^2 \left[\left(\lambda^2 - \frac{1}{5}h_b^2 + \frac{13}{10}h_\tau^2 \right) M_1' + \lambda^2 A_\lambda - \frac{1}{5}h_b^2 A_b + \frac{13}{10}h_\tau^2 A_\tau \right] \\
&\quad + 12g_2^4 \left(3N_g - \frac{7}{2} \right) M_2 + \frac{36}{5}g_1^4 \left(3N_g + \frac{3}{2} \right) M_1 + \frac{14}{5}g_1'^4 \left(3N_g + \frac{3}{4} \right) M_1' \\
&\quad + \frac{18}{5}g_2^2 g_1^2 (M_2 + M_1) + \frac{39}{10}g_2^2 g_1'^2 (M_2 + M_1') + \frac{51}{50}g_1^2 g_1'^2 (M_1 + M_1'),
\end{aligned}$$

whereas

$$\begin{aligned}
\Sigma_{A_\lambda} &= \lambda_1^2 A_{\lambda_1} + \lambda_2^2 A_{\lambda_2} + \lambda_3^2 A_{\lambda_3}, & \Sigma_{A_\kappa} &= \kappa_1^2 A_{\kappa_1} + \kappa_2^2 A_{\kappa_2} + \kappa_3^2 A_{\kappa_3}, \\
\Pi_\lambda &= \lambda_1^4 A_{\lambda_1} + \lambda_2^4 A_{\lambda_2} + \lambda_3^4 A_{\lambda_3}, & \Pi_\kappa &= \kappa_1^4 A_{\kappa_1} + \kappa_2^4 A_{\kappa_2} + \kappa_3^4 A_{\kappa_3}.
\end{aligned}$$

The one-loop RGEs for the soft scalar masses can be written as

$$\begin{aligned}
\frac{dm_{S_i}^2}{dt} &= \frac{1}{(4\pi)^2} \left[\sum_{j=1..3} 4\lambda_j^2 \left(m_{H_j^u}^2 + m_{H_j^d}^2 + m_S^2 + A_{\lambda_j}^2 \right) \delta_{i3} \right. \\
&\quad \left. + \sum_{j=1..3} 6\kappa_j^2 \left(m_S^2 + m_{D_j}^2 + m_{\overline{D}_j}^2 + A_{\kappa_j}^2 \right) \delta_{i3} - 5g_1'^2 M_1'^2 + \frac{g_1'^2}{4} \Sigma_1' \right], \\
\frac{dm_{H_i^u}^2}{dt} &= \frac{1}{(4\pi)^2} \left[2\lambda_i^2 \left(m_{H_i^u}^2 + m_{H_i^d}^2 + m_S^2 + A_{\lambda_i}^2 \right) + 6h_t^2 \left(m_{H_u}^2 + m_Q^2 + m_{t^c}^2 + A_t^2 \right) \delta_{i3} \right. \\
&\quad \left. - 6g_2^2 M_2^2 - \frac{6}{5}g_1^2 M_1^2 - \frac{4}{5}g_1'^2 M_1'^2 + \frac{3}{5}g_1^2 \Sigma_1 - \frac{g_1'^2}{10} \Sigma_1' \right],
\end{aligned}$$

$$\begin{aligned}
\frac{dm_{H_i^d}^2}{dt} &= \frac{1}{(4\pi)^2} \left[2\lambda_i^2 \left(m_{H_i^u}^2 + m_{H_i^d}^2 + m_S^2 + A_{\lambda_i}^2 \right) + 6h_b^2 \left(m_{H_d}^2 + m_Q^2 + m_{b^c}^2 + A_b^2 \right) \delta_{i3} \right. \\
&\quad \left. + 2h_\tau^2 \left(m_{H_d}^2 + m_L^2 + m_{\tau^c}^2 + A_\tau^2 \right) \delta_{i3} - 6g_2^2 M_2^2 - \frac{6}{5}g_1^2 M_1^2 - \frac{9}{5}g_1'^2 M_1'^2 \right. \\
&\quad \left. - \frac{3}{5}g_1^2 \Sigma_1 - \frac{3}{20}g_1'^2 \Sigma_1' \right], \\
\frac{dm_{Q_i}^2}{dt} &= \frac{1}{(4\pi)^2} \left[2h_t^2 \left(m_{H_u}^2 + m_Q^2 + m_{t^c}^2 + A_t^2 \right) \delta_{i3} + 2h_b^2 \left(m_{H_d}^2 + m_Q^2 + m_{b^c}^2 + A_b^2 \right) \delta_{i3} \right. \\
&\quad \left. - \frac{32}{3}g_3^2 M_3^2 - 6g_2^2 M_2^2 - \frac{2}{15}g_1^2 M_1^2 - \frac{1}{5}g_1'^2 M_1'^2 + \frac{1}{5}g_1^2 \Sigma_1 + \frac{g_1'^2}{20} \Sigma_1' \right], \\
\frac{dm_{u_i^c}^2}{dt} &= \frac{1}{(4\pi)^2} \left[4h_t^2 \left(m_{H_u}^2 + m_Q^2 + m_{t^c}^2 + A_t^2 \right) \delta_{i3} - \frac{32}{3}g_3^2 M_3^2 - \frac{32}{15}g_1^2 M_1^2 - \frac{1}{5}g_1'^2 M_1'^2 \right. \\
&\quad \left. - \frac{4}{5}g_1^2 \Sigma_1 + \frac{g_1'^2}{20} \Sigma_1' \right], \\
\frac{dm_{d_i^c}^2}{dt} &= \frac{1}{(4\pi)^2} \left[4h_b^2 \left(m_{H_d}^2 + m_Q^2 + m_{b^c}^2 + A_b^2 \right) \delta_{i3} - \frac{32}{3}g_3^2 M_3^2 - \frac{8}{15}g_1^2 M_1^2 - \frac{4}{5}g_1'^2 M_1'^2 \right. \\
&\quad \left. + \frac{2}{5}g_1^2 \Sigma_1 + \frac{g_1'^2}{10} \Sigma_1' \right], \\
\frac{dm_{L_i}^2}{dt} &= \frac{1}{(4\pi)^2} \left[2h_\tau^2 \left(m_{H_d}^2 + m_L^2 + m_{\tau^c}^2 + A_\tau^2 \right) \delta_{i3} + -6g_2^2 M_2^2 - \frac{6}{5}g_1^2 M_1^2 - \frac{4}{5}g_1'^2 M_1'^2 \right. \\
&\quad \left. - \frac{3}{5}g_1^2 \Sigma_1 + \frac{g_1'^2}{10} \Sigma_1' \right], \quad (\text{B.8}) \\
\frac{dm_{e_i^c}^2}{dt} &= \frac{1}{(4\pi)^2} \left[4h_\tau^2 \left(m_{H_d}^2 + m_L^2 + m_{\tau^c}^2 + A_\tau^2 \right) \delta_{i3} - \frac{24}{5}g_1^2 M_1^2 - \frac{1}{5}g_1'^2 M_1'^2 \right. \\
&\quad \left. + \frac{6}{5}g_1^2 \Sigma_1 + \frac{g_1'^2}{20} \Sigma_1' \right], \\
\frac{dm_{D_i}^2}{dt} &= \frac{1}{(4\pi)^2} \left[2\kappa_i^2 \left(m_S^2 + m_{D_i}^2 + m_{D_i}^2 + A_{\kappa_i}^2 \right) - \frac{32}{3}g_3^2 M_3^2 - \frac{8}{15}g_1^2 M_1^2 - \frac{4}{5}g_1'^2 M_1'^2 \right. \\
&\quad \left. - \frac{2}{5}g_1^2 \Sigma_1 - \frac{g_1'^2}{10} \Sigma_1' \right], \\
\frac{dm_{\bar{D}_i}^2}{dt} &= \frac{1}{(4\pi)^2} \left[2\kappa_i^2 \left(m_S^2 + m_{D_i}^2 + m_{D_i}^2 + A_{\kappa_i}^2 \right) - \frac{32}{3}g_3^2 M_3^2 - \frac{8}{15}g_1^2 M_1^2 - \frac{9}{5}g_1'^2 M_1'^2 \right. \\
&\quad \left. + \frac{2}{5}g_1^2 \Sigma_1 - \frac{3}{20}g_1'^2 \Sigma_1' \right], \\
\frac{dm_{H'}^2}{dt} &= \frac{1}{(4\pi)^2} \left[-6g_2^2 M_2^2 - \frac{6}{5}g_1^2 M_1^2 - \frac{4}{5}g_1'^2 M_1'^2 - \frac{3}{5}g_1^2 \Sigma_1 + \frac{g_1'^2}{10} \Sigma_1' \right], \\
\frac{dm_{\bar{H}'}^2}{dt} &= \frac{1}{(4\pi)^2} \left[-6g_2^2 M_2^2 - \frac{6}{5}g_1^2 M_1^2 - \frac{4}{5}g_1'^2 M_1'^2 + \frac{3}{5}g_1^2 \Sigma_1 - \frac{g_1'^2}{10} \Sigma_1' \right],
\end{aligned}$$

where

$$\begin{aligned}
\Sigma_1 &= \sum_{i=1}^3 \left(m_{Q_i}^2 - 2m_{u_i^c}^2 + m_{d_i^c}^2 + m_{e_i^c}^2 - m_{L_i}^2 + m_{H_i^u}^2 - m_{H_i^d}^2 + m_{D_i}^2 - m_{\bar{D}_i}^2 \right) - m_{H'}^2 + m_{\bar{H}'}^2, \\
\Sigma_1' &= \sum_{i=1}^3 \left(6m_{Q_i}^2 + 3m_{u_i^c}^2 + 6m_{d_i^c}^2 + m_{e_i^c}^2 + 4m_{L_i}^2 - 4m_{H_i^u}^2 - 6m_{H_i^d}^2 + 5m_{S_i}^2 - 9m_{D_i}^2 - 6m_{\bar{D}_i}^2 \right) + 4m_{H'}^2 - 4m_{\bar{H}'}^2.
\end{aligned}$$

References

- [1] H.P. Nilles, Phys. Rept. **110** (1984) 1; A.B. Lahanas, D.V. Nanopoulos, Phys. Rept. **145** (1987) 1.
- [2] A. H. Chamseddine, R. L. Arnowitt and P. Nath, Phys. Rev. Lett. **49** (1982) 970; R. Barbieri, S. Ferrara, C. Savoy, Phys. Lett. B **119** (1982) 343; H. P. Nilles, M. Srednicki, D. Wyler, Phys. Lett. B **120** (1983) 345; L. Hall, J. Lykken, S. Weinberg, Phys. Rev. D **27** (1983) 2359; S. K. Soni, H. A. Weldon, Phys. Lett. B **126** (1983) 215. P. Nath, R. L. Arnowitt and A. H. Chamseddine, Nucl. Phys. B **227** (1983) 121.
- [3] E. Witten, Nucl. Phys. B **188** (1981) 513; N. Sakai, Z. Phys. C **11** (1981) 153; S. Dimopoulos, H. Georgi, Nucl. Phys. B **193** (1981) 150; R. K. Kaul, P. Majumdar, Nucl. Phys. B **199** (1982) 36.
- [4] D. J. H. Chung, L. L. Everett, G. L. Kane, S. F. King, J. Lykken, L. T. Wang, Phys. Rept. **407** (2005) 1.
- [5] L. Girardello, M.T. Grisaru, Nucl. Phys. B **194** (1982) 65.
- [6] J. Ellis, S. Kelley, D. V. Nanopoulos, Phys. Lett. B **249** (1990) 441; J. Ellis, S. Kelley, D. V. Nanopoulos, Phys. Lett. B **260** (1991) 131; U. Amaldi, W. de Boer, H. Furstenau, Phys. Lett. B **260** (1991) 447; P. Langacker, M. Luo, Phys. Rev. D **44** (1991) 817.
- [7] H. Georgi, S. L. Glashow, Phys. Rev. Lett. **32** (1974) 438.
- [8] A. Salam, J. Strathdee, Phys. Rev. D **11** (1975) 1521; M. T. Grisaru, W. Siegel, M. Rocek, Nucl. Phys. B **159** (1979) 429.
- [9] M. B. Green, J. H. Schwarz, E. Witten, “Superstring Theory” (Cambridge University Press, 1987).
- [10] P. Horava, E. Witten, Nucl. Phys. B **460** (1996) 506 and Nucl. Phys. B **475** (1996) 94.
- [11] E. Witten, Nucl. Phys. B **471** (1996) 135; T. Banks, M. Dine, Nucl. Phys. B **479** (1996) 173; K. Choi, H. B. Kim, C. Muñoz, Phys. Rev. D **57** (1998) 7521.
- [12] F. del Aguila, G. A. Blair, M. Daniel, G. G. Ross, Nucl. Phys. B **272** (1986) 413.
- [13] V.S. Kaplunovsky, J. Louis, Phys. Lett. B **306** (1993) 269; A. Brignole, L.E. Ibañez, C. Muñoz, Nucl. Phys. B **422** (1994) 125 [Erratum-ibid. B **436** (1995) 747].

- [14] Y. Hosotani, Phys. Lett. B **129** (1983) 193.
- [15] J.L. Hewett, T.G. Rizzo, Phys. Rept. **183** (1989) 193.
- [16] P. Athron, S. F. King, D. J. Miller, S. Moretti, R. Nevzorov, J. Phys. Conf. Ser. **110** (2008) 072001.
- [17] H. P. Nilles, M. Srednicki, D. Wyler, Phys. Lett. B **120** (1983) 346; J. M. Frere, D. R. T. Jones, S. Raby, Nucl. Phys. B **222** (1983) 11; J. P. Derendinger, C. A. Savoy, Nucl. Phys. B **237** (1984) 307; M. I. Vysotsky, K. A. Ter-Martirosian, Sov. Phys. JETP **63** (1986) 489; J. Ellis, J. F. Gunion, H. Haber, L. Roszkowski, F. Zwirner, Phys. Rev. D **39** (1989) 844; L. Durand, J. L. Lopez, Phys. Lett. B **217** (1989) 463; M. Drees, Int. J. Mod. Phys. A **4** (1989) 3635; C. Panagiotakopoulos, K. Tamvakis, Phys. Lett. B **446** (1999) 224 and Phys. Lett. B **469** (1999) 145; C. Panagiotakopoulos, A. Pilaftsis, Phys. Rev. D **63** (2001) 055003; A. Dedes, C. Hugonie, S. Moretti, K. Tamvakis, Phys. Rev. D **63** (2001) 055009.
- [18] S. A. Abel, S. Sarkar, P. L. White, Nucl. Phys. B **454** (1995) 663.
- [19] J. F. Gunion, H. E. Haber, G. L. Kane, S. Dawson, “The Higgs Hunter’s Guide” (Westview Press, 2000) [Erratum arXiv:hep-ph/9302272]; P. Binetruy, S. Dawson, I. Hinchliffe, M. Sher, Nucl. Phys. B **273** (1986) 501; J. R. Ellis, K. Enqvist, D. V. Nanopoulos, F. Zwirner, Mod. Phys. Lett. A **1** (1986) 57. L. E. Ibanez, J. Mas, Nucl. Phys. B **286** (1987) 107; J. F. Gunion, L. Roszkowski, H. E. Haber, Phys. Lett. B **189** (1987) 409; H. E. Haber, M. Sher, Phys. Rev. D **35** (1987) 2206; J. R. Ellis, D. V. Nanopoulos, S. T. Petcov, F. Zwirner, Nucl. Phys. B **283** (1987) 93; M. Drees, Phys. Rev. D **35** (1987) 2910; J. F. Gunion, L. Roszkowski, H. E. Haber, Phys. Lett. B **189** (1987) 409. H. Baer, D. Dicus, M. Drees, X. Tata, Phys. Rev. D **36** (1987) 1363; J. F. Gunion, L. Roszkowski, H. E. Haber, Phys. Rev. D **38** (1988) 105.
- [20] M. Cvetič, P. Langacker, Phys. Rev. D **54** (1996) 3570; M. Cvetič, P. Langacker, Mod. Phys. Lett. A **11** (1996) 1247; M. Cvetič, D. Demir, J. R. Espinosa, L. L. Everett, P. Langacker, Phys. Rev. D **56** (1997) 2861 [Erratum-ibid. D **58** (1998) 119905].
- [21] P. Langacker, J. Wang, Phys. Rev. D **58** (1998) 115010.
- [22] D. Suematsu, Y. Yamagishi, Int. J. Mod. Phys. A **10** (1995) 4521.
- [23] E. Keith, E. Ma, Phys. Rev. D **56** (1997) 7155.
- [24] Y. Daikoku, D. Suematsu, Phys. Rev. D **62** (2000) 095006.

- [25] J. H. Kang, P. Langacker, T. J. Li, Phys. Rev. D **71** (2005) 015012.
- [26] E. Ma, Phys. Lett. B **380** (1996) 286.
- [27] T. Hambye, E. Ma, M. Raidal, U. Sarkar, Phys. Lett. B **512** (2001) 373.
- [28] S. F. King, R. Luo, D. J. Miller, R. Nevzorov, JHEP **0812** (2008) 042.
- [29] E. Ma, M. Raidal, J. Phys. G **28** (2002) 95; J. Kang, P. Langacker, T.-J. Li, T. Liu, Phys. Rev. Lett. **94** (2005) 061801.
- [30] J. A. Grifols, J. Sola, A. Mendez, Phys. Rev. Lett. **57** (1986) 2348; D. A. Morris, Phys. Rev. D **37** (1988) 2012.
- [31] D. Suematsu, Mod. Phys. Lett. A **12** (1997) 1709.
- [32] D. Suematsu, Phys. Lett. B **416** (1998) 108.
- [33] S. F. King, S. Moretti, R. Nevzorov, Phys. Rev. D **73** (2006) 035009.
- [34] S. F. King, S. Moretti, R. Nevzorov, Phys. Lett. B **634** (2006) 278.
- [35] D. Suematsu, Phys. Rev. D **57** (1998) 1738.
- [36] E. Keith, E. Ma, Phys. Rev. D **54** (1996) 3587.
- [37] P. Athron, S. F. King, D. J. Miller, S. Moretti, R. Nevzorov, arXiv:0901.1192 [hep-ph].
- [38] P. Athron, S. F. King, D. J. Miller, S. Moretti, R. Nevzorov, arXiv:0810.0617 [hep-ph].
- [39] J. Rich, M. Spiro, J. Lloyd–Owen, Phys. Rept. **151** (1987) 239; P. F. Smith, Contemp. Phys. **29** (1988) 159; T. K. Hemmick et al., Phys. Rev. D **41** (1990) 2074.
- [40] S. Wolfram, Phys. Lett. B **82** (1979) 65; C. B. Dover, T. K. Gaisser, G. Steigman, Phys. Rev. Lett. **42** (1979) 1117.
- [41] S. F. King, S. Moretti, R. Nevzorov, Phys. Lett. B **650** (2007) 57.
- [42] Y. Kawamura, Prog. Theor. Phys. **105** (2001) 999; G. Altarelli, F. Feruglio, Phys. Lett. B **511** (2001) 257; L. J. Hall, Y. Nomura, Phys. Rev. D **64** (2001) 055003; A. Hebecker, J. March-Russell, Nucl. Phys. B **613** (2001) 3; T. Asaka, W. Buchmuller, L. Covi, Phys. Lett. B **523** (2001) 199; L. J. Hall, Y. Nomura, T. Okui, D. R. Smith, Phys. Rev. D **65** (2002) 035008.

- [43] S. F. King, S. Moretti, R. Nevzorov, arXiv:hep-ph/0601269; S. Kraml *et al.* (eds.), *Workshop on CP studies and non-standard Higgs physics*, CERN–2006–009, hep-ph/0608079; S. F. King, S. Moretti, R. Nevzorov, AIP Conf. Proc. **881** (2007) 138; R. Howl, S. F. King, JHEP **0801** (2008) 030; S. F. King, S. Moretti, R. Nevzorov, *In *Moscow 2006, ICHEP* 1125-1128.*
- [44] G. F. Giudice, A. Masiero, Phys. Lett. B **206** (1988) 480; J. A. Casas, C. Muñoz, Phys. Lett. B **306** (1993) 288.
- [45] R. Howl, S. F. King, JHEP **0805** (2008) 008.
- [46] M. Fukugita, T. Yanagida, Phys. Lett. B **174** (1986) 45.
- [47] M. Yu. Khlopov, A. D. Linde, Phys. Lett. B **138** (1984) 265; J. R. Ellis, J. E. Kim,, D. V. Nanopoulos, Phys. Lett. B **145** (1984) 181.
- [48] V. A. Kuzmin, V. A. Rubakov, M. E. Shaposhnikov, Phys. Lett. B **155** (1985) 36; V. A. Rubakov, M. E. Shaposhnikov, Usp. Fiz. Nauk, **166** (1996) 493.
- [49] L. E. Ibáñez, G. G. Ross, Phys. Lett. B **110** (1982) 215; J. R. Ellis, D. V. Nanopoulos, K. Tamvakis, Phys. Lett. B **121** (1983) 123; J. R. Ellis, J. Hagelin, D. V. Nanopoulos, K. Tamvakis, Phys. Lett. B **125** (1983) 275; L. Alvarez-Gaumé, J. Polchinski, M. Wise, Nucl. Phys. B **221** (1983) 495.
- [50] D. Suematsu, Phys. Rev. D **59** (1999) 055017.
- [51] K. S. Babu, C. Kolda, J. March–Russell, Phys. Rev. D **54** (1996) 4635; T. G. Rizzo, Phys. Rev. D **59** (1999) 015020.
- [52] P. Abreu *et al.* [DELPHI Collaboration], Phys. Lett. B **485** (2000) 45; R. Barate *et al.* [ALEPH Collaboration], Eur. Phys. J. C **12** (2000) 183.
- [53] J. F. Grivaz, arXiv:0809.0531 [hep-ex] and references therein.
- [54] A. C. Kraan, hep-ex/0505002.
- [55] S. Hesselbach, F. Franke, H. Fraas, Eur. Phys. J. C **23** (2002) 149.
- [56] T. Gherghetta, T. A. Kaeding, G. L. Kane, Phys. Rev. D **57** (1998) 3178.
- [57] P. A. Kovalenko, R. B. Nevzorov, K. A. Ter-Martirosian, Phys. Atom. Nucl. **61** (1998) 812 [Yad. Fiz. **61** (1998) 898]; R. B. Nevzorov, M. A. Trusov, J. Exp. Theor. Phys. **91** (2000) 1079 [Zh. Eksp. Teor. Fiz. **91** (2000) 1251]; R. B. Nevzorov, K. A. Ter-Martirosyan, M. A. Trusov, Phys. Atom. Nucl. **65** (2002) 285 [Yad. Fiz. **65** (2002) 311].

- [58] B. C. Allanach, *Comput. Phys. Commun.* **143** (2002) 305.
- [59] A. Aktas *et al.* [H1 Collaboration], *Phys. Lett. B* **629** (2005) 9.
- [60] F. Abe *et al.* [CDF Collaboration], <http://www-cdf.fnal.gov/physics/>, see CDF Notes 9246.
- [61] P. Athron, S. F. King, D. J. Miller, S. Moretti, R. Nevzorov, in preparation.
- [62] J. Kalinowski, S. F. King, J. P. Roberts, *JHEP* **0901** (2009) 066.
- [63] D. R. T. Jones, *Phys. Rev. D* **25** (1982) 581; M. E. Machacek, M. T. Vaughn, *Nucl. Phys. B* **222** (1983) 83; M. E. Machacek, M. T. Vaughn, *Nucl. Phys. B* **236** (1984) 221; S. P. Martin, M. T. Vaughn, *Phys. Rev. D* **50** (1994) 2282.
- [64] D. I. Kazakov, *Phys. Lett. B* **449** (1999) 201.